# Pea fractionation into functional ingredients

## A structural perspective

Anna Cäcilie Möller

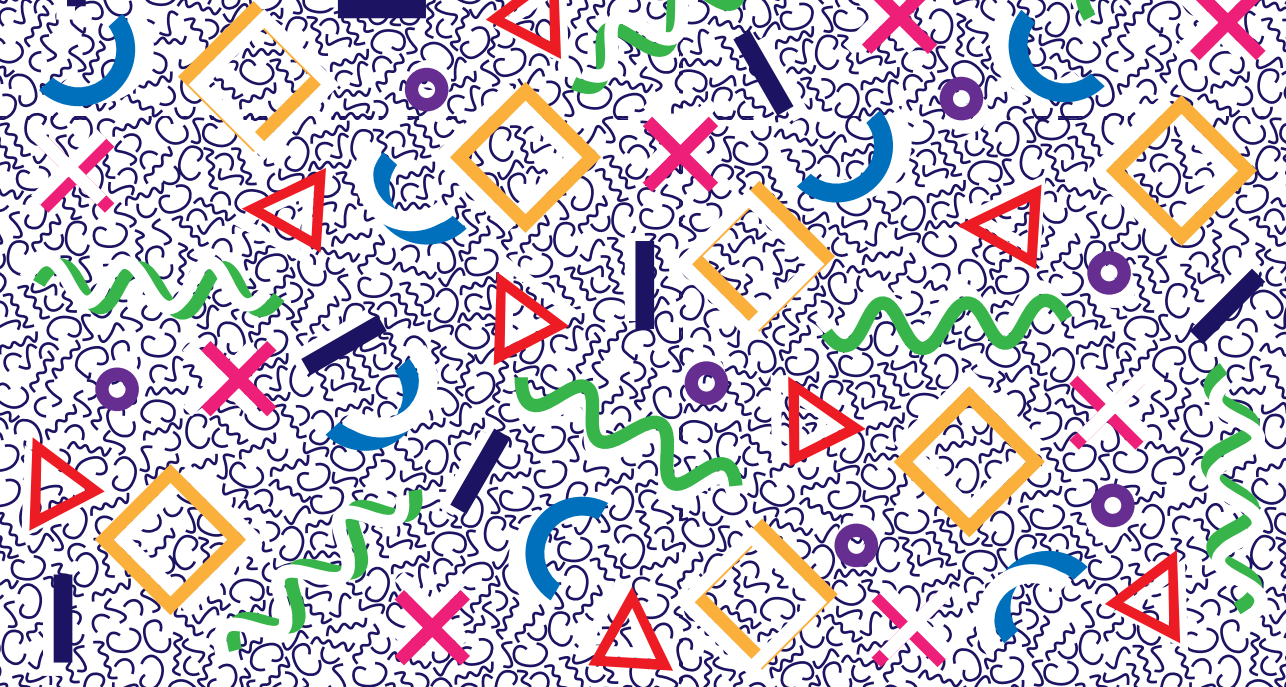

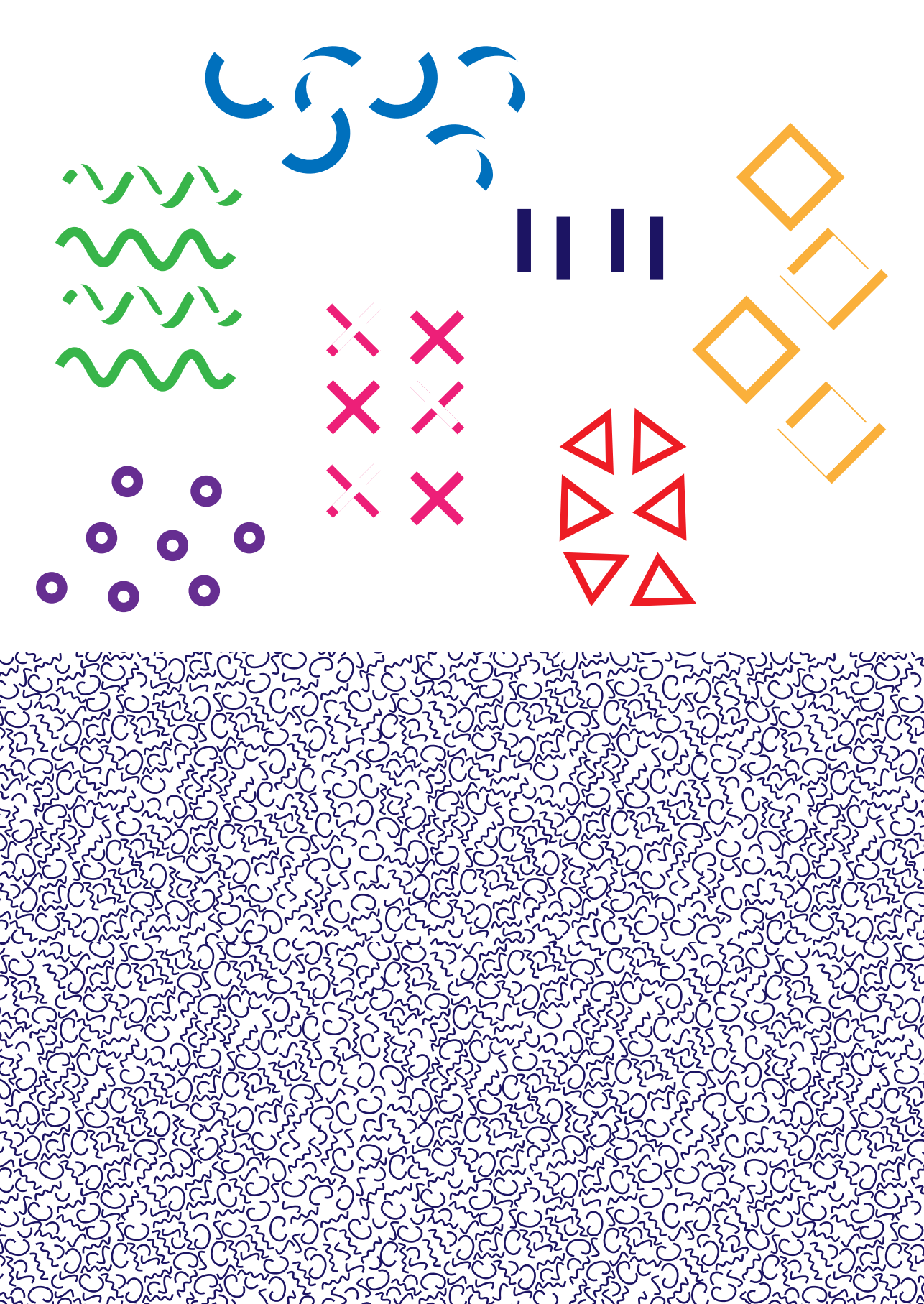

# Propositions

1. A biopolymer is as soluble as the selected definition of solubility allows.
   (this thesis)

2. Instead of re-inventing the wheel, we only have to apply the know-how from dairy industry to develop fractionation processes for plant-based ingredients.
   (this thesis)

3. Academic performance should be evaluated on team achievements, because modern research thrives on collaboration.

4. Creativity in research demands the unique skill of sensitive guidance without discouragement.

5. Only when confronted with the uncertainty of sickness do we realize the ease of a healthy life.

6. Human interaction is essential for happiness.

Propositions belonging to the thesis, entitled

Pea fractionation into functional ingredients
A structural perspective

Anna Cäcilie Möller

Wageningen, 14. October 2022

# Pea fractionation into functional ingredients A structural perspective

Anna Cäcilie Möller

## Thesis committee

### Promotors

Prof. Dr A. van der Padt
Special Professor at Food Process Engineering
Wageningen University & Research

Prof. Dr A. J. van der Goot
Personal chair at Food Process Engineering
Wageningen University & Research

### Other members

Prof. Dr M. A. Stieger, Wageningen University & Research

Prof. Dr H. Jäger, University of Natural Resources & Life Sciences, Vienna, Austria

Dr C. Dotremont, FrieslandCampina, Wageningen, The Netherlands

Dr E. Scholten, Wageningen University & Research

This research was conducted under the auspices of graduate school VLAG
(Advanced Studies in Food Technology, Agrobiotechnology, Nutrition and Health Sciences)

# Pea fractionation into functional ingredients A structural perspective

Anna Cäcilie Möller

Thesis
submitted in fulfilment of the requirements for the degree of doctor
at Wageningen University
by the authority of the Rector Magnificus,
Prof. Dr A.P.J. Mol,
in the presence of the
Thesis Committee appointed by the Academic Board
to be defended in public
on Friday 14 October 2022
at 4 p.m. at the Omnia Auditorium.

Anna Cäcilie Möller
Pea fractionation into functional ingredients
A structural perspective
207 pages
PhD thesis, Wageningen University, Wageningen, the Netherlands (2022)
With references, with summary in English
ISBN: 978-94-6447-364-3
DOI: 10.18174/575339

# Contents

# Chapter 1

## Introduction

Food structure is an important characteristic of most foods we consume. A distinction can be made between 'naturally' developed structures in plant and animal tissue or prefabricated structures via food processing (Morris & Groves, 2013). Natural structures are, for example, the muscle tissue of meat, where macromolecules form a hierarchical fibrous structure, starch granules in which polysaccharides assemble into discrete packets or the fleshy structure of fruits and vegetables, where plant cells form network structures bound by the cell walls (Parada & Aguilera, 2007). In 'natural' and prefabricated structures, the main building blocks are proteins, fats, and carbohydrates, which are self-assembled in natural foods. These building blocks can form high-order structures that can be sub-structures of even more complex structures, e.g. polysaccharides form starch granules that are embedded in a wheat grain structure (Morris & Groves, 2013). To produce prefabricated structures in the food industry, the 'natural' structure of the raw material needs to be broken down and reassembled with other ingredients into new structures. This procedure becomes clear when analysing the bread making process. Cereal grains are milled into flour, rich in carbohydrates and proteins, and are reassembled with water, yeast and salt into bread. For some products, all components from the raw material are used (whole-grain bread), while for others, specific components are extracted before structure formation (white flour bread).

## 1.1 Legume protein for prefabricated structures

Legumes are usually a food product on their own, and only minor processing is required to transform them into edible and appealing food products. However, interest has grown in producing prefabricated food structures from legume protein in the past decade.

Legumes are a major food source for centuries worldwide, and are one of the few plant groups almost distributed globally (Isely, 1982). They exist in a wide range of species, are well accepted, have high protein contents and are available at low cost (Tiwari, Gowen, & McKenna, 2011).

Yellow pea is one of the oldest field crops of the family Leguminosae. Peas can tolerate low temperatures during germination and growth (Chao, Jung, & Aluko, 2018). Furthermore, yellow pea contains around 21% protein with low allergenic potential, 45% starch, and nourishing minerals and vitamins (Roy, Boye, & Simpson, 2010).

With an increased interest in legume proteins, the food industry enhanced their focus on extracting the proteins from the legumes. Often, the aim is to create highly pure protein isolates and streams of starch, fibre and soluble material. Different methods exist to extract protein from pulses. For starch-rich legumes, the flour is dispersed, and the starch is separated in a centrifugal separator. The most common method to extract the protein from the remaining slurry is an alkaline extraction of the protein followed by its isoelectric precipitation. The dispersion is adjusted to an alkaline pH, which results in solubilisation of the core proteins. Residual insoluble components are separated via centrifugation. Subsequently, the pH of the aqueous phase is adjusted to the isoelectric point of the core proteins, which results in their precipitation. The protein pellet obtained can be immediately dried or dried after another pH adjustment to neutral pH (Boye, Zare, & Pletch, 2010). Legumes contain a variety of proteins, which have different isoelectric points (pI). Pea globulins' pI is between pH 4-5 (Boye, Zare, & Pletch, 2010), while albumins are still soluble at that pH (Djoullah, Djemaoune, Husson, & Saurel, 2015). This consequently results in the loss of albumins into the residual material during isoelectric precipitation as these proteins do not precipitate completely. Efforts are taken to valorise the side streams obtained from these protein isolation methods to ensure the process and economic sustainability of the manufacturing process. However, their application still lacks a commercial scale (Ratnayake, 2021).

Nowadays, an interest is rising for alternative processes that are milder, but still lead to sufficiently high purities of the ingredients. Milder processes comprise dry fractionation methods, such as air classification and electrostatic separation. These techniques require no use of water and hence no drying step,

which results in considerably lower energy consumption of the processes. Air classification works with a difference in size and density of the protein-rich and protein-poor particles in legumes (Schutyser, Pelgrom, van der Goot, & Boom, 2015). Electrostatic separation based on triboelectric charging could be more suitable for particles of similar size but differences in composition and hence a different charging behaviour. The particles are charged and subsequently separated in an electric field created by two electrodes, which attract the oppositely charged particles (Wang, Smits, Boom, & Schutyser, 2015).
Alternatively, mild wet fractionation techniques were introduced where milder steps, such as ultrafiltration and diafiltration replaced isoelectric precipitation of proteins subsequent to alkaline extraction (Boye, Aksay, et al., 2010).

## 1.2 Relevant properties to structure proteins into food products

Ingredients containing proteins, are widely analysed for their techno-functional properties. Specifically, the influence of the fractionation method on the ingredient properties is investigated (Boye, Zare, & Pletch, 2010). Harsh processing methods, such as alkaline extraction and isoelectric precipitation can have a detrimental effect on functionality, which explains why commercial protein isolates have a reputation for having poor techno-functional properties (Nikbakht Nasrabadi, Sedaghat Doost, & Mezzenga, 2021), especially in comparison to dairy protein. These poor properties, including low solubility, are primarily owed to the denaturation and aggregation of proteins, caused by the extraction process (Tanger, Engel, & Kulozik, 2020). Protein solubility is considered one of the most important properties of food proteins. However, other properties such a water holding capacity and rheological properties are nowadays also considered as important properties to create different food products.
When solid structures are made with food proteins, the processes usually follow three main steps (Gonzalez-Perez & Arellano, 2009). Initially, the proteins are denatured by, e.g. coagulation to produce curd, which is both a require-

ment to produce cheese and tofu. The coagulation can be induced by salt, acid or enzymatic coagulants. The curd is then further processed, which usually includes a re-organization and re-orientation step for the proteins. To stay with the example of cheese and tofu, the curd is stretched or pulled in hot water to produce pasta filata, a technique in Italian cheese manufacture. It is also possible to fill the curd into vessels to solidify for soft tofu or to produce firm tofu by draining and pressing. Finally, the structure is bound and stiffened. Especially the processing of pasta filata is of interest when mimicking meat structures. The curd is kneaded to obtain a stringy and elastic structure after coagulation.

## 1.3. Aim and Outline of this thesis

This thesis describes the research on the fractionation of peas from structured seed into structured product. The structure is therefore the main determinant of the choices in this thesis. The aim of the thesis is to understand the role of the material structure before, during and after mild fractionation when reassembling the mild fractions into food products. To do so the interactions between the components in dry and wet state are quantified.

*Chapter 2* describes the potential of pearling as a pre-fractionation method beyond dehulling. The aim is to pearl off 20 % of the outer pea cotyledon and investigate if the resulting fractions from the inner and outer kernel will be enriched in protein or starch by compositional analysis.

In *Chapter 3*, a relation between the structure of the yellow pea flour particles and their composition will be established. The structure break-up is investigated during milling, and the structural composition in the fractions after dry and mild wet fractionation is determined.

*Chapter 4* builds on the results of *Chapter 3* by developing a mild wet fractionation technique to obtain higher yield and purity fractions. The use of only water for fractionation is analysed on the fractionation efficiency. Multiple washing steps are applied to enhance separation, and ultrafiltration is investigated to

concentrate the soluble protein fraction. A techno-economic evaluation on the upscaling of the process is included as well.

*Chapter 5* describes the solubility characteristics of the pea proteins in the soluble and non-soluble protein fraction obtained from mild wet fractionation. Both fractions are further separated into albumin and globulin-rich fractions and analysed for their composition. The protein solubility is investigated at different concentrations and varying pH for all fractions. Furthermore, the gelling properties are assessed, to demonstrate how functional properties depend on composition.

In *Chapter 6*, the water distribution and component phase behaviours in multi-component blends of starch, protein and fibre from pea is determined. The motivation is to better understand the role of component interactions in such blends. The viscoelastic properties of pea isolates and blends thereof are measured, and predictions of the water distribution are made with the polymer blending law.

*Chapter 7* introduces a structuring method developed for the polymer industry, with which stratified structures can be produced. Here, the potential of this structuring method is investigated to structure food. Combinations of different materials are structured, and the structure uniformity is assessed. Finally, the potential of the method for food structuring is discussed.

The thesis is concluded in *Chapter 8* with a general discussion on the main findings of the presented work and final conclusions. Additionally, the chapter includes a summary of opportunities to develop the research further.

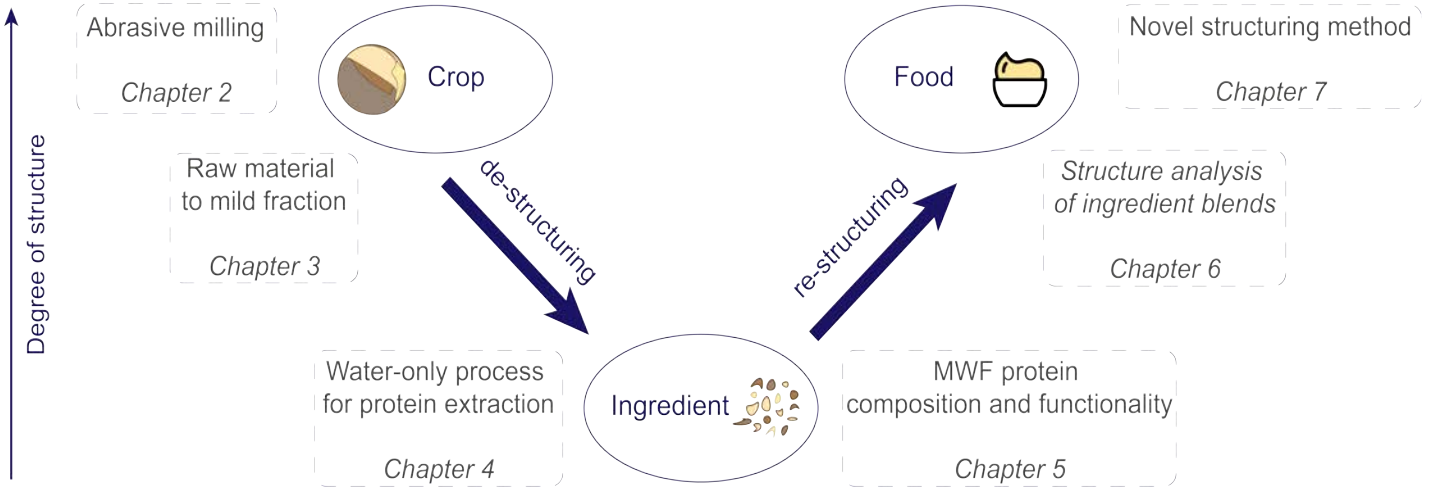


Figure 1.1: Contextual outline of this thesis

# Chapter 2

## Abrasive milling: A method to pre-fractionate testa and embryonic axis from yellow pea

Anna Cäcilie Möller, Albert van der Padt, Atze Jan van der Goot

Published in LWT, 151, (2021), 112087

## Abstract

Making use of crops structural break-up during pearling and subsequent fractionation into starch or protein enriched fractions was investigated using stepwise pearling as a method. In first instance, pearling resulted in separation of pea testa and embryonic axis from the cotyledon. Further around 20% of the yellow pea cotyledon was pearled off and collected separately from the inner kernel. All four fractions were finely ground and their composition analysed. Due to the di-cotyledon structure of the pea, solely pearling the outer kernel couldn't be guaranteed. Therefore, the process was repeated by hand-dissection, to ensure only separation of the outer 20% cotyledon. Pearling resulted in size reduction and separation of testa, embryonic axis and the outer and inner part of the cotyledon. Although, no considerable enrichment was achieved in protein or starch content in the pearled fraction of the outer and inner cotyledon, pearling gave the opportunity to obtain the testa fraction, which according to literature is rich in dietary fibre. Moreover, the protein-rich embryonic axis was separated and collected. The testa fraction accounts for 7–8% of the whole pea and contains little protein and starch, which makes it a promising dietary fibre rich ingredient in food application.

## 2.1 Introduction

An increasing trend in food industry is shifting from animal-based proteins to plant-based proteins. This leads to the necessity to investigate methods to extract proteins from plant materials. Promising plant materials to extract proteins from are crops like legumes, as they naturally have high protein contents. To contribute to a more sustainable food production process, mild fractionation techniques were investigated (Geerts, Mienis, Nikiforidis, van der Padt, & van der Goot, 2017; Pelgrom, Berghout, van der Goot, Boom, & Schutyser, 2014; Pelgrom, Vissers, Boom, & Schutyser, 2013) valorising the whole crop. One crop is the yellow field pea, consisting of 21–30% protein, around 50% carbohydrates, 10% crude fibres and 2–3% fat (de Almeida Costa, da Silva Queiroz-Monici, Pissini Machado Reis, & de Oliveira, 2006). The pea is a spherical seed with an outer skin, the testa. The core of the seed is di-cotyledonous, hence contains two embryonic leaves, which function as storage organs in the pea and are connected by an embryonic axis.

The cotyledons mainly consist of protein bodies (1–3 μm) and starch granules (5–20 μm), which comprise the storage tissue of the pea cells. The concentrations of protein, fat, starch and dietary fibre change towards the outer part of the cotyledon, when compared to the inner part (Kosson, Czuchajowska, & Pomeranz, 1994; Otto, Baik, & Czuchajowska, 1997). Van Donkelaar, Noordman, Boom, & Van Der Goot, (2015) showed that by step-wise pearling of the barley kernel the protein and starch content could be altered. In one fraction the protein content doubled while the starch content reduced by almost threefold. Hence, pearling provided a route for enrichment of protein and starch in different fractions. The barley is like the yellow pea a starch rich seed. Barley is mono-cotyledonous with a starchy endosperm where, similar to the pea cotyledon, the starch granules are embedded in a proteinaceous matrix including protein bodies. However, the barley kernel is distinctly different in structure compared to yellow pea. The starchy endosperm is surrounded by distinct layers including the aleurone layer, testa, pericarp and husk. These layers vary in composition

and structure. Protein is next to the endosperm also present in aleurone cells in the aleurone layer. However, similarly to the pea cotyledons, the outer region of the barley endosperm is richer in protein, compared to the endosperm centre (MacGregor, 2003). Therefore, this similarity in enriched and depleted areas of protein and starch within the kernels, and the starch rich endosperm structure suggested that pearling of pea could be promising to introduce as a size reduction step while simultaneously producing enriched fractions from the pea testa and outer and inner layer of the pea cotyledon. To the best of our knowledge, so far pearling of di-cotyledon seeds beyond dehulling to produce enriched fractions has not been studied. Therefore, the aim of this research was to investigate the potential of pearling as a fractionation method to obtain fractions enriched in protein or starch.

## 2.2 Materials & Methods

Pre-dried yellow peas (*Pisum sativum L.*), harvested in 2017 in the U.S. and stored in bulk in a warehouse silo were purchased from Alimex (Sint Kruis, The Netherlands). The dried yellow peas were pearled in a Satake TM05 testing mill. In a first step, the seeds were subjected to the pearling machine only for a short time of 10 s to separate the testa from the cotyledon which could be collected in separate baskets. Subsequently, the pea cotyledons were again subjected to the pearling and a second longer pearling step was performed of around 30 s, to pearl off around 20 % w/w from the pea cotyledon. The pearled off cotyledon fraction was called fraction 1, while the remaining cotyledons were called fraction 2. Both were ground in a laboratory rotor mill prior to further analysis (Fritsch, type pulverisette 14 equipped with a 500 µm screen). The yield of both fractions was defined as the weight percentage of the pearled off fraction based on the initial weight. In a second approach testa and cotyledon were separated accordingly and the embryonic axes were hand-picked from the separated testa fraction. Furthermore, the outer layer of the pea cotyledons was dissected by

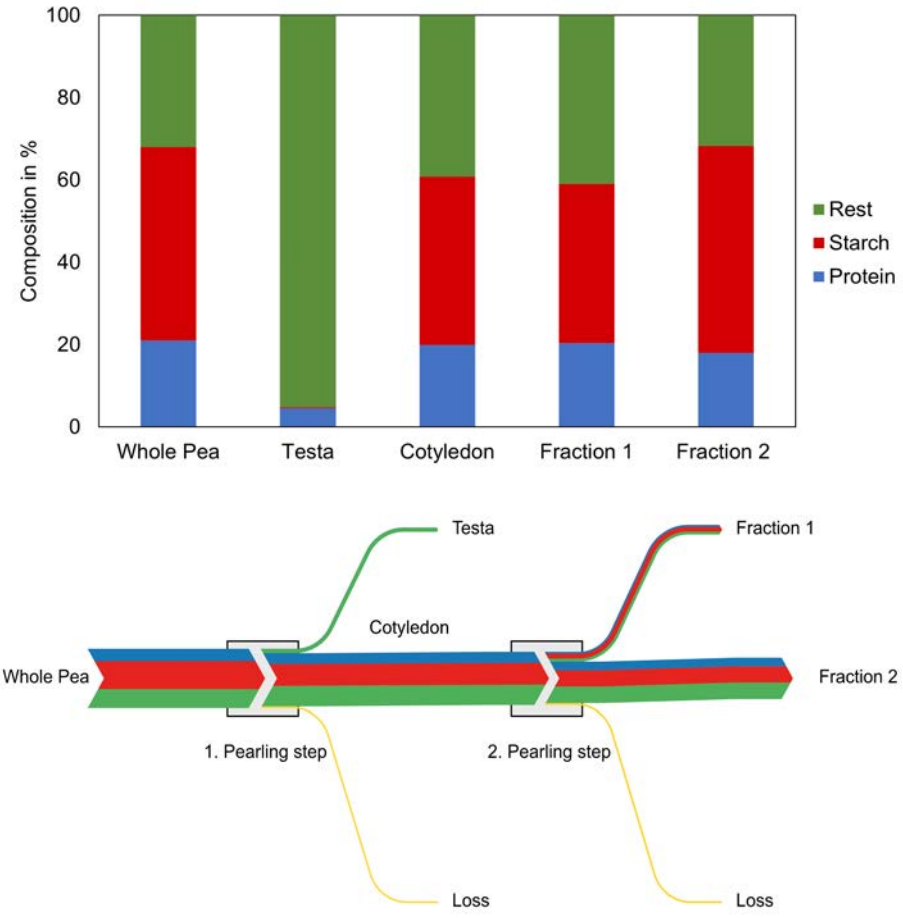


Figure 2.1 The composition of the fractions obtained from the two pearling steps is depicted in a compositional bar chart and a Grassmann diagram. In the first pearling step the testa was separated from the cotyledon, subsequently the cotyeldon was pearled in a second step to obtain fraction 1 and 2. The colours indicate the protein, starch, rest, and loss content of the streams.

hand with a sharp razor blade. And both the outer layer and the inner layer were ground for further analysis according to fraction 1 and 2. The dry matter content of the peas was determined by oven drying at 105 °C overnight, to calculate the yields. The protein content of the fractions was determined using a Dumas analysis (Nitrogen analyser, FlashEA 1112 series, Thermo Scientific, Interscience, Breda, The Netherlands) using a protein conversion factor of 5.52 (Holt & Sosulski, 1979). The total starch content was determined using the Total Starch Amyloglucosidase/α-Amylase Assay Kit (Megazyme International Ireland Ltd., Bray, Ireland).

## 2.3 Results

The whole peas (138.8 g) were dehulled, resulting in a testa fraction of 7.4 % of the total pea. During dehulling around 3.0 % material was lost. With the separation of the testa, the embryonic axis was concurrently separated from the cotyledons, which resulted from splitting of the peas. Some embryonic axes remained in a small pocket inside the testa, hence ended up in the testa fraction (Appendix, Figure A 2.1). The cotyledons (124.4 g) were subsequently pearled, resulting in a fraction of the outer layer (fraction 1) of around 18.3 % of the cotyledons. The remaining parts were milled and collected as the inner layer fraction (fraction 2) accounting to 78 % of the cotyledons. The pearling steps resulted in a material loss of 3.7 % (Appendix, Table A 2.1). Figure 2.1 depicts the composition of each fraction in grams, the colours indicating the amount of protein, starch and rest in the fractions. The Grassmann diagram is added to visualize the pearling process and yield of each fraction. The protein content in the testa was assumed to be derived from embryonic axes remaining in the testa fraction, as pea testa contain nearly no protein and starch (Bain & Mercert, 1966). Embryonic axes were hand-picked, and their composition was analysed to account to about 40 % protein and 5 % starch content on a dry matter basis. The remaining embryonic axes could hence account to the protein content in

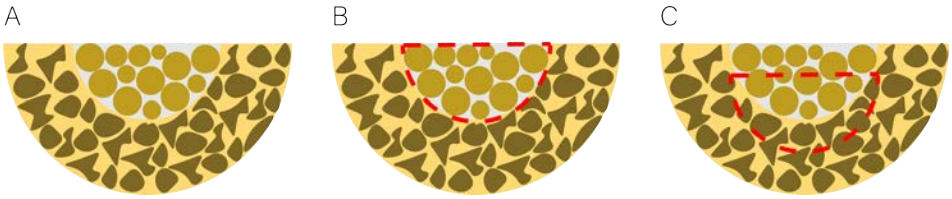


Figure 2.2. Representation of a split cotyledon leaf of pea. The outer part underlined in yellow represents the assumed protein enriched outer part of the pea, while the grey underlined inner part is the assumed starch enriched part (A,B,C). The red dotted line in (B) represents the desired pearling profile, while the red line in (C) represents a less optimal pearling profile.

the testa fraction. The whole peas contained 21.0 % protein and 47.0 % starch, fraction 1 contained 20.4 % protein and 38.7% starch and fraction 2 contained 18.0 % protein and 50.3 % starch. Hence, pearling resulted in a slight depletion (fraction 1) and enrichment (fraction 2) of starch in the respective fractions, when compared to whole peas. However, a significant enrichment or depletion of protein could not be achieved in either of the fractions by pearling. Comparing the pea seed to the barley seed, the pea is a dicotyledonous seed and splits when dehulled. It was therefore considered that upon pearling not only the outer layer was pearled off. Two possible pearling profiles are depicted in Figure 2.2 (B, C). (B) represents the desired pearling profile, while (C) depicts a less optimal profile according to the hypothesis that the outer and inner layer are distinct in their starch and protein distribution. To understand the results depicted in Figure 2.1 and connect them to the hypothesis of the pearling profiles, additional experiments were performed. Both a thick and a thin layer were cut off the cotyledons, respectively and their protein content was determined. With hand dissection the cutting line in (B) was assumed to be followed, as no part of the flat inner surface of the cotyledon was dissected. Remarkably, no differences in protein content between the different outer and inner fractions could

be observed (Appendix, Figure A 2.2, A), in contrast to the barley endosperm. The results of both experiments give the indication that, in contrast to barley, protein is homogeneously distributed over the cotyledon. Hence, pearling will not lead to protein and starch enrichment during structural break-up.

## 2.4 Conclusions

Pearling was shown to be a suitable first size-reduction step, prior to a milling step in the laboratory mill, the process leads to a dietary fibre enriched fraction, composed of the pea testa. Further, pearling of the cotyledon did not lead to protein or starch enrichment in the respective outer and inner fraction. It was shown that no different results are obtained for when pearling or hand-dissecting the pea cotyledon, which indicated that the structural locations of protein and starch do not allow separation by stepwise pearling. Therefore, pearling is considered effective for removing and collecting the testa, however, does not serve as a fractionation method for the pea cotyledon. Additionally, with pearling the embryo was successfully separated, it was confirmed that the embryonic axis contained a considerable amount of protein, next to only little starch, which makes it an interesting part of the pea to isolate.

# Appendix

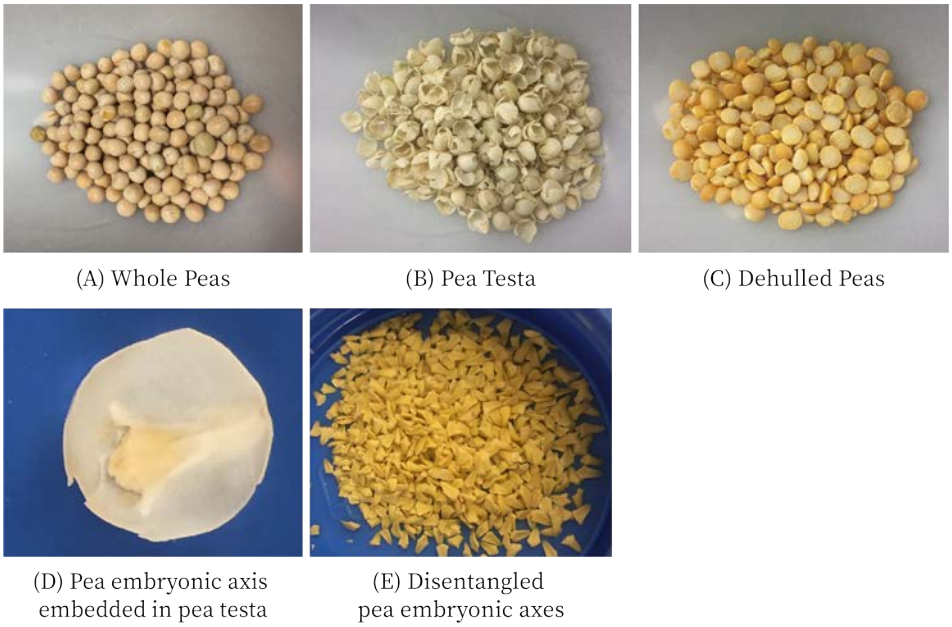

(A) Whole Peas (B) Pea Testa (C) Dehulled Peas

(D) Pea embryonic axis embedded in pea testa (E) Disentangled pea embryonic axes

Figure A 2.1. Images of whole peas (A), pea testa (B) and split pea cotyledons (C) after dehulling. Further a fragment of a pea testa with an embryonic axis embedded in a pocket of the pea testa is depicted (D) and disentangled embryonic axes (E). The observation explained the presence of embryonic axes in the testa fraction and indicated that the protein content in the fraction was attributed to the embryonic axes.

Table A 2.1. Yields of the fractions throughout the pearling process. The averages are given in grams [g] and the respective percentages were calculated from the absolute values including the deviations. The numbers reflect the reproducibility of the pearling process.

| Fraction | [%] | [g] | [%] | [g] |
|---|---|---|---|---|
| Whole Pea | 100.0 | 138.8 ± 1.4 | | |
| Testa | 7.4 ± 0.3 | 10.3 ± 0.3 | | |
| Cotyledon | 89.6 ± 1.4 | 124.4 ± 0.8 | | |
| Loss Dehulling | 3.0 ± 1.7 | 4.2 ± 2.4 | | |
| Inner + Outer Layer | | | 100.0 | 119.8 ± 0.2 |
| Pearled Outer Layer | | | 18.3 | 97.0 ± 0.3 |
| Pearled Inner Layer | | | 78.0 | 22.8 ± 0.1 |
| Loss Pearling | | | 3.7 | 4.6 ± 0.9 |

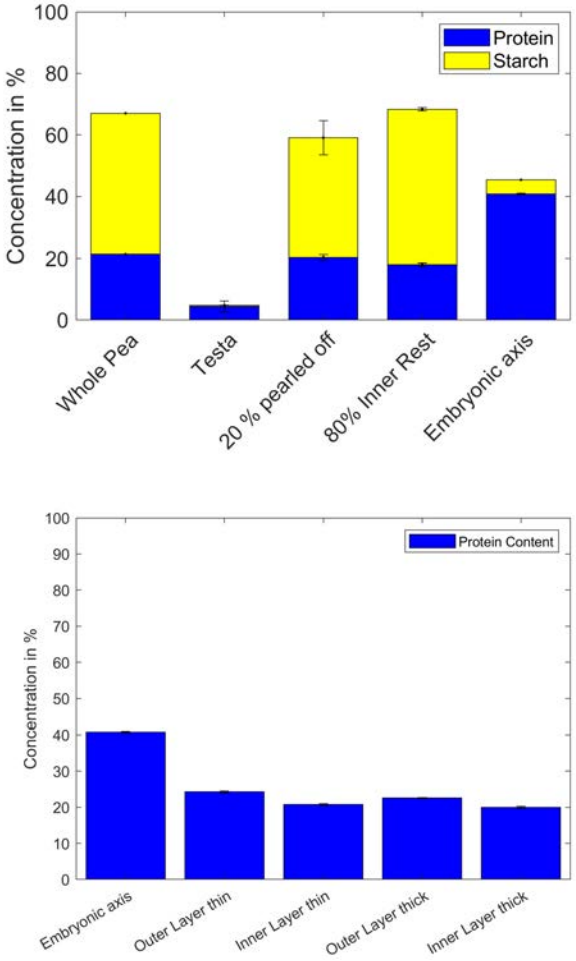


Figure A 2.2 Protein and starch content on a dry matter basis of fractions obtained through pearling process (top). Protein content on a dry matter basis of hand dissected pea cotyledon fractions (bottom). Both thin and thick layers were dissected from the cotyledons and analysed for their protein content separately. Slight enrichment in protein is observed for the Outer layer when compared to the Inner layer. It was however not considered to be a sufficient amount (< 10%).

# Chapter 3

## From raw material to mildly refined ingredient - Linking structure to composition to understand fractionation processes

Anna Cäcilie Möller, Albert van der Padt, Atze Jan van der Goot

Published in Journal of Food Engineering, 291, (2021), 110321

## Abstract

The relation between the structure of yellow pea and its optimal fractionation process was investigated using scanning electron microscopy (SEM) and energy-dispersive X-ray spectroscopy (EDS). Different fractionations obtained by milling and various methods were investigated and compared to pea flour. Milling resulted in structure break-up and a distinction of particles in shape and size. Different particles were identified using the mapping of the elements (EDS), carbon, oxygen and nitrogen, indicating the presence of starch, protein and other carbohydrates, in the form of protein bodies, starch granules and cell wall fragments. It was further observed that not only protein bodies contained protein, but also particles that were presumed to be cell wall material contained protein, although in considerably lower concentrations. With both fractionation methods protein and starch could be partly separated, but wet fractionation resulted in a higher purity in both the soluble and nonsoluble protein fractions.

## 3.1 Introduction

Most ingredients that are used in food products are highly purified, i.e. starch, sugar, oils or proteins. The production of these ingredients requires large amounts of water and energy, and results in large side streams (Augustin et al., 2016; Ladha-Sabur, Bakalis, Fryer, & Lopez-Quiroga, 2019; Van Der Goot et al., 2016). Therefore, alternative processing and fractionation routes were investigated, where either the valorization of the produced side streams is investigated (Schieber, 2017) or routes to omit side streams by producing less pure ingredients (Geerts, Mienis, Nikiforidis, van der Padt, & van der Goot, 2017; Pelgrom, Berghout, van der Goot, Boom, & Schutyser, 2014; Pelgrom, Vissers, Boom, & Schutyser, 2013). So far, a relation seems to exist between the harshness of the process and the obtained purification. It is therefore interesting to better understand which factors determine possible limits in purification and further develop the proposed route towards less refined ingredients to increase the process efficiency.

Yellow field pea has been widely studied before and is gaining increasing popularity as an ingredient in plant-based products. The pea is a spherical seed with an outer skin, the Testa or hull. The core of the seed is di-cotyledonous, hence contains two embryonic leaves, which together form the spherical shape. The cotyledons function as storage organs in the pea and are connected by the embryonic axis. Within the cotyledons, protein bodies and starch granules are embedded in the storage tissues of pea cells. The protein bodies are spherical organelles and, in the field-pea have a diameter of around 1–3 μm. The starch granules have round elongated shapes, ranging in size from 2 to 40 μm (Ratnayake, Hoover, & Warkentin, 2002) and are tightly embedded in a matrix of the protein bodies (Huang, 1985; Pernollet, 1978). The field pea contains around 21–30% protein, about 50% carbohydrates, 10% crude fiber and about 2–3% lipids (de Almeida Costa et al., 2006).

A range of fractionation processes have been investigated for yellow field pea, including air classification as a dry fractionation process (Pelgrom, Vissers, et

al., 2013; Silventoinen, Sipponen, Holopainen-Mantila, Poutanen, & Sozer, 2018; Wu & Nichols, 2005) and mild wet fractionation, where chemicals are omitted (Geerts et al., 2017; Peng, Kersten, Kyriakopoulou, & van der Goot, 2020). Milling is usually the first step when producing a concentrate or an isolate (Assatory, Vitelli, Rajabzadeh, & Legge, 2019; Boursier, B; Delevarre, M; Lis, J; Marquilly, 2008; Geerts et al., 2017; Muneer et al., 2018; Pelgrom, Vissers, et al., 2013). Ideally, milling leads to initial structure break-up that separates the components into discrete particles already. In yellow pea, starch and protein are naturally present in separate entities, which suggests potential of being broken up along those entities (Pelgrom, Boom, & Schutyser, 2015). In this paper, we investigate how efficient peas are broken-up along the different entities. The different structural levels of the pea seed have been visualized and analyzed using microscopic imaging before. Especially the structures in the pea storage cell and the disentangled starch granules were imaged by various authors using different microscopic methods (Bertoft, Qin, & Manelius, 1993; Colonna, Gallant, & Mercier, 1980; Craig, Goodchild, & Millerd, 1979; Kornet et al., 2020; Otto et al., 1997; Pelgrom, Schutyser, & Boom, 2013; Reichert & Youngs, 1978). The extensive research on the microstructure of the pea storage cell lead to an identification of the structures in the cell, based on their composition. During structure break-up and fractionation however, these structures are disentangled and might be modified in size and shape, which limits the particle identification in the obtained fractions. Therefore, the aim of this work was to investigate the structure break-up during milling and investigate the structural composition during dry and mild wet fractionation. By understanding the structure and composition of the flour particles we aim at understanding the potential of the fractionation methods to create possibilities for further optimization thereof.

## 3.2 Materials and Methods

Pre-dried yellow peas (*Pisum sativum L.*), were purchased from Alimex (Sint Kruis, The Netherlands).

### 3.2.1 Milling

The peas were pre-milled into grits using a pin mill (LV 15M, Condux-Werk, Wolfgang bei Hanau, Germany) at room temperature. The grits were subsequently milled into fine flour using a ZPS50 impact mill (Hosokawa-Alpine, Augsburg, Germany), with an impact mill speed of 8000 rpm, the air flow at 52 $m^3$/h, the classifier wheel speed at 5000 rpm and a feed rate of 2 rpm (method adopted from Pelgrom et al., 2015). A thermometer inside the mill was used to control the temperature between 16 and 34 °C.

### 3.2.2 Dry fractionation

Air classification was used according to the method of Pelgrom, Vissers, Boom and Schutyser (2013) using an ATP50 classifier (Hosokawa-Alpine, Augsburg, Germany). With a fixed air flow at 52 $m^3$/h, the classifier wheel speed at 5000 rpm, and the feed rate at 20 rpm a protein fraction (FF), enriched in protein and a starch fraction (DF), enriched in starch were obtained.

### 3.2.3 Mild wet fractionation

Secondly mild wet fractionation was performed according to the method of Geerts, Nikiforidis, van der Goot, & van der Padt (2017). 11.4 g of pea flour was suspended in 100 g ultrapure water (Milli-Q) and stirred for at least an hour. The suspension was then centrifuged at 1500 g at 20 °C for 1 s, resulting in a starch enriched pellet, defined as the starch fraction (SF) and a supernatant. The supernatant was then subjected to a second centrifugation step of 10000 g at 20 °C for 30 min, resulting in a pellet further called non-soluble protein fraction (NSPF) and a supernatant, soluble protein fraction (SPF). All three fractions were freeze dried for further analysis using a Pilot freeze dryer (Christ Epsilon

2-6D, Osterode am Harz, Germany).
A batch of the pre-dried peas was dehulled in a Satake TM05 pearling machine (Japan) to obtain a hull fraction. The remaining dehulled peas were not considered for further analysis.

3.2.4 Scanning electron microscopy (SEM) and energy-dispersive X-ray spectroscopy (EDS)
SEM was used to visualize the morphology of the pea flours and the respective fractions. The samples were mounted on SEM stubs (Aluminium Pin-Type Mounts 12.7 mm, Jeol, Nieuw-Vennep, The Netherlands) by carbon adhesive tabs (12 mm carbon tabs, SPI Supplies Division of Structure Probe, Inc., West Chester, PA, USA) and subsequently coated with 12 nm Iridium using a High Vacuum Coating system (Leica MED 020, Leica Microsystems B.V., Amsterdam, The Netherlands). Samples were analyzed at 2 kV, 13 pA, in a field emission scanning electron microscope including the energy-dispersive X-ray spectroscopy detector (Magellan 400, FEI, Eindhoven, The Netherlands). Elemental maps of the samples were produced using energy-dispersive X-ray spectroscopy. An electron beam is focused on the sample, the interaction of the beam with the specimen produces backscattered x-rays whose specific energies provide a fingerprint that is specific to each element due to their different and unique atomic numbers (Goldstein et al., 2018). In addition to the elemental maps, spectral analysis was performed on the surface of differently shaped particles to aid particle identification. Therefore, a scan area is selected. With the elemental scans the atomic percentages were calculated from the weight percentages using the following equation (Goldstein et al., 2018). Where n is the number of elements detected in the scan area.

$$atomic\% = \frac{\frac{wt.\%}{m_{element}}}{\sum_{1}^{n} \frac{wt.\%}{m_{element}}} \cdot 100\% \qquad 3.1$$

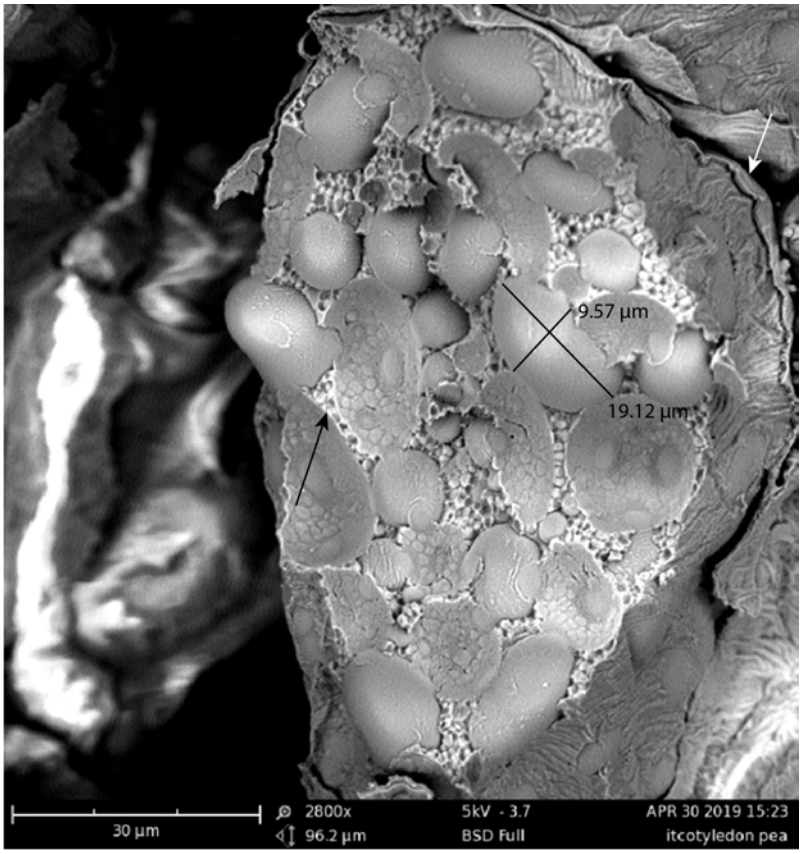


Figure 3.1 Scanning electron microscope (SEM) image of a storage cell from yellow pea. The long and short side of a starch granule is measured with 19.12 µm and 9.57 µm, respectively. The particulate matrix embedding the starch granules is highlighted with the black arrow. The storage cell is surrounded by a sheet-like structure, marked with a white arrow.

### 3.2.5 Image analysis

Image analyses was performed using the image processing and analysis open source software ImageJ (version 1.52, Laboratory for Optical and Computational Instrumentation, University of Wisconsin-Madison, USA). The scale bar of the image was converted into the software and the measures of the different shapes in the images were added.

## 3.3 Results and Discussion

Pea structure break-up during milling was investigated by identifying the particles based on their composition using Scanning electron microscopy (SEM) and energy-dispersive spectroscopy (EDS). Two different fractionation methods were performed, and the protein and starch separation potentials were analyzed by combining the compositional analysis of the fractions with elemental maps and image analysis of the particles.

### 3.3.1 Structure break-up from pea storage cell to pea flour

The pea cotyledon consists of storage cells in which starch granules are embedded in a cellular matrix, rich in protein. The protein in this matrix was reported to be present in protein bodies (Pernollet, 1978). An identification of the structures in the storage cell using cryo-scanning electron microscopy and energy-dispersive X-ray spectroscopy was previously reported by (Kornet et al., 2019). In this study, elongated particles in the cell, of rounded shapes and sizes of 10–30 μm were identified as starch granules and the matrix surrounding these particles was confirmed to contain proteins. The protein in this matrix was reported to be present in protein bodies (Pernollet, 1978). The elemental composition of the cell wall was not discussed and can also not be clearly identified in the images presented. Reichert and Youngs (1978) however reported that the cell wall of the pea storage cell contains 5 wt% protein in dry matter. Figure 3.1 shows a SEM image of a pea storage cell. The elongated particles in

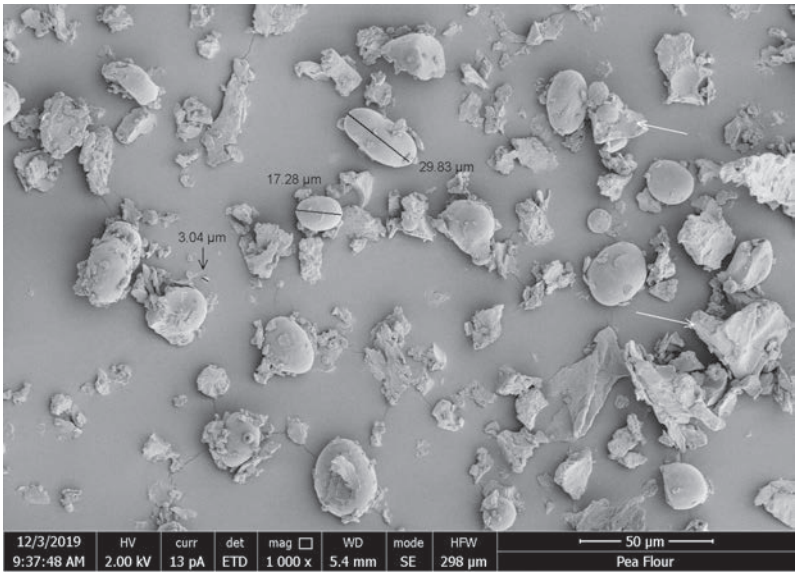


Figure 3.2 Scanning Electron Microscope (SEM) image of pea flour milled with the impact mill at 5000 rpm according to Pelgrom et al. (2013). The length of two elongated particles are included with 29.83 µm and 17.28 µm, respectively. The length of a smaller round particle is marked with 3.04 µm. Examples of insufficiently broken up structures are marked with white arrows.

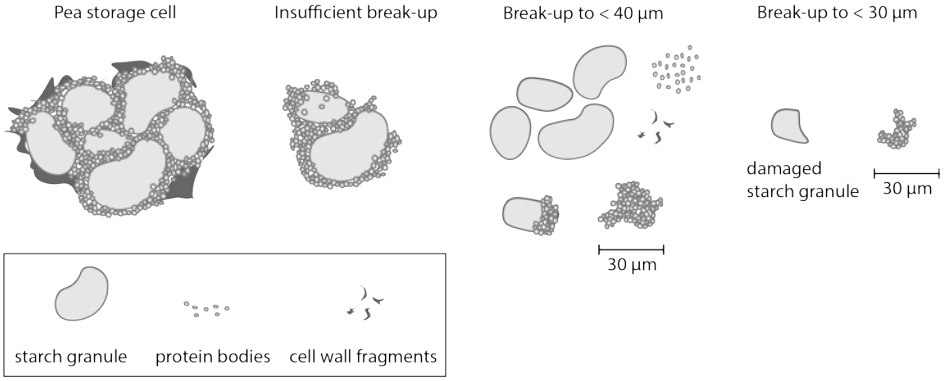


Figure 3.3 Illustration of pea structure break-up during milling, depicting a whole storage cell, insufficiently broken-up particles, fully disentangled particles and damaged starch granules (partly adopted from Schutyser, Pelgrom, van der Goot, & Boom, (2015).

the cell have a length of about 10–20 µm, which according to Kornet et al. (2019) are starch granules. These granules are embedded in a matrix of smaller round particles (Figure 3.1, black arrow), presumably protein bodies. Further, the storage cell is surrounded by sheet-like structures (Figure 3.1, white arrow), which might form the cell wall.

Figure 3.1 underlines that thorough disentanglement of protein and starch requires structure break-up of the pea cotyledon to a particle size range of 10 µm < D0.5 < 40 µm (Pelgrom, Vissers, et al., 2013). They found that impact milling at a classification speed of 4000 rpm resulted in optimal disentanglement of protein bodies and starch granules, with limited to no starch damage. This further resulted in a good protein and starch separation during air classification. The results are in line with previous findings. The non-uniform particle size of the starch granules makes full disentanglement without damage of the granules difficult to achieve in practice (Bertoft et al., 1993; Huang, 1985; Pernollet, 1978; Ratnayake et al., 2002; Vose, Basterrechea, Gorin, Finlayson, & G, 1976). Too coarse milling leads to aggregates of protein bodies, starch granules and other cell material, while too fine milling results in extensive starch damage, which was reported to negatively affect the component separation (Boye, Zare, & Pletch, 2010). Figure 3.2 shows a fraction of the pea flour, milled according to Pelgrom et al. (2013), where the cells were successfully broken-up into small particles. The elongated and round shapes of around 10–30 µm, representing starch granules, are disentangled from the cellular structure. However, upon close observation, particles of different sizes and roughness are still attached to the starch granules. Other particles of varying shapes and sizes are also visible, among others also larger particles, of which the morphology suggest insufficient break-up of the cell structures, i.e. a round, starch granule like particle, still entangled with the particulate cellular matrix (Figure 3.2, white arrows). However, these particles are similar in size as some starch granules, hence their structure break-up would also induce starch damage. For a better visualization of the structure break-up of the pea an illustration was

added (Figure 3.3). The illustration depicts a pea storage cell, containing starch granules, embedded in a particulate matrix and surrounded by a sheet like cell wall. Further a particle >30 µm is depicted which is a representation of an insufficiently broken up cell fragment. Structure break-up to <40 µm depicts the fully disentangled particles and some insufficient structure break-up, in form of an aggregate of a starch granule and protein bodies, which have approximately the same size as the fully disentangled starch granules. Lastly, structure break-up to <30 µm is depicted to illustrate starch damage.

### 3.3.2 SEM and EDS of pea flour

Figure 3.4 shows SEM images and elemental maps of particles obtained after milling. The elongated, round particle in (A) is a starch granule, given its size (27.35 µm) and shape. It is further, poor in nitrogen, see Figure 3.4 (B). The particles adhering to the surface of the granule, however, are rich in nitrogen, they have a diameter of about 3 µm and vary in shape and surface roughness. The size of these particles corresponds to the approximate sizes of protein bodies (~3 µm) reported in previous studies (Pernollet, 1978). However, the difference of the two particles, in shape and roughness indicates that they might be of different nature. The second particle (see Figure 3.4 (C)) looks distinctly different in shape and structure as the starch granule. The particle itself consists of smaller round particles sticking together, indicated by the black arrow. Large dents with a width of around 10 µm and a smooth surface are visible in the particle structure that might be the negative forms of starch granules according to their size and round shape. These observations suggest that the particle is a fragment of the intercellular matrix in which the starch granules were embedded (Huang, 1985; Pernollet, 1978). On its surface additional round particles (~3 µm) are adhering, which seem to have adhered to the fragment only after structure break-up, as they are positioned on the smooth surfaces where the starch granules were assumed to be in the original structure (see Figure 3.1). The small particles adhering to the surface of the fragment also contain nitro-

gen and could according to their shape, size (3 µm) and composition be protein bodies that were disentangled from the intercellular matrix and are re-adhering to the fragment. The elemental map reveals an even distribution of nitrogen over the whole particle, indicating that the whole fragment contains protein. This underlines the assumption that the particle is indeed a fragment of the intercellular matrix, rich in protein.

The identification of the particles, which adhere to the starch granules and matrix fragment, was extended by the spectral analysis of the clear surfaces of a starch granule and from two differently shaped particles adhering to the granule (Figure 3.5). Spectra 1 detected the elements on a clear starch granules' surface. In the scan area, no nitrogen was detected (see Table 3.1), which correlates with the results from the overall elemental map (Figure 3.4 B, D). The ratio of carbon to oxygen in starch is 6:5 according to the molecular structure of amylose and amylopectin. The large difference in the proportion of carbon to oxygen (5:1), might be induced by the carbonization of molecules by the electron beam leading to dehydration and thereby a loss of oxygen (Funke and Ziegler, 2010). The area of spectra 2 is from the surface of a round shaped particle, supposedly a protein body, adhering to the starch granule. The atomic nitrogen percentage of the surface is 15 %, if converted to protein using the nitrogen conversion factor of 5.52 for pea (Holt and Sosulski, 1979), this corresponds to 80 % protein. The organelle protein concentration in a protein body of different legume species was reported to be on average between 60 and 90 % (on dry weight basis) (Pernollet, 1978). That supports the hypothesis that the particle is a protein body. The average ratio of carbon to nitrogen based on the amino acid composition of pea proteins, was calculated to be around 4 carbon atoms per 1 nitrogen atom. This corresponds to the ratio of carbon to nitrogen detected on the surface of the protein body. It is therefore assumed that no depletion of nitrogen is occurring through, i.e. the electron beam. Spectra 3 is of the surface of a small flat shaped particle, which as well is adhering to the starch granule, but according to its flat shape might not be a protein body.

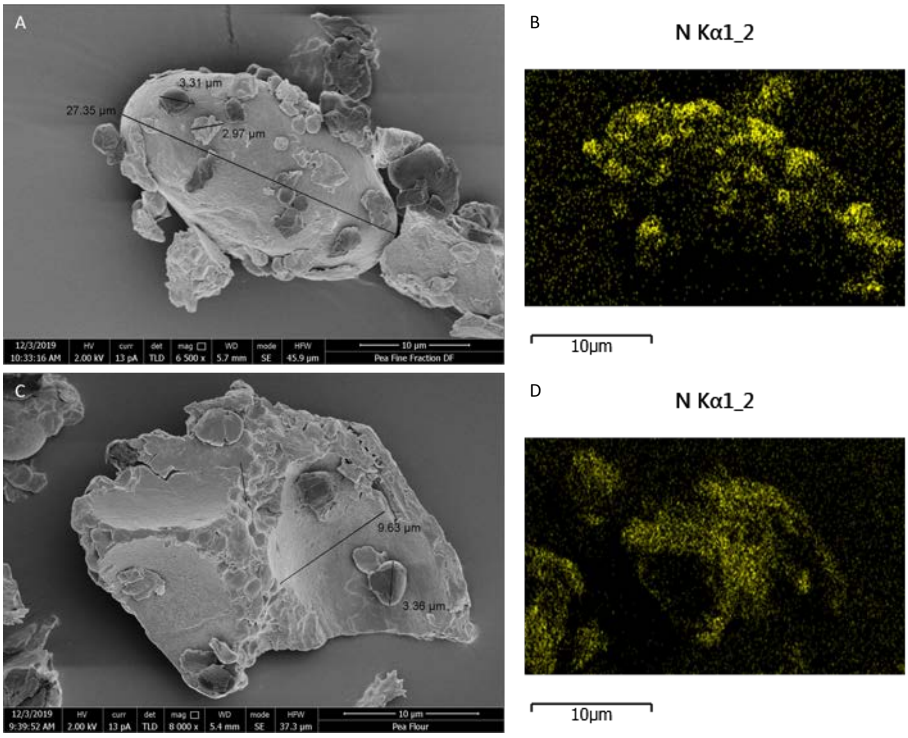


Figure 3.4 Scanning electron microscope (SEM) (A and C), and elemental maps (EDS) of pea flour particle depicting the abundance of nitrogen (B and D). (A) Measures for the different particles are included in the image with 27.35 µm, 3.31 µm and 2.97 µm, respectively. (C) The measure of a particle adhering to the structure is included with 3.36 µm. The width of one of the smoother areas of the big particle is included with 9.63 µm. The black arrow highlights the particulate structure of the particle.

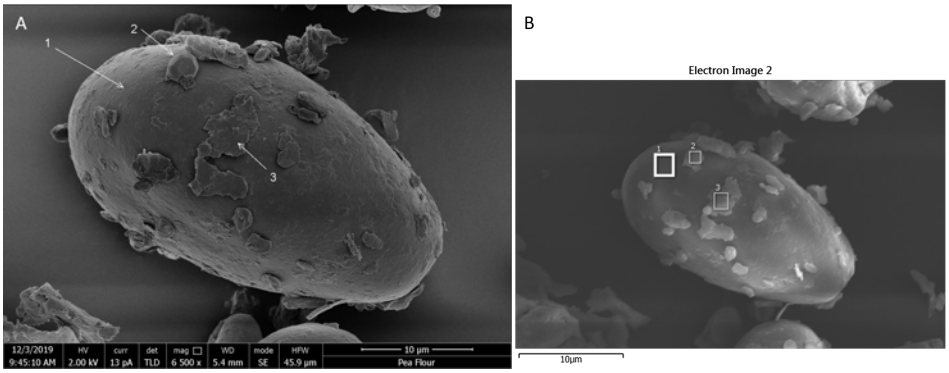


Figure 3.5 SEM image of individual starch granule (A), with indication of spectra locations 1,2 and 3 (B). In (A) the spectra locations are highlighted with white arrows and numbered accordingly.

It contains 2.26 atomic-% nitrogen (see Table 3.1), corresponding to 12.45 % protein (Nx5.52) which is a considerably lower amount when compared to the protein body of Spectra 2. The cell wall of legumes contains next to dietary fiber also some cell wall proteins (Reichert and Youngs, 1978), therefore the flat particle is probably a fragment of the cell wall. Although the spectra are only a representation of the surface of the particle and limited by the penetration depth of the x-rays, the atomic percentages of the surfaces allow an estimation of the total protein content of the particles. A more reliable insight, however is derived from the ratios between the elements that make a distinction and identification of the particles, based on their composition possible.
This distinction and identification of the particles, might help to predict the separation potentials of fractionation methods for different crops. If the particle structure serves to determine the composition, i.e. using morphology analysis techniques, together with the cut-off size of the air classification method a rough prediction of the separation potential might be possible.

The particle adhesion of the smaller particles, i.e. protein bodies and cell wall fragments, to the bigger particles, i.e. starch granules and cellular matrix fragments (Figures 3.4 and 3.5), could be caused by different mechanisms. Firstly, the particles are not fully disentangled from each other during milling, and therefore still adhere to the granule. Another possibility is that the particles are charged during milling, resulting in attraction and adhesion of smaller to bigger particles. The charging is caused by contact electrification when two surfaces contact and separate again and is dependent on the surface properties of the material (Horn and Smith, 1992; Kwetkus, 1998). These contacting surfaces are particle-wall contact surfaces between the particles and the mill, and particle-particle contact surfaces. With decreasing particle size the electrification of the particles increases, due to the increased surface-volume ratio of smaller particles (Gajewski, 1989), which means the charging also depends on the particle size of the flour. To investigate the adhesion mechanisms, different milling materials and speeds would need to be investigated. This was however out of scope for this research question. Instead, the SEM images after fractionation might provide an indication of the cause of the adhesion.

### 3.3.3 SEM and EDS of dry fractionated samples

Figure 3.6 depicts a protein-enriched fraction and a starch-enriched fraction, which were obtained using air classification. Compared to the SEM images of the flour, the starch-enriched fraction (see Figure 3.6 A) shows mostly starch granules, and few other bigger fragments, indicated by the black arrows. The surface of the starch granules is much cleaner after air classification when compared to the starch particles present in the flour. The protein-enriched fraction contains a much broader variety of particles. Here still some starch granules are visible (white arrows), as well as irregularly shaped particles (black arrows). Further, smaller particles are visible that adhere to the present bigger particles. In the protein fraction (A), more particle adhesion is visible, compared to the starch fraction. Next to the imaging, the

Table 3.1 Results of the spectral elemental analysis using SEM EDX as depicted in Figure 3.5, with the weight atomic percentages of the elements present within the area of the different spectral scans.

| chemical element | weight % Spectra 1 | atomic % Spectra 1 | weight % Spectra 2 | atomic % Spectra 2 | weight % Spectra 3 | atomic % Spectra 3 |
|---|---|---|---|---|---|---|
| C | 77.42 | 82.35 | 61.62 | 67.33 | 80.23 | 84.47 |
| N | | | 15.57 | 14.58 | 2.5 | 2.26 |
| O | 21.80 | 17.39 | 21.49 | 17.61 | 16.49 | 13.02 |
| Mg | | | 0.16 | 0.09 | | |
| K | 0.78 | 0.25 | 1.17 | 0.39 | 0.78 | 0.25 |

protein and starch content of the protein-enriched fraction and the starch-enriched fraction was determined, the results are listed in Table 3.2. According to the compositional analysis there is still around 13 % (Nx5.52) of protein present in the starch-enriched fraction. The starch granules in the starch fraction (DF) show, however, clean surfaces, indicating no protein is adhering to the granules which could explain the remaining protein content. Hence, air classification leads to loosening of the adhering particles to the starch granules allowing their separation, based on the particle size. This supports the hypothesis that the smaller particles are only adhering to the granules after structure break-up. The remaining protein is probably due to the presence of minor impurities or might be entangled in the insufficiently broken up particles (Figure 3.6 (B), black arrows) of >30 µm present in the starch-enriched fraction. The protein fraction (A) has a remaining starch content of 11 % (Table 3.2), which can be explained by the starch granules present in the fraction. Overall, the dry fractionation method leads to good protein – starch separation, however, the method is limited by the insufficient disentanglement during milling. Pelgrom et al. (2015)

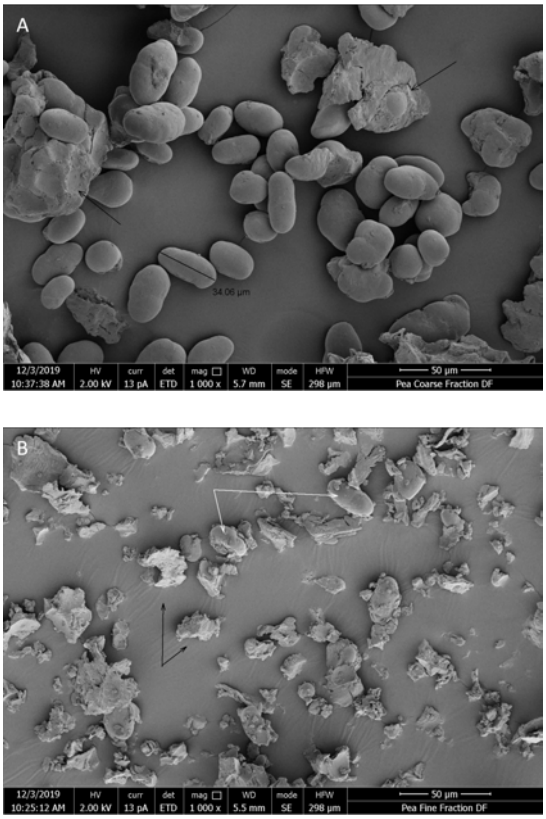


Figure 3.6 Scanning electron microscopy (SEM) images of pea starch-enriched fraction (A) and protein-enriched fraction (B) obtained by air classification of finely milled pea flour as adopted from (Pelgrom et al., 2015). In (A) the measure of a starch granule is included (34.06 µm), insufficiently broken up particles are highlighted with black arrows. In (B) starch granules are highlighted with white and irregularly shaped fragments are highlighted with black arrows.

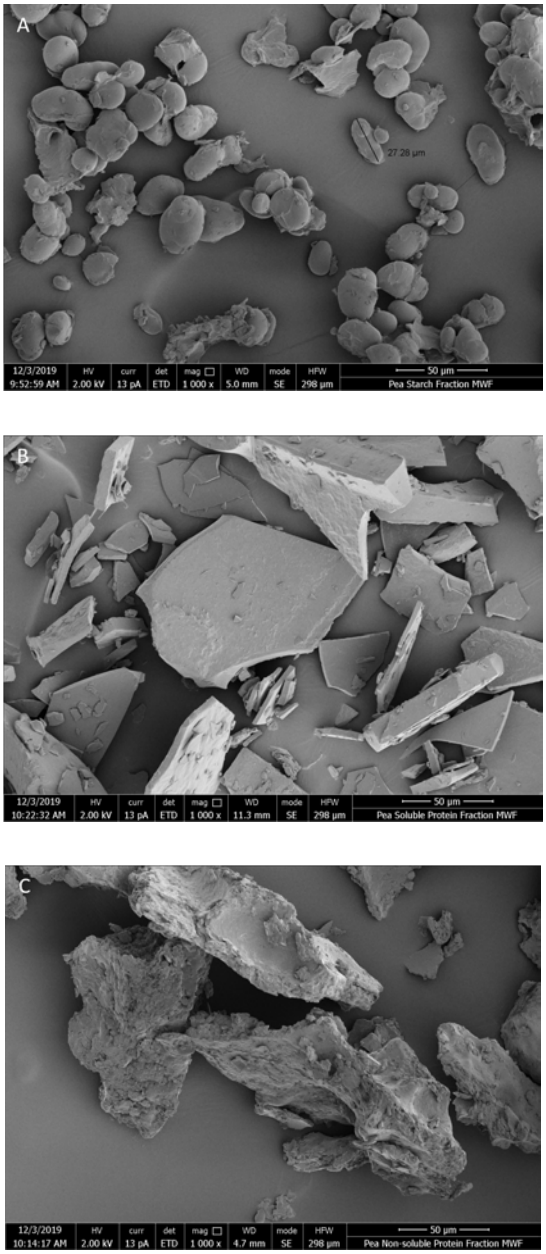


Figure 3.7 Scanning electron microscopy (SEM) of (A) starch enriched fraction, (B) soluble protein fraction (C) non-soluble protein fraction obtained by mild wet fractionation according to the method of (Geerts et al., 2017). (A) The measure of a starch granule is included (27.28 µm).

investigated a broad range of process conditions to find the optimal milling conditions, for maximal protein separation efficiency during air classification. The trade-off found was between highest disentanglement of protein and starch at lowest damage of starch granules.

### 3.3.4 SEM and EDS of mild wet fractionated samples

Mild wet fractionation was used to produce a starch enriched and two protein enriched fractions. Freeze drying was chosen as a mild drying process. These fractions were compared to the coarse and protein fraction (DF) from air classification and the native pea flour. Figure 3.7 (A) shows an image of the freeze dried and crushed starch fraction obtained after the first centrifugation step, (B) depicts the soluble protein fraction, freeze dried and crushed, and (C) the non-soluble protein fraction respectively. In addition to the SEM images, the compositional analysis of the fractions was performed, and the results are listed in Table 3.2 under mild wet fractionation.

SEM-images were used to compare the non-soluble protein fraction (NSPF) to the soluble protein fraction (SPF). On the surface of the NSPF particle a nitrogen atomic percentage of 11.70 % was calculated, which would result in a protein content of 64.58 % (Nx5.52). The nitrogen atomic-% calculated for the SPF particle surface was 8.99 %, corresponding to a protein content of 49.62 % (Nx5.52). The percentages of the spectral analysis were compared to the composition obtained through chemical analysis of the fractions. The protein purity of both SPF and NSPF are equal with around 52 %, see Table 3.2. This shows that the nitrogen detection of a particle surface does not exactly represent the protein content of the whole fraction. The compositions of the particles within the fraction are likely to be a bit different from each other which would explain over- or underestimations of the actual composition, when just looking at small sections. Further analyses showed that NSPF contains a slightly higher amount of starch than SPF, resulting from remaining starch from the first centrifugation step, which sedimented during the second step due to the longer time and

Table 3.2 Compositional analysis of pea flour and the protein and starch enriched fractions obtained through dry fractionation and mild wet fractionation. The nitrogen conversion factor used was Nx5.52 (Nx6.25 is provided in brackets for comparison) and the values are given in g/100g dry matter.

| Component | Before fractionation | Dry fractionation | | MWF | | |
|---|---|---|---|---|---|---|
| | Flour | Starch fraction | Protein fraction | Starch fraction | Protein fraction 1 (SPF) | Protein fraction 2 (NSPF) |
| Protein | 18.5 ± 0.6 | 13.2 ± 0.7 | 37.0 ± 3.6 | 4.6 ± 0.4 | 51.5 ± 1.4 | 54.0 ± 1.2 |
| | (23.4 ± 0.7) | (14.2 ± 0.8) | (41.9 ± 4.0) | (5.2 ± 0.5) | (58.3 ± 1.6) | (61.1 ± 1.3) |
| Starch | 44.7 ± 1.5 | 62.3 ± 0.0 | 11.4 ± 0.0 | 70.4 ± 1.1 | 1.8 ± 0.1 | 5.1 ± 1.4) |
| Other | 36.8 ± 2.1 | 24.5 ± 0.7 | 51.6 ± 3.6 | 25.0 ± 1.5 | 46.7 ± 1.5 | 40.9 ± 2.5 |

higher force.

The SEM images of the starch fraction (MWF) and the starch fraction (DF) both depict mainly elongated round particles of around 30 µm. Based on their compositional analysis, both fractions contain similar amounts of other components (Table 3.2), but the starch fraction (MWF) is more enriched in starch and more depleted of protein. The starch granules of the starch fraction (MWF) have a similarly clean surface compared to the granules in the starch fraction (DF), however thin lines or marks can be observed spun across the surface, see Figure 3.8 (A), white arrows. To get a better understanding of the origin of these marks an elemental map of a starch granule is depicted in Figure 3.8 (B). When investigating the SEM image, no distinct particles or protein bodies are attached to the starch granules anymore, but the marks or lines which are now visual on the surface are enriched in nitrogen, hence protein is present (Figure 3.8 B). In the SEM images of the SPF and NSPF also no protein bodies were observable, instead platelet structures typical for freeze drying were formed (Figure 3.7 B, C). Both the observation in the starch fraction (MWF) and the SPF and NSPF suggest that the protein bodies were partly of fully dissolved upon addition of water and formed new structures during freeze drying. For the starch fraction the solubilisation of the proteins most likely resulted in films around the granules upon freeze-drying, which explains the presence of nitrogen on the whole granule (Figure 3.8 B). Hence, with centrifugation dissolved proteins remain in the pellet with the interstitial water and form films around the granules upon drying. The findings show that the solubilization with water lead to the washing off of the smaller particles form the starch granules, resulting in a starch-enriched fraction of ~70 % and two protein enriched fractions of each ~50 % (Table 3.2). The solubilization of the protein in water and the fact that some water remains in the pellet in form of interstitial water, point out the potential of the fractionation method, as an increase in purity could be achieved by additional pellet washing steps. Further, protein is not the only component solubilizing in water, i.e. soluble dietary fiber and small sugars probably also solubilise. This

indicates that with water, soluble and insoluble components can be separated to a certain extent.

The comparison of fractions obtained through mild wet fractionation to those obtained through dry fractionation, highlights that the MWF fractions are all more enriched in either protein or starch. The protein content of the SPF and NSPF is around 10 % higher and the starch content in SPF and NSPF is 10 % and 6 % lower, respectively, compared to those in the protein fraction (DF). Similar results are found for the starch fractions, where the starch content of the starch fraction (MWF) is 8 % higher than the starch content of the starch fraction (DF). The protein content in the starch fraction (MWF) is about 8 % lower than the protein content in the starch fraction (DF). This indicates that MWF is more efficient when compared to DF, based on component separation. In both dry and mild wet fractionation, the smaller particles are disentangled from the granules. Hence the adhesion between the particles could be overcome using both methods. Therefore, the remaining explanation for the further enrichment of the fractions obtained through mild wet fractionation, is the addition of water and hence the solubilisation of some components in the flour. It is assumed that in MWF the insufficiently milled flour fragments could dissolve in the water, which lead to more disentangled starch granules and protein bodies that could be fractionated into the respective fractions.

The MWF process offers potential to extract more protein from the interstitial water in the starch fraction, applying washing steps. However, the complete extraction is limited by the simple techniques of using only water and centrifugal forces. Additionally, to increase the purity in the respective fractions even further, a removal of other components is necessary. Such a removal, is limited by the solubility properties of the components, i.e. the separation of soluble dietary fiber and soluble protein might require other methods or additional solvents. These other methods or solvents would, in turn, interfere with the mildness of the conditions. Therefore, both the trade-off between mild fractionation and protein enrichment, as well as, yield reduction and protein enrichment

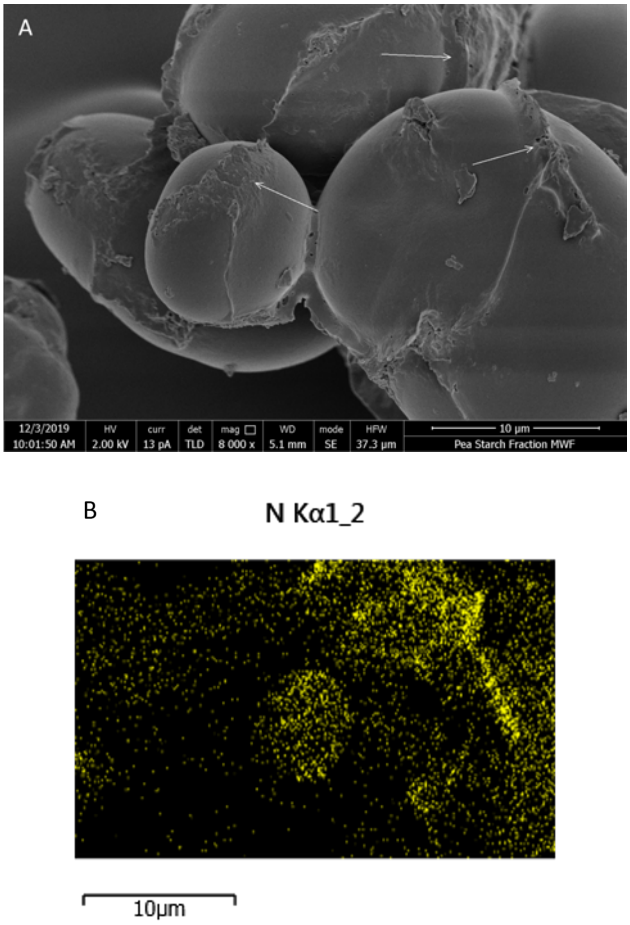


Figure 3.8 Scanning electron microscopy (SEM) (A) and elemental map (EDS-SEM) (B) of starch granules from the starch fraction (MWF). (B) depicting the abundance of nitrogen.

would need to be assessed together with a method on how to further enrich the respective fraction. Finally, the observation of the equally high protein purity of the NSPF compared to the SPF offers further potential to investigate the route with emphasis on the properties of NSPF, to make full use of all proteins obtained. The presented approach could be a suitable method to also investigate the structure break-up and fractionation potential of other starch rich legumes and cereals. The application of the fractions obtained through DF and MWF is next to their composition also dependent on their functional properties. MWF fractions would be more relevant in food products, where solubility characteristics and a higher purity is required, i.e. the SPF in milk-like systems, high protein drinks, etc. The functional properties of the NSPF still have to be determined in future studies, especially as it can be expected that due to their difference in solubility, the SPF and NSPF also differ in their functional properties. Both the dry and mild wet fractionated starch fraction show good gelling behavior and could therefore serve as ingredients to enforce or stabilize gels. The other components present in the fractions were shown to rather improve the functional properties of the fractions (Geerts, Strijbos, van der Padt, & van der Goot, 2017; Pelgrom, Boom, & Schutyser, 2014). A tool to predict the functional properties of the fractions based on their composition could help to close this gap. A key element of such a tool would be the inclusion of potential interactions between the components.

## 3.4 Conclusions

This study revealed that both dry and wet fractionation can be used to enrich and purify yellow peas, but adhesion between small and big particles occurring after structure break-up hinders full separation of yellow peas into their pure components. Enhanced separation in case of wet fractionation was explained by the fact that water addition solubilized fragments that were not fully disentangled and would by default in dry fractionation reach the coarse fraction.

Thus, water addition provided an additional driving force that resulted in further disentanglement of fragments and consequently better separation. The results presented above show that a relation between the structure and purity of the fractions can be established and used to judge on the potential of the fractionation method.

# Chapter 4

## A water-only process to fractionate yellow peas into its constituents

Anna Cäcilie Möller, Junni Li, Atze Jan van der Goot, Albert van der Padt

Published in Innovative Food Science and Emerging Technologies, 75, (2022) 102894

## Abstract

To meet the consumer demand for minimally processed foods and clean labels, the potential of processes where chemicals are omitted and only water is used needs to be explored. Mild wet fractionation of yellow pea, a water-only process, is investigated on maximum separation and efficient water use. By only using water, starch and protein from pea could be successfully separated, resulting in fractions high in yield and purity. Multiple washing steps of both the starch and the non-soluble protein fraction were performed to enhance separation. As a result of starch- and non-soluble protein pellet washing, the starch fraction was further depleted in protein and the protein solubility in the non-soluble protein fraction decreased. Ultrafiltration of the soluble protein fraction served to concentrate and the extracted water has potential to be reused in the process. Small solutes were concurrently extracted, which resulted in a higher protein purity in the soluble protein concentrate of 75%. The presented method has potential for upscale use in industry to produce protein fractions comparable to protein isolates obtained through conventional fractionation.

## 4.1 Introduction

Mild fractionation of crops to produce ingredients aims towards the omittance of chemicals and the reduction of water and energy use in the food production chain. For yellow pea, different mild fractionation routes have been investigated and compared to conventional wet fractionation techniques in regard of their resource use efficiency (Geerts, van Veghel, Zisopoulos, van der Padt, & van der Goot, 2018). From both dry (Pelgrom, Vissers, Boom, & Schutyser, 2013) and mild wet fractionation (Geerts, Mienis, Nikiforidis, van der Padt, & van der Goot, 2017) of yellow peas, concentrates enriched in protein or starch are obtained. The fractions obtained from dry fractionation yield lower purities (Pelgrom et al., 2013) than those from mild wet fractionation and are both less pure than isolates obtained from conventional fractionation (Geerts, Nikiforidis, van der Goot, & van der Padt, 2017). In terms of rational exergy efficiency, dry fractionation is most efficient, followed by mild wet fractionation and conventional wet fractionation.

The efficiencies are mostly influenced by material loss (Geerts et al., 2018). In a previous study (Möller, van der Padt, & van der Goot, 2021), the potential of mild fractionation processes was studied in more detail through comparing mild wet fractionation and dry fractionation of yellow peas on their purity performance. The results indicated that higher purities in mild wet fractionation are owed to additional disentanglement of the flour particles upon dispersion in water. It was found that the soluble components in the pea flour fragments are solubilized indeed, which explained better separation. This led to the conclusion that water provides a promising additional driving force in mild fractionation.

It was further hypothesized that pellet washing in mild wet fractionation could lead to higher purities in the respective fractions (Möller et al., 2021). To further investigate the role of water in mild wet fractionation and to optimize the process in regard of yield and purity, we explore a more efficient use of water in this study. Therefore, the aim of this study is to develop mild wet fraction-

ation further into a method comparable to conventional fractionation regarding purity and yield by a more efficient employment of water and the omittance of chemicals.

## 4.2 Materials & Methods

Pre-dried yellow peas (*Pisum sativum L.*), were purchased from Alimex (Sint Kruis, The Netherlands).

### 4.2.1 Milling

The peas were pre-milled into grits using a pin mill (LV 15 M, Condux-Werk, Wolfgang bei Hanau, Germany) at room temperature.
The grits were subsequently milled into fine flour using a ZPS50 impact mill (Hosokawa-Alpine, Augsburg, Germany), with an impact mill speed of 8000 rpm, an air flow at 52 $m^3$/h, a classifier wheel speed of 4000 rpm and a feed rate of 2 rpm (method adopted from (Pelgrom, Boom, & Schutyser, 2014). A thermometer inside the mill was used to monitor temperature.

### 4.2.2 Mild wet fractionation

Mild wet fractionation (MWF) was performed following the method of (Geerts, Nikiforidis, van der Goot, & van der Padt, 2017) with minor modifications. The following water-flour dispersions were prepared: 10 g flour and 20, 50, 80, 90, 100, 110, 120, 150, 200 and 500 g Milli-Q water (resistivity 18.2 MΩ.cm, Merck Millipore, France), respectively.
The mixtures were stirred at room temperature for 1 h. Then, the dispersions were submitted to a first centrifugation step at 1500 g for 1 s. During this step the insoluble starch granules were separated into the pellet. The supernatant was submitted to a second centrifugation step at 10000 g for 30 min. The pellet of this second centrifugation step yielded the so-called non-soluble protein fraction (NSPF) and the supernatant yielded the soluble protein fraction (SPF). The

obtained fractions were freeze dried for further analysis using a Pilot freeze dryer (Christ Epsilon 2-6D, Osterode am Harz, Germany). Previous results from mild wet fractionation were performed with the water/flour ratios 10:1, 8:1 (Geerts, Nikiforidis, van der Goot, & van der Padt, 2017).

4.2.3 Compositional analysis

The dry matter content was determined using an infrared moisture analyzer (MA35, Sartorius, Germany) at 120 °C, until a constant weight was reached. The protein content of the fractions was determined using Dumas analysis (Nitrogen analyzer, FlashEA 1112 series, Thermo Scientific, Interscience, Breda, The Netherlands) using a protein conversion factor of 5.52 (Holt & Sosulski, 1979). The total starch content was determined using the Total Starch Amyloglucosidase/α-Amylase Assay Kit, AOAC Method 996.11 (Megazyme International Ireland Ltd., Bray, Ireland). The protein yield (*Y*) (%) based on the total protein present in the flour was calculated with equation 4.1.

$$Y = \frac{m_x \cdot x_{p,x}}{m_f \cdot x_{p,f}} \cdot 100\% \qquad 4.1$$

Here $m_x$ is the mass in (g) and $x_{p,x}$ the protein content in (g/g) of the obtained fraction, $m_f$ is the mass in (g) and $x_{p,f}$ the protein content in (g/g) of the initial flour used for the fractionation. The protein purity (*P*) (%) was calculated with equation 4.2, by dividing the protein mass in the fraction ($m_{p,x}$) by the total mass of the fraction ($m_x$):

$$P = \frac{m_{p,x}}{m_x} \cdot 100\% \qquad 4.2$$

4.2.4 Protein solubility

Different definitions of protein solubility are described in literature. The measure used in this study is based on the percent protein solubility. It is defined as

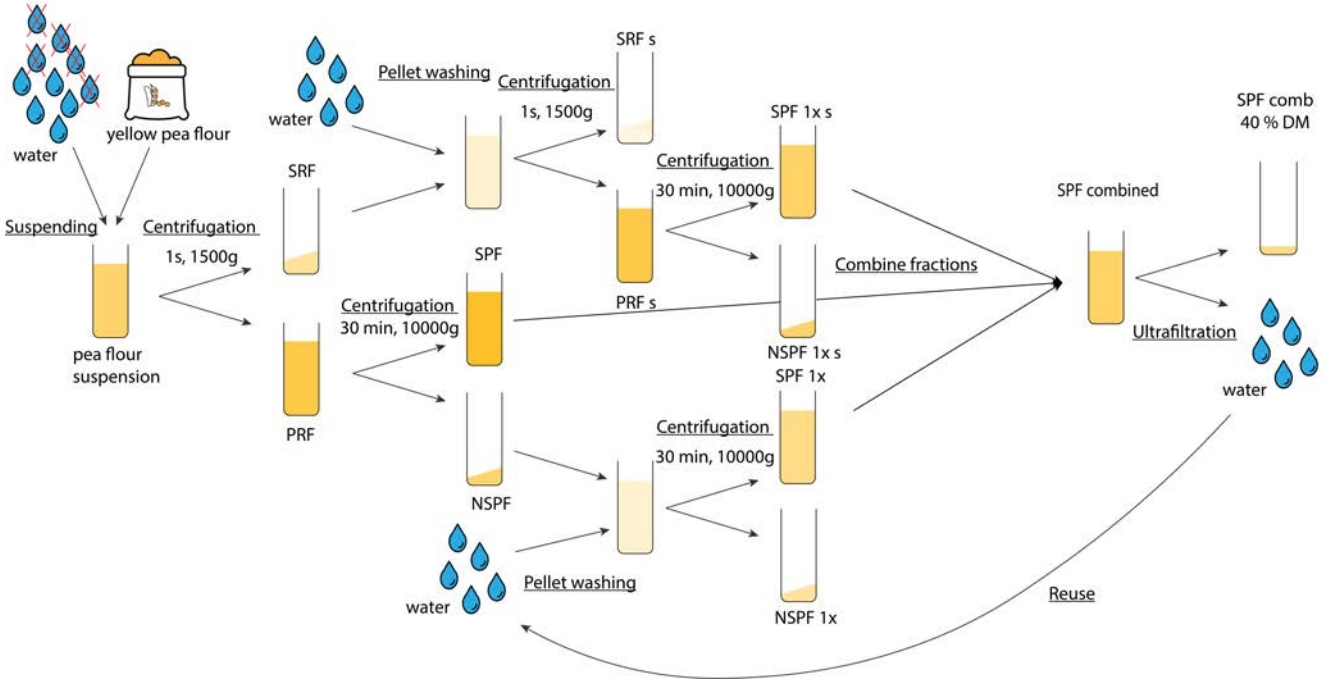


Figure 4.1 Graphic representation of the mild wet fractionation process (adopted from (Geerts, Nikiforidis, van der Goot, & van der Padt, 2017) with adaptations and additions) including one washing step of the starch rich fraction (SRF) an the non-soluble protein fraction (NSPF), and a subsequent ultrafiltration step of the soluble protein fraction (SPF). PRF is the protein rich fraction, 1× indicates obtained after one washing step, the small 's' indicates the fractions' origin from the starch fraction.

the percent amount of protein in the supernatant to total amount of protein in the sample before centrifugation (Vojdani, 1996). The determination for protein solubility was partly adopted from (Tanger, Engel, & Kulozik, 2020). Protein solutions of 0.1 % were made with both the SPF and NSPF fractions, before washing and after two washing steps. The solutions were rotated using a rotator (Stuart, UK) for 1 hour, after which the pH was determined. The samples were then centrifuged again at 6,000 g at 20 °C for 15 min. The supernatant was separated and used to determine the protein content using a PierceTM Bicinchoninic acid protein assay kit (ThermoFisher Scientific Inc., USA). Bovine serum albumin (BSA) with a known concentration was used to prepare a standard curve (ThermoFisher Scientific Inc., USA). The method was performed according to the standard protocol and the absorbance of the colorimetric reaction was measured 562 nm using a spectrophotometer (Beckman DU720 UV-Vis spectrophotometer (Beckman-Coulter Inc., USA). The protein solubility ($S$) (%) in the fractions was determined by dividing the protein content determined with BCA ($x_{p,BCA}$) (g/g) by the initial protein content in the solution ($x_s$) (g/g) using equation 4.3:

$$S = \frac{x_{p,BCA}}{x_s} \cdot 100\% \qquad 4.3$$

4.2.5 Pellet washing

Water and flour were mixed in a ratio of 5:1 and MWF was performed, according to the method of (Geerts et al., 2017). The pellets were re-dispersed in water to a ratio of 5:1 water to pellet and stirred at room temperature for 1 hour. After a second centrifugation was applied, 1500 g for 1 s at 20 °C for the starch pellet and 10,000 g for 30 min at 20 °C for the NSPF pellet. The pellets were washed twice in triplicates, respectively, (Figure 4.1). The obtained SPF and NSPF fractions were combined, their protein yields were summed, and their protein purities were averaged over the combined protein fractions and corrected for

their proportion. The combined protein yield (%) of the protein rich fractions ($Y_{cm}$), the normalized protein yield ($Y_{Norm}$) (%), which is the relation between the protein yield in one fraction and the combined protein yield of the protein rich fractions, and the averaged protein purity ($P_{av}$) (%) of the washed protein rich fractions were calculated with equations 4.4 - 4.6:

$$Y_{cm} = Y_{p,SPF} + Y_{p,NSPF} \tag{4.4}$$

$$Y_{Norm} = \frac{Y_{p,x}}{Y_{cm}} \cdot 100\% \tag{4.5}$$

$$P_{av} = \frac{\sum m_{p,x}}{\sum m_x} \cdot 100\% \tag{4.6}$$

Here $Y_{p,SPF}$ and $Y_{p,NSPF}$ are the protein yields (%) in the soluble and non-soluble protein fraction, respectively and $Y_{p,x}$ is either of them according to equation 4.1. $m_{p,x}$ is the protein mass (g) in, and $m_x$ the total mass (g) of the respective fraction.

### 4.2.6 Ultrafiltration

Approximately 200 mL of the soluble protein fraction was subjected to batch ultrafiltration using an Amicon® stirred cell, 400 mL (Millipore Merck KGaA, Darmstadt, Germany). The smallest protein present in pea is PA2, a dimer of 8 kDa size (Croy et al., 1984; Higgins et al., 1986). Therefore, a membrane pore size of 3 kDa was chosen to have a sufficiently small cut off size for the ultrafiltration process. The ultrafiltration was performed in single step and repeated in multiple steps with a mass reduction factor (*MRF*) of 1.7 per step. After each step a sample of the permeate and retentate was analysed for its dry matter and protein content. The mass reduction factor for this batch system is defined by equation 4.7:

$$MRF = \frac{m_{fd}}{m_{ret}} \tag{4.7}$$

Where $m_{fd}$ is the initial feed mass and $m_{ret}$ is the obtained retentate mass both in (g).

4.2.7 Membrane characterization and modelling

For designing and predicting a continuous ultrafiltration process the retention coefficient ($R$) was calculated from the permeate and retentate concentrations obtained with the batch system ultrafiltration. Equation (8) defines the retention:

$$R = 1 - \frac{x_{per}}{x_{ret}} \tag{4.8}$$

where $x_{per}$ and $x_{ret}$ are the measured permeate and retentate mass fractions in (g/g), respectively. The retention coefficients for both the protein and non-protein stream were determined with the batch experiments described in Section 4.2.6.

The measured retention coefficient and mass reduction factor from the batch system were used to calculate the yield and purity in a continuous membrane system of 10 stages, equation 4.9. Firstly, the component mass fraction $x_{ret,c}$ in the retentate can be calculated with the given retention coefficient and mass reduction factor:

$$x_{ret,c} = \frac{MRF \cdot x_{fd,c}}{1 + (MRF - 1) \cdot (1 - R)} \tag{4.9}$$

The component mass fraction in the permeate can then be calculated using equation 4.8.

With $x_{ret,c}$ and $x_{per,c}$ the permeate $\Phi_{per}$ and retentate $\Phi_{per}$ mass flows both in (g/s) can be calculated. For each stage the equations 4.10 and 4.11 hold:

$$\phi_{fd} \cdot x_{fd,c} = \phi_{ret} \cdot x_{ret,c} + \phi_{per} \cdot x_{per,c} \quad 4.10$$

$$\phi_{fd} + \phi_{d} = \phi_{ret} + \phi_{per} \quad 4.11$$

Here $\Phi_{fd}$ is the mass flow (g/s) and $x_{fd,c}$ the component mass fraction (g/g) of the feed stream. The equations apply for both the protein and the non-protein components in the streams. Equation 4.11 considers the addition of diawater, which is added to dilute the feed stream, avoiding polarization concentration at the membrane surface. Here $\Phi_{d}$ is the diawater mass flow (g/s).
The protein yield and purity of the streams of each stage were then calculated using equations 4.1 and 4.2; for the yield, the mass and protein content of the fraction are divided by the mass and protein content of the initial feed stream. For calculations of a batch system, $\Phi_{fd}$ should be replaced by the initial mass $m_{fd}$ and $\Phi_{ret}$ and $\Phi_{per}$ by the retentate mass $m_{ret}$ and the permeate mass $m_{per}$, respectively.

### 4.2.8 Permeate characterization

High Performance Size Exclusion Chromatography (HPSEC) was carried out in an UltiMate 3000 chromatographer (ThermoFisher Scientific Inc., USA) through a dual column system with TSK gel columns G3000SWXL and G2000SWXL for proteins and peptides. An aqueous solution of 30% acetonitrile (Actu All Chemicals, The Netherlands) and 0.1 % trifluoroacetic acid was used as eluent. Signals were measured with UV detector set at 214 nm. Data analysis was performed in Chromeleon 7.2 CDS software (ThermoFisher Scientific Inc., USA). The processing step was adjusted to integrate peaks between molecular weight ranges. A calibration curve of molecular weight on a logarithmic scale against elution time was plotted for thyroglobulin (670 kDa),γ-globulin (158 kDa), ovalbumin (44.3 kDa), α-lactalbumin (14 kDa), aprotinin (6.51 kDa), bacitracin (1.42 kDa) and phenylalanine (165 Da).

## 4.3 Results & Discussion

The efficiency of mild wet fractionation was investigated in view of the obtained yields and purities in the respective fractions. The mild wet fractionation process was adopted from Geerts et al. (2017) with modifications in the employment of water. The method as previously reported included a hydration step of 1 to about 12 h. A two-step centrifugation was used to, separate the suspension into a starch rich, a soluble protein rich and a non-soluble protein rich fraction. In the following sections several process adaptations will be discussed to increase the water use efficiency.

### 4.3.1 Optimizing the water use in single step mild wet fractionation

To optimize the water-use for MWF, the effect of water content in the initial hydration step at the minimum constant hydration time of 1 h was studied. Mild wet fractionation was performed using varying water/flour ratios. The process yielded a constant purity of around 52 % protein content in the soluble protein fraction (SPF) for all ratios. The purity of the non-soluble protein fraction (NSPF) was constant at around 53 % protein content for all ratios except for the lowest at water/flour ratio 2:1 (Figure 4.2 A).

Differences in outcomes due to a variation in water/flour ratios are more prominent when looking at the protein yield. The combined protein yield depicts the protein yield in both the SPF and NSPF based on the protein initially present in yellow pea flour (equation 4.3, Appendix Figure A 4.1). The increase in combined protein yield indicates that with an increase in water more protein is extracted from the starch fraction. Moreover, the constant purity in both fractions (52 and 53 %, respectively) suggests that other components solubilized with protein in a similar manner. A constant protein yield at higher water/flour ratios indicates a critical water-flour ratio, above which no further extraction was achieved. The maximum combined protein yield of SPF and NSPF was determined around 86 % at ratio 9:1. Consequently, at least 14 % of the initial protein remained in the starch fraction. Further, the cumulative yield of protein

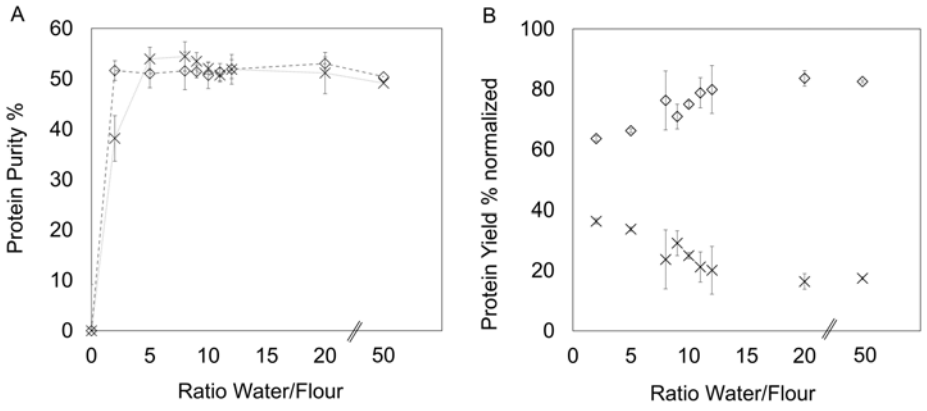


Figure 4.2 The protein purity (%) (A) of the SPF ◊ and NSPF X and normalized protein yield % (B) of SPF ◊ and NSPF X (equation 4.3) are depicted at varying water/flour ratios. The lines are meant to guide the eye.

Table 4.1 Protein purity and protein yield of the three fractions obtained through mild wet fractionation of yellow pea flour. The purities of 1 wash and 2 washes are the averaged protein purities (aver.) as calculated in equation 4.4, the protein yields of 1 wash and 2 wash are added up from the respective fractions to represent the combined streams (comb.).

| Fraction | no wash | | 1 wash | | 2 washes | |
|---|---|---|---|---|---|---|
| | Yield (%) | Purity (%) | Yield (%) comb. | Purity (%) aver. | Yield (%) comb. | Purity (%) aver. |
| SPF | 44.5 | 47.0 | 60.5 | 47.5 | 64.7 | 47.6 |
| NSPF | 33.2 | 66.7 | 34.6 | 68.5 | 31.9 | 66.1 |
| Starch | 22.3 | 8.7 | 4.9 | 3.7 | 3.4 | 2.1 |

was approximately constant above a ratio of 2.
Next, protein yields of SPF and NSPF were normalized to the combined protein yield of the protein rich fractions, for a clearer representation of the protein distribution between both fractions, Figure 4.2 B. Protein yield in the SPF increased, while protein yield of NSPF decreased with increasing water/flour ratios. However, at a ratio of 20 and above the protein yields of both fractions remain constant at 83 % and 17 %, respectively. Hence with the employment of more water, no more soluble protein is extracted from the NSPF. This indicates that above a ratio of 20, protein solubility is independent of water ratio, which might imply that all soluble protein is in the SPF and all non-soluble protein in the NSPF. From the results obtained it was concluded that the previously reported water/flour ratios of 8:1 and 10:1 are not needed in regard of water use efficiency. Instead a ratio of 5:1 can be chosen to yield the same purities and the same combined yield, while decreasing the amount of water employed in the fractionation step. To recover the protein remaining in the starch fraction and to investigate the protein distribution between SPF and NSPF, pellet washing steps were introduced to investigate extra protein extraction.

### 4.3.2 Multiple pellet washing steps for further purification in mild wet fractionation

Previously, a hypothesis was introduced that additional pellet washing steps could lead to further enrichment in mild wet fractionation (Möller et al., 2021). During centrifugation interstitial water remains in the pellets, in which proteins and other soluble components are solubilized. This hypothesis could explain the presence of residual protein in the starch fraction. Therefore, multiple pellet washing steps were added to the mild wet fractionation process and the effect on yield and purity in the respective fractions was investigated. Multiple SPF and NSPF streams were obtained after two-step washing of both the starch fraction and the NSPF, which were combined into one SPF and one NSPF streams. Figure 4.3 depicts a representation of the dry matter mass flow

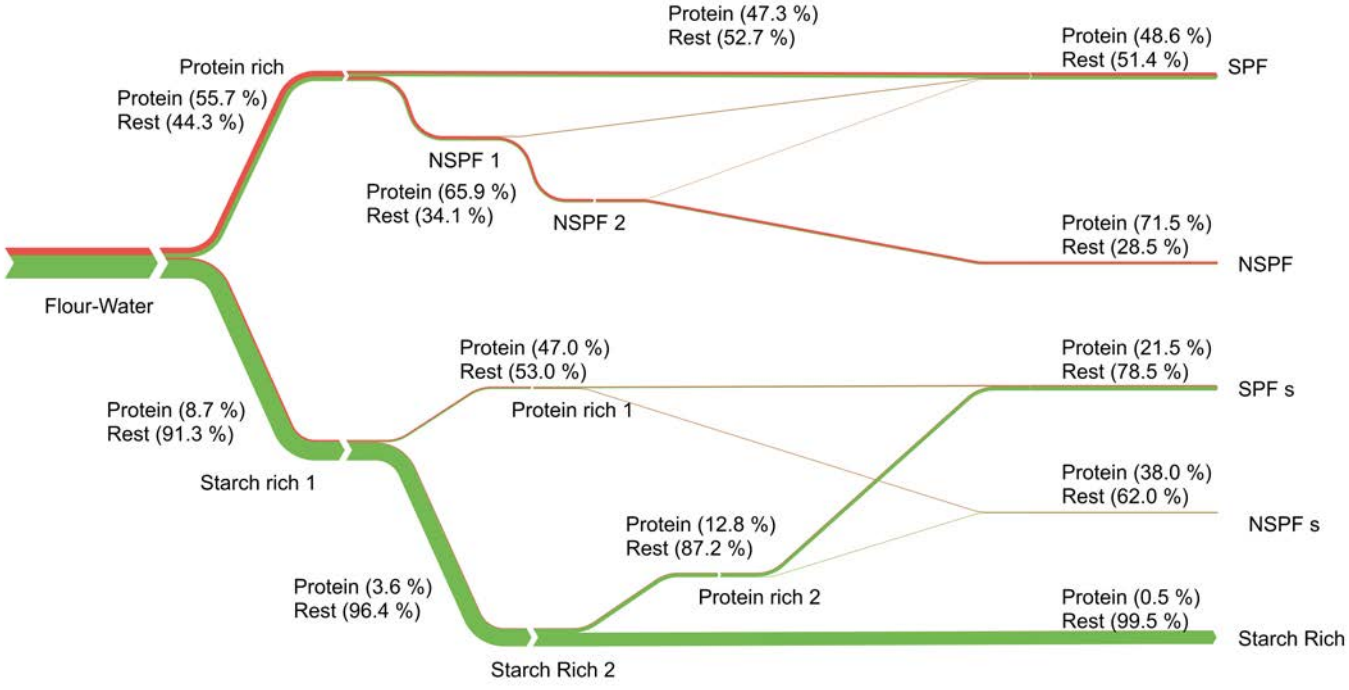


Figure 4.3 Mass representation of the dry matter streams during mild wet fractionation and combination of the according fractions into a SPF-, NSPF- and a starch fraction stream. The red stream represents the protein content in dry matter, the green stream represents the rest content in dry matter. Percentages of the main streams indicate purities of the streams and were added to depict the effect of pellet washing.

during mild wet fractionation including two pellet washing steps for both the starch fraction and the NSPF. After the first separation step, the main part of the protein is collected in the protein rich fraction, and the main part of the rest in the starch rich fraction. The second centrifugation step separates the protein rich stream into the SPF and NSPF. With each starch pellet washing step, more protein was extracted from the starch fraction into the soluble and non-soluble protein fraction, enriching both streams. NSPF pellet washing resulted in an extraction of protein from the NSPF into a secondary and tertiary SPF. All SPF and NSPF streams obtained from pellet washing can be combined respectively and would result in the depicted streams, Figure 4.3. Next to protein also rest is extracted with each washing step. The extraction of the rest explains why the protein purity only slightly increases in the SPF and NSPF, while the protein yield is mainly increasing. It is assumed that the non-protein components extracted from the starch fraction through pellet washing do not contain starch, due to its insolubility at room temperature.

The protein yields and purities of the fractions were determined during fractionation and after each pellet washing step. The results are listed in Table 4.1. The purities and yields after one and two washes are from the cumulative fractions. In the SPF, the protein yield increased with each washing step. While in the NSPF, the protein yield increased with the first washing step and decreased with the second washing step. In the starch fraction, protein purity and yield decreased with each washing step. Hence, more protein could indeed be extracted from the starch fraction and was distributed over the protein fractions. The average purity of SPF slightly increases with each washing step, while the averaged protein purity of the combined NSPF increases with the first and decreases with the second washing step. For the NSPFs, the purity of the primary pellets increased stepwise; however, the protein purity of the secondary NSPF obtained from starch pellet washing has a lower protein purity due to a higher rest content, decreasing the cumulative purity after two washing steps.

### 4.3.3 Protein fractionation into the soluble and non-soluble protein fractions and the effect of pellet washing

The separation of the SPF and NSPF indicates that mild wet fractionation, allows additional fractionation of the proteins based on their solubility characteristics, on top of the separation of protein and starch. This hypothesis was supported by the constant yield in both SPF and NSPF obtained at water/flour ratios above 20 (Appendix Figure A 4.1), indicating that around 17 % of the protein is indeed insoluble. It was further hypothesized that pellet washing of the NSPF would extract soluble protein from the NSPF, which otherwise remained in the fraction with the interstitial water. To further investigate the solubility characteristics of SPF and NSPF, the fractions were diluted to 0.1 % protein solutions and the solubility of the proteins in the fractions was determined. The solubility characteristics of SPF and NSPF obtained after one and two pellet washes was accordingly determined. Due to the dependency of protein solubility on pH (Zayas, 1997), the pH was measured for all protein solutions. The pH was between pH 6.5–7 for all samples. Figure 4.4 depicts the relative amounts of soluble and non-soluble protein to total protein in the respective SPF and NSPF streams, after the first centrifugation step, and the two pellet washing steps. Neither the SPF nor the NSPF consists of pure soluble or non-soluble protein, respectively. With pellet washing, mainly soluble protein is extracted from the NSPF. However, with each washing step, a smaller proportion of non-soluble protein is extracted as well. Yet, using mild wet fractionation the majority of soluble and non-soluble protein was successfully separated. Solubility is one of the main functionalities often analysed for plant-proteins (Lam, Can Karaca, Tyler, & Nickerson, 2018). Therefore, including fractionation into soluble and non-soluble protein, next to component fractionation, highlights the potential of mild wet fractionation for industrial application.

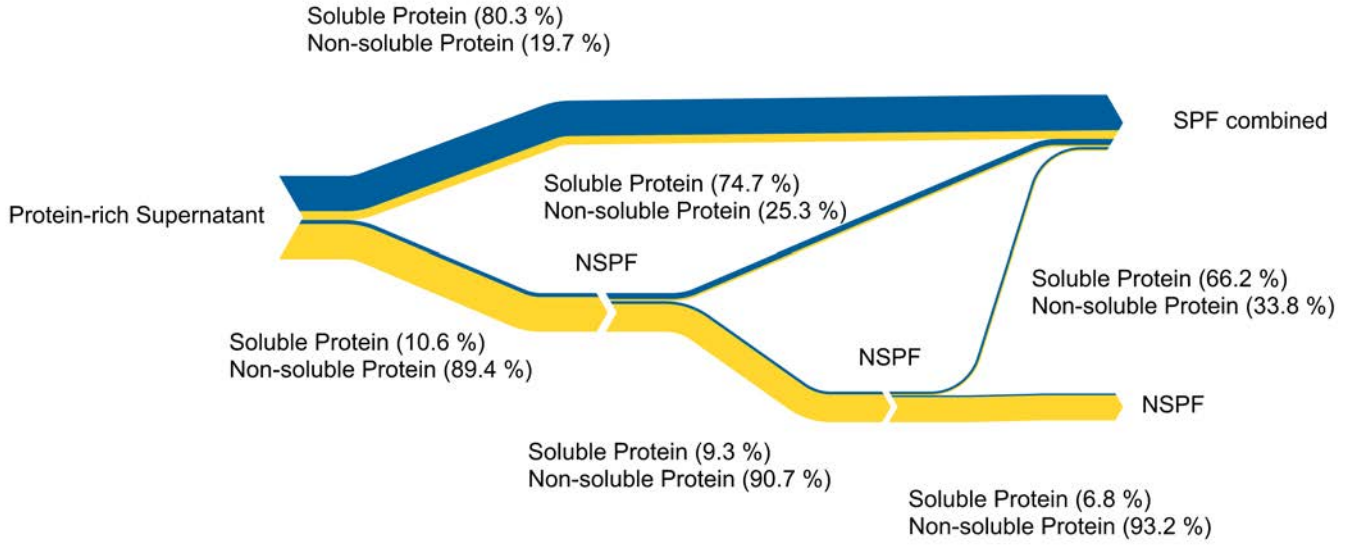


Figure 4.4 Graphical representation of the proportion of soluble and non-soluble protein in the protein rich stream after the first centrifugation step. The blue stream represents the relative amount of soluble protein and the yellow stream the non-soluble protein. Two pellet washing steps were performed on the NSPF stream and the obtained supernatants were combined to the SPF stream.

### 4.3.4 Concentration of SPF with ultrafiltration

With the addition of the pellet washing steps to the mild wet fractionation method, more water was introduced into the process. The NSPF and the starch fraction before and after pellet washing have relatively constant dry matters of around 20 and 30 %, respectively. The additional water introduced during pellet washing therefore ended up in the SPF mainly, decreasing the cumulative dry matter content of that fraction with every washing step. Ultrafiltration is commonly used in dairy industry for whey protein separation and concentration. Further, ultrafiltration was previously used to produce pea protein isolates, with enhanced functionality, higher protein yields (Boye, Aksay, et al., 2010) and lower amounts of antinutritional factors (Mondor, Tuyishime, & Drolet, 2012). In these studies, ultrafiltration was used subsequent to alkaline extraction, to substitute isoelectric precipitation. Here, ultrafiltration of SPF was performed to extract the excess water from the fraction. Ultrafiltration increased the dry matter content of SPF from approximately 4 % to 38 %. Moreover, the protein purity increased to 75 %. However, the permeate after ultrafiltration to such high dry matter contents had a dry matter content of around 2 % of which 19 % was protein. Additionally, filtration to such high dry matter contents of around 40 % leads to a gel layer formation on the ultrafiltration membrane and the process becomes ineffective. Therefore, the ultrafiltration process was repeated in three steps, using a mass reduction factor of approximately 1.7. The protein retention coefficient was for all samples around 0.95–0.97.

During step wise ultrafiltration, it was observed that the purity of SPF already increased to 63 % when the dry matter content was only increased to around 7 %, (Appendix Table A 4.1). To check whether the retention could be considered constant, the three-step ultrafiltration was additionally calculated using the equations introduced in section 2.6 and 2.7. The same mass reduction factor was chosen for the continuous membrane system of three stages. A constant protein retention coefficient was chosen at 0.97, which resulted in a non-protein retention coefficient of 0.48 in order to achieve similar filtration results as

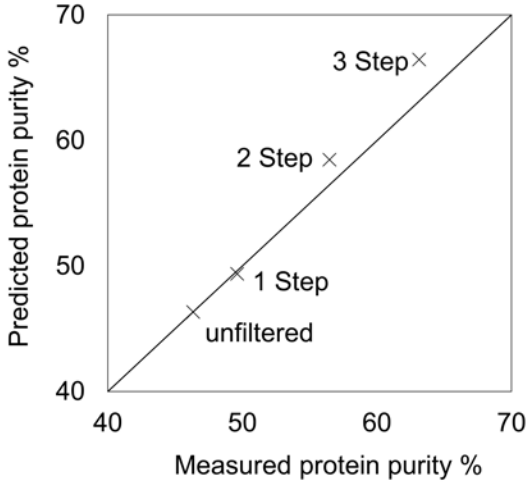


Figure 4.5 Prediction of protein purity in retentate over measured protein purity in retentate after 3 step ultrafiltration with an average concentration factor of 1.7, and a protein retention coefficient of 0.97. The line is added to guide the eye.

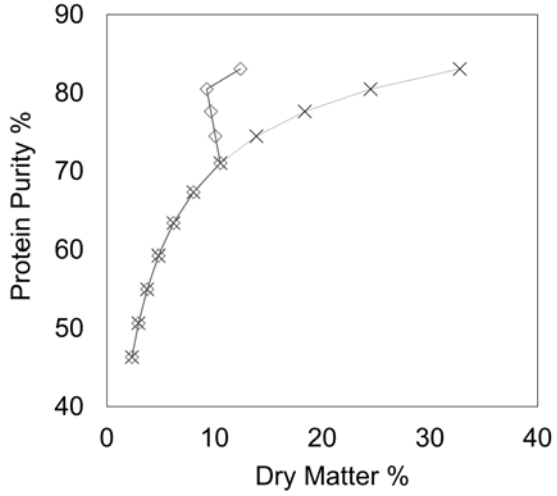


Figure 4.6 Predicted protein purity in retentate over predicted dry matter content in retentate after 10 step ultrafiltration with a concentration factor of 1.4, and a retention coefficient of 0.97 for protein. (x) indicates ultrafiltration without addition of diawater, (◊) indicate the addition of diawater in step, 7, 8 and 9 to avoid concentration polarization.

measured with the batch system. With an initial dry matter content in SPF of 2.3 % and a protein content of 46 % per dm the dry matter and protein purity increased with each step (Appendix Table A 4.2).
The predicted and measured protein purity are plotted in Figure 4.5. The protein purity in step 2 and 3 is slightly overpredicted using the ultrafiltration calculations; however, the prediction is quite close to the measured purities. To elucidate the potential of a continuous ultrafiltration system further, a calculation is added to predict the dry matter content and protein purity in a ten-stage ultrafiltration process.

4.3.5 Preliminary design of a ten-stage continuous ultrafiltration system
Therefore, the calculations were used to further extend and optimize the ultrafiltration prediction to a ten-step continuous ultrafiltration process (Figure 4.6). To obtain a dry matter content of 30 % with a retention coefficient of 0.97 for protein, the mass reduction factor was lowered to 1.4 in a ten-stage system. The employment of stepwise ultrafiltration could allow to increase the protein purity in the SPF to more than 80 % and a dry matter content of >30 %. It was however observed that at a dry matter content above 10 %, the purity gain reduced. In dairy industry, diawater is often added in ultrafiltration processes to obtain high protein purities and to reduce concentration polarization, protein gel layer formation, on the membrane surface. Such a combination can yield subsequently dried protein powders of about 85% protein purity (Henning, Baer, Hassan, & Dave, 2006). Therefore, the ultrafiltration was predicted a second time with an addition of diawater after a dry matter content of ≥10 % was reached. The addition of diawater had no influence on the protein purity, on dry matter bases, but lead to a constant dry matter content around 10 %.

4.3.6 Quantification of the permeate stream
The permeate samples were additionally subjected to size exclusion chromatography, to determine the approximate size of the proteins (Figure 4.7, Permeate

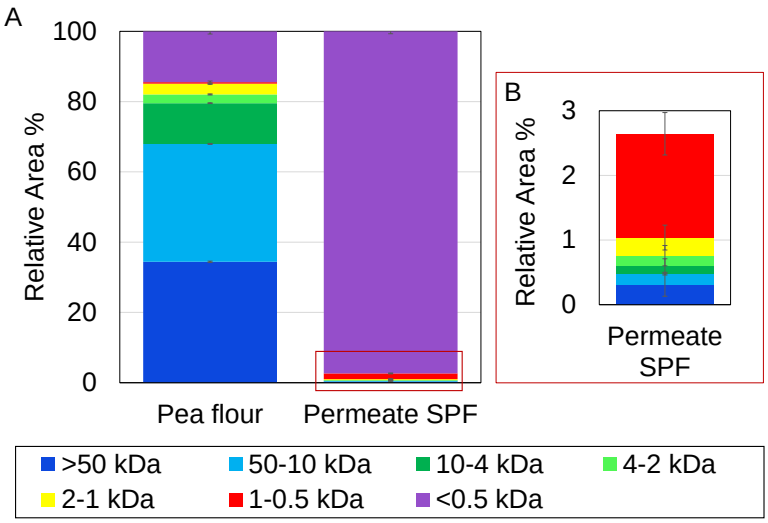


Figure 4.7 (A) Peptide profile integrated from size exclusion chromatograms of Pea flour, and SPF permeates obtained from step wise ultrafiltration. The pea flour profile was determined in triplicate. The SPF Permeate includes duplicate ultrafiltration runs determined in triplicates. The bars depict the relative amount of peptides/proteins in the respective size range. The error bars depict a confidence interval of 0.95. (B) Zoom in of the permeate SPF relative area profile for molecules > 0.5 kDa, red box.

SPF). More than 95 % of the peptides present in the UF permeate are smaller than 0.5 kDa. To understand the nature of the presence of peptides in the protein fraction, pea flour was diluted in water and size exclusion chromatography was performed right after solubilization (<10 min in solution) (Figure 4.7, Pea flour). Around 15 % of the proteins and peptides present in pea flour have a size of less than 1 kDa. The protein yield of the UF permeate, based on the initial protein present in pea flour, was around 14 %. Hence, the amount of small peptides present in the SPF approximates the amount of small peptides initially present in the pea flour. Indicating that the protein loss during ultrafiltration into the permeate is actually a loss of small peptides. Due to a difference in functional properties and taste of peptides and proteins such a separation could be desired. Furthermore, a separation could enable the analysis of the peptides in regard of their bioactivity and a coordinated employment of the peptides in foods depending on their various functional properties (Karami & Akbari-adergani, 2019).

### 4.3.7 Comparison to conventional wet fractionation

The adapted mild wet fractionation process offers potential to replace the conventional wet fractionation method. Omitting chemicals throughout the process allows to recover and reuse the water in the process. The addition of the ultrafiltration step of SPF to the fractionation process increases the protein purity to more than 75 % in the SPF (Figure 4.8). Hence, the process becomes more comparable to conventional wet fractionation (CWF), where protein purities of around 75 % (Nx5.52) are obtained (Roquette-Freres, 2021). The cumulative protein yield of the SPF and NSPF, subtracting the 14 % peptides lost during ultrafiltration, is approximately 83 %. CWF can yield up to approximately 76 % (Geerts et al., 2018) to 82 % (Lie-Piang, Braconi, Boom, & van der Padt, 2021) of the initial protein in the protein isolate (protein in pea flour 21.4 %). To obtain these high purities and yields in CWF alkaline extraction and isoelectric precipitation are used, by changing the pH of the solution, to first solubilize all

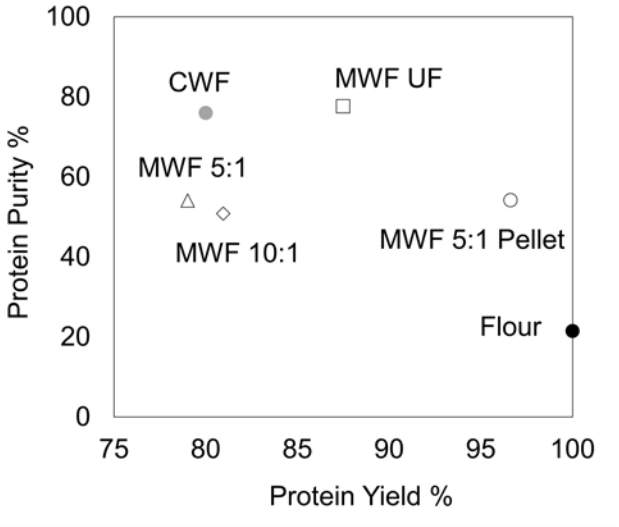


Figure 4.8 Yield-purity curve of fractionation methods discussed in this research. CWF, MWF 10:1 (mild wet fractionation as performed by (Geerts, Nikiforidis, et al., 2017), MWF 5:1 (mild wet fractionation at ratio 5:1), MWF 5:1 washed (mild wet fractionation with additional pellet washing steps), MWF 5:1 UF (mild wet fractionation at ratio 5:1 with pellet washing and ultrafiltration) and pea flour. The purities of SPF and NSPF were averaged per proportion, the yields were added up.

proteins and separate them from non-protein components and secondly precipitate proteins for further purification. However, the use of chemicals affects the structure and functionality of pea proteins. Moreover, alkaline extraction is responsible for adverse chemical reactions of the amino acid side chains (Lam et al., 2018). Isoelectric precipitation also influences the protein conformation and functionality (Boye, Aksay, et al., 2010). Hence, omitting the use of chemicals can not only yield comparable purities and yields but additionally limits the modification of the protein nativity.

With the method presented above, we therefore show possibilities to mildly fractionate proteins from yellow pea, while omitting chemicals. The protein concentrates and isolates can be obtained with different protein purities and yields, according to the process intensity. Besides, the method enables the separation of proteins into soluble and nonsoluble protein, potentially offering a wider functional spectrum of the ingredients. Mild wet fractionation introduces the possibility to adjust and alter the composition and functionality of the ingredients based on the application. Performing less, or more processing steps, the protein purity and separation can be controlled, which in turn has an influence on the resource use efficiency and functionality of the final ingredient.

For the fractionation process, including pellet washing step and ultrafiltration, without the addition of diawater, about 23 kg water are necessary to fractionate 1 kg of pea flour. Due to these large amounts of water, the recovery and reuse of water in the process becomes increasingly important. Moreover, as the use of chemicals was fully omitted in this processing technology, the reuse and recovery of water is possible and has no influence on the following fractionation processes. In Figure 4.9 the mild wet fractionation process including two pellet washing steps is depicted with subsequent steps to recover the water using ultrafiltration followed by a nanofiltration water purification step. Per kg of pea flour, around 20 kg of water can be recirculated with the proposed process. The recovered water could be reused in the fractionation process, which notably decreases the amount of fresh water necessary for fractionation. Figure 4.9

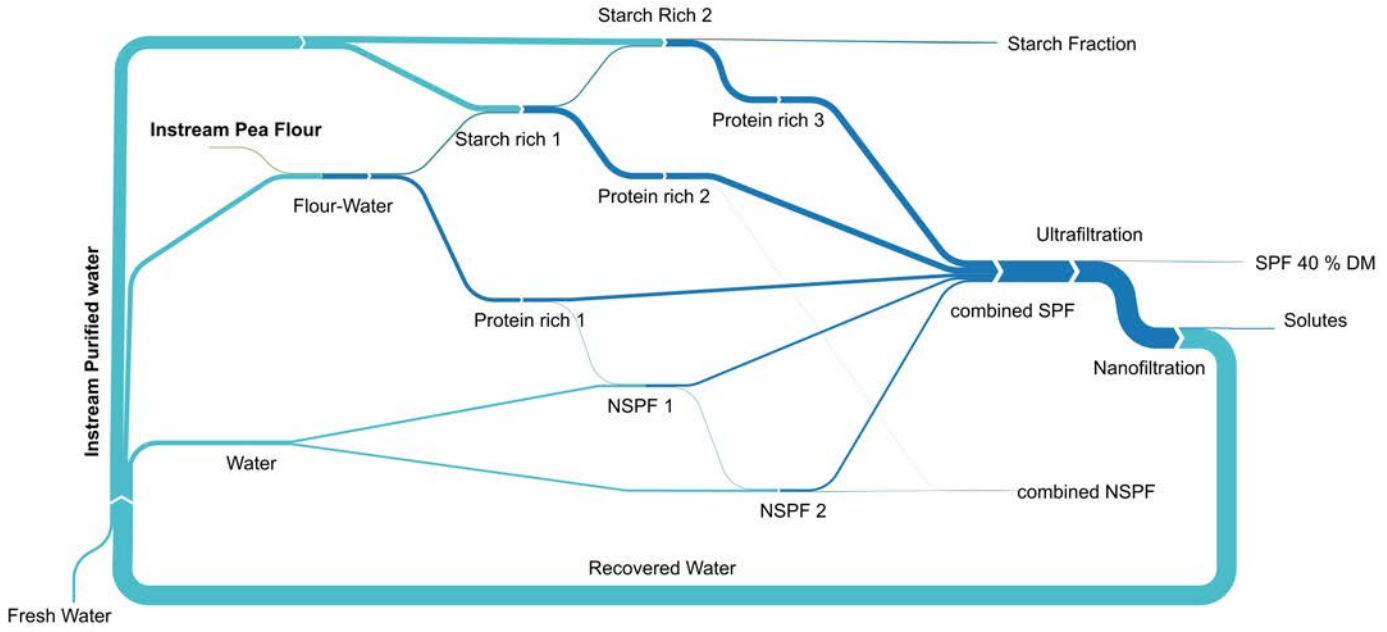


Figure 4.9 Graphic representation of mass flow during mild wet fractionation including pellet washings and the potential of recovery and reuse of water after ultrafiltration and water purification. Fresh water is light blue, dispersions are dark blue. The flow quantities are summarized in the Appendix Table A 4.3 as kg stream/ kg pea flour.

depicts the potential of upscaling the mild fractionation process showing a concept, how mild wet fractionation could be applied to produce protein and starch isolates without the use of chemicals. In the presented process the centrifugation and pellet washing steps could be replaced with two decanters to separate starch and protein.
This would on top decrease the water consumption in the initial process phase. Ultrafiltration of protein solutions is frequently applied in diary industry, e.g. for the production of protein concentrates from whey and for the pre-concentrations of milk, both processes of cheese manufacture (Berk, 2013). The calculated water usage for the presented pea fractionation upscale is around 100 kg water/ kg pea protein (i.e. see Figure 4.8 and Figure 4.9, 20 kg water/ 0.2 kg protein). To provide a reference, the diawater consumption for whey protein isolate (WPI) production from thick whey (35% DM) was calculated using the same methodology. A water usage of 62 kg water/ kg whey protein was estimated to produce WPI. The water consumption of both processes was evaluated to be around the same order of magnitude, as a proper diafiltration design will reduce the water usage of the pea fractionation process, which was demonstrated by (Gavazzi-April, Benoit, Doyen, Britten, & Pouliot, 2018; Lipnizki, Boelsmand, & Madsen, 2002). Moreover, so far the presented values are based on lab scale experiments. Therefore, this paper could form the basis to set-up pilot scale experiments to arrive at a conceptual design for industrial pea protein isolation using only water.

## 4.4 Conclusions

With the well-directed employment of water in mild wet fractionation we present a promising method for the extraction of high purity and yield protein and starch fractions. The protein purity in the SPF can be increased to around 75 % according to our experiments, and potentially even to around 85 % comparable to purities obtained in dairy industry, when using a combination of pellet washing with ultrafiltration.

Pellet washing of the starch fraction increased the cumulative yield in the protein fractions. While pellet washing of the NSPF led to a further separation of soluble and non-soluble protein in the respective fractions. Ultrafiltration of the SPF extracted small soluble non-protein components from the fractions, together with small peptides, resulting in increased protein purity in the SPF, despite the extraction of the peptides. The mild wet fractionation process offers the potential to produce similar fractions compared to conventional wet fractionation, with the advantage to omit chemicals, recirculate water and limit changes in techno-functional properties. Furthermore, the introduced process shows the potential to add or skip processing steps depending on the desired final ingredient composition and functionality. The presented research highlights that the extensive knowhow of whey protein isolation applied in plant protein purification could provide new routes to more effective plant ingredient production.

# Appendix

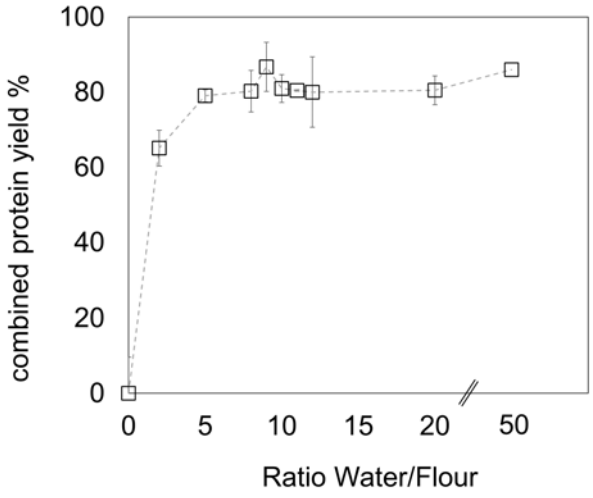


Figure A 4.1. The combined protein yield % (Equation (4.2) of the sum of SPF and NSPF are depicted at varying water/flour ratios. The line is meant to guide the eye.

Table A 4.1 Measured results of 3 step batch ultrafiltration. After each filtration a sample for the compositional analysis was taken, resulting in the mass difference in output and input retentate. Results are depicted in Figure 4.5.

| Filtration | | Sample | Total (g) | Total Dry Matter (g) | Total protein (g) | Dry Matter (g) | Protein/ DM % | Retention coefficient DM (g/g) | Retention coefficient Protein (g/g) | MRF |
|---|---|---|---|---|---|---|---|---|---|---|
| 1. | Feed | SPF | 200.41 | 4.66 | 2.16 | 2.33 | 46.33 | 0.91 | 0.98 | 1.27 |
| | Out | Retentate 1 | 157.52 | 4.26 | 2.11 | 2.70 | 49.61 | | | |
| | Out | Permeate 1 | 42.89 | 0.36 | 0.05 | 0.84 | 13.09 | | | |
| 2. | Feed | Retentate 1 | 132.87 | 3.59 | 1.78 | 2.70 | 49.61 | 0.81 | 0.93 | 1.96 |
| | Out | Retentate 2 | 68.06 | 2.92 | 1.65 | 4.29 | 56.47 | | | |
| | Out | Permeate 2 | 64.81 | 0.66 | 0.08 | 1.02 | 12.20 | | | |
| 3. | Feed | Retentate 2 | 50.17 | 2.12 | 1.20 | 4.29 | 56.74 | 0.86 | 0.96 | 1.87 |
| | Out | Retentate 3 | 26.80 | 1.82 | 1.15 | 6.80 | 63.13 | | | |
| | Out | Permeate 3 | 23.37 | 0.30 | 0.04 | 1.29 | 11.87 | | | |

Table A 4.2 Calculated 3 step ultrafiltration for designing a continuous ultrafiltration system with a constant protein retention coefficient of 0.97. Results are depicted in Figure 4.5.

| Filtration | | Sample | Total (g) | Total Dry Matter (g) | Total protein (g) | Dry Matter % | Protein/ DM % | Retention coefficient DM (g/g) | MRF |
|---|---|---|---|---|---|---|---|---|---|
| 1. | In | SPF | 200 | 4.66 | 2.16 | 2.33 | 46.33 | 0.75 | 1.27 |
| | Out | Retentate 1 | 157 | 4.33 | 2.14 | 2.75 | 49.37 | | |
| | Out | Permeate 1 | 43 | 0.33 | 0.02 | 0.77 | 6.09 | | |
| 2. | Feed | Retentate 1 | 157 | 4.33 | 2.14 | 2.75 | 49.37 | 0.75 | 1.96 |
| | Out | Retentate 2 | 81 | 3.54 | 2.07 | 4.40 | 58.47 | | |
| | Out | Permeate 2 | 77 | 0.79 | 0.07 | 1.03 | 8.55 | | |
| 3. | Feed | Retentate 2 | 81 | 3.54 | 2.07 | 4.40 | 58.47 | 0.75 | 1.87 |
| | Out | Retentate 3 | 43 | 3.02 | 2.01 | 7.03 | 66.46 | | |
| | Out | Permeate 3 | 38 | 0.52 | 0.06 | 1.38 | 11.63 | | |

Table A 4.3 Mass flows during mild wet fractionation from Figure 4.9. Presented as kg stream/ kg pea flour to be fractionated.

| Stream name | Stream quantity (kg/kg pea flour) |
|---|---|
| Flour-water | 6.00 |
| Starch rich 1 | 1.32 |
| Protein rich 1 | 4.68 |
| Water to Starch rich 1 | 6.25 |
| Starch rich 2 | 1.06 |
| Protein rich 2 | 6.51 |
| Water to Starch rich 2 | 6.25 |
| Water to NSPF 1 | 2.50 |
| NSPF 1 | 0.46 |
| Water to NSPF 2 | 2.50 |
| NSPF 2 | 0.38 |
| Starch fraction | 0.97 |
| Combined SPF | 22.07 |
| Combined NSPF | 0.46 |
| SPF 40 wt.% | 0.62 |
| Solutes | 1.20 |
| Recovered water | 20.25 |
| Fresh water | 2.25 |

# Chapter 5

## Influence of the fractionation method on the protein composition and functional properties

Anna Cäcilie Möller, Albert van der Padt, Atze Jan van der Goot

Published in Innovative Food Science and Emerging Technologies, 81, (2022) 103144

## Abstract

Mild wet fractionation can separate pea proteins into a soluble and a non-soluble fraction. Soluble proteins and solutes are extracted into the soluble protein fraction, insoluble proteins are collected in the non-soluble protein fraction. The protein composition in the respective fractions was investigated by further fractionating the protein fractions with isoelectric precipitation. The molecular mass of the proteins in the fractions was determined by SDS-PAGE and size exclusion chromatography. The protein fractions' solubility was determined in excess water, and the gelation properties were investigated at the same protein concentration. With mild wet fractionation, compared to conventional wet fractionation, both globulins and albumins are extracted. The protein fractions were mixtures of both proteins, although the non-soluble protein fraction contained mainly globulins. Solubility and gelation properties varied with protein type, composition and protein state; isoelectric precipitation decreased the gelation capacity of the protein fractions.

## 5.1 Introduction

Pea proteins are a popular plant protein in the developing market of plant protein products (Boukid, Rosell, & Castellari, 2021). Accordingly, pea ingredients are investigated for food application, their nutritional and functional properties (Saldanha do Carmo et al., 2019; Zhao, Shen, Wu, Zhang, & Xu, 2020). The extraction method influences plant proteins' functional and nutritional properties (Boukid et al., 2021), which consequently explains the interest in novel fractionation methods. Different studies describe the functional properties of pea albumins, globulins, and mixes thereof. These functional properties varied depending on the protein composition (Kornet, Penris, et al., 2021; Kornet, Yang, Venema, van der Linden, & Sagis, 2022; Yang et al., 2022).

Protein in pea can be divided into several different classes. The proteins present in legumes are commonly classified based on their solubility (Osborne, 1909). Such a classification results from the perception that solubility is one of the mostly analysed and thus important functional properties of proteins (Lam et al., 2018a). In pea, the primary proteins are classified as albumins (15-25 %) and globulins (65-80 %) (Boye, Zare, & Pletch, 2010). The major globulins in yellow pea are legumin (360-410 kDa), built of six double-stranded subunits (60 kDa) (Croy, Gatehouse, Evans, & Boulter, 1980a); convicilin (210-290 kDa), a tetrameric protein with subunits of 46 and 67 kDa (Croy, Gatehouse, Evans, & Boulter, 1980b; UniProt Consortium, 2019); and vicilin (150-200 kDa), a trimeric protein with subunits of 50 kDa and 30-35 kDa (Croy, Gatehouse, Evans, et al., 1980b). The major albumins are PA2, in its dimeric (48-52 kDa) or monomeric (22-26 kDa) form, lipoxygenase (94 kDa), PA1 dimer (10 kDa) and lectins (18 kDa) (Croy, Hoque, Gatehouse, & Boulter, 1984; UniProt Consortium, 2019).

In conventional pea protein fractionation, proteins are extracted through isoelectric precipitation. However, the isoelectric point of pea albumins is generally higher than that of pea globulins (Dziuba, Szerszunowicz, Nałecz, & Dziuba, 2014). The isoelectric precipitation is carried out around the isoelectric point of the globulins (pH 4.5), which generally leads to loss of albumins in that

fraction (Passe, D; Fouache C; Verrin, J-M; Bureau, 2008). Kornet et al. (2020) showed that mainly globulins precipitated after isoelectric precipitation of pea proteins at pH 4.5, while albumins and small subunits remained soluble. This suggests that conventional fractionation techniques only extract the globulins from the pea, and thus do not valorise the entire protein content in the pea. Mild wet fractionation is a method to obtain high purity and yield protein isolates (Möller, Li, van der Goot, & van der Padt, 2021). Geerts, Mienis, Nikiforidis, van der Padt, & van der Goot (2017) introduced the method to obtain soluble and non-soluble protein concentrates. This mild fractionation is based on the use of water only to fractionate the pea into its constituents, and the fractionation is based on the solubility characteristics of the components at extraction conditions. Due to the high protein yield in the fractions, it is assumed that both albumins and globulins were extracted into the soluble (SPF) and non-soluble (NSPF) protein fractions. Djoullah, Djemaoune, Husson, & Saurel (2015) determined the solubility characteristics of albumins and globulins of pea over a pH range of 2-10. According to their research, both albumins and globulins can be soluble at the extraction pH of mild wet fractionation. Therefore, it is interesting to understand which types of proteins are present in SPF and NSPF. It is even more relevant to understand the effect of the protein composition on the functional properties of the ingredients. That is why this study aims to determine the protein composition of SPF and NSPF and to investigate the effect of the protein composition on the functional properties. It is assumed that both fractions contain mixtures of albumin and globulin. The analysis of the fractions' protein solubility characteristics and protein gelation properties can be used to establish a link between composition and functional properties.

## 5.2 Materials and Methods

The pre-dried yellow peas (*Pisum sativum L.*) were purchased from Alimex (Sint Kruis, The Netherlands).

### 5.2.1 Milling

The peas were pre-milled into grits at room temperature using a pin mill (LV 15M, Condux-Werk, Wolfgang bei Hanau, Germany). The grits were milled into a fine flour (protein content 21.6 %, 91.1 wt.%) with a ZPS50 impact mill (Hosokawa-Alpine, Augsburg, Germany), an impact mill speed of 8000 rpm, an airflow at 52 $m^3$/h, a classifier wheel speed of 5000 rpm and a feed rate of 2 rpm (Pelgrom et al., 2015). The temperature in the mill was monitored to remain between 16 and 34 °C, with a thermometer placed inside the mill.

### 5.2.2 Mild wet fractionation

Mild wet fractionation (MWF) was performed following the method of (Geerts et al., 2017) with minor modifications according to (Möller, Li, et al. 2021). The flour was dispersed in Milli-Q water (resistivity 18.2 MΩ.cm, Merck Millipore, France) to a 20 wt.% dispersion. The mixture was stirred at room temperature for one hour. Then, the dispersion was submitted to a first centrifugation step at 1500 g for one second. During this step, the insoluble starch granules were collected into the pellet. The supernatant (PRF) was submitted to a second centrifugation step at 10000 g for 30 min. The pellet of this second centrifugation step yielded the so-called non-soluble protein fraction (NSPF), and the supernatant contained the soluble protein fraction (SPF). Parts of the obtained fractions were freeze-dried for further analysis using a Pilot freeze dryer (Christ Epsilon 2-6D, Osterode am Harz, Germany).

### 5.2.3 Albumin and Globulin extraction

SPF and NSPF were further fractionated into an albumin and globulin rich fraction each, according to the method of (Kornet, Penris, et al., 2021), with minor

modifications. The NSPF was diluted to a 2 % protein suspension to match the protein content of SPF. The pH of both fractions was adjusted to pH 4.5 with a 1 M HCl solution and was moderately stirred for one hour. The dispersion was then again centrifuged at 10000 g at 20 °C for 30 min to separate the precipitated globulins from the albumins. The pellet was resolubilised, and both dispersions were readjusted to pH 7 and subsequently freeze-dried for further analysis. The complete fractionation process, including mild wet fractionation and isoelectric precipitation, is depicted in Figure 5.1.

### 5.2.4 Compositional analysis

The dry matter content was determined by oven drying at 105 °C until a constant weight was reached. The protein content of the fractions was determined using Dumas analysis (Nitrogen analyzer, FlashEA 1112 series, Thermo Scientific, Interscience, Breda, The Netherlands) with a protein conversion factor of 5.52 (Holt & Sosulski, 1979).

### 5.2.5 Protein solubility

In literature, different definitions exist to describe protein solubility. Here, protein solubility is defined as the ratio between the protein dissolved in the supernatant and the total amount of protein in the sample before centrifugation (Vojdani, 1996). Mild wet fractionation is based on the solubility characteristics of the components. Therefore, it was decided to choose the same centrifugation settings for the protein solubility analysis as for the second mild wet fractionation step. Protein solutions of 0.1 % were made from SPF, NSPF, and the GLB and ALB fractions. The pH of the protein solutions was adjusted to a range of pH 3-9, and the samples were mixed using a rotator (Stuart, UK) for 1 hour, after which the pH was controlled and readjusted, if necessary. According to the mild wet fractionation method, the samples were then centrifuged at 10000 g at 20 °C for 30 min. The supernatant was separated, and the protein content was determined using a PierceTM Bicinchoninic acid protein assay kit (ThermoFisher

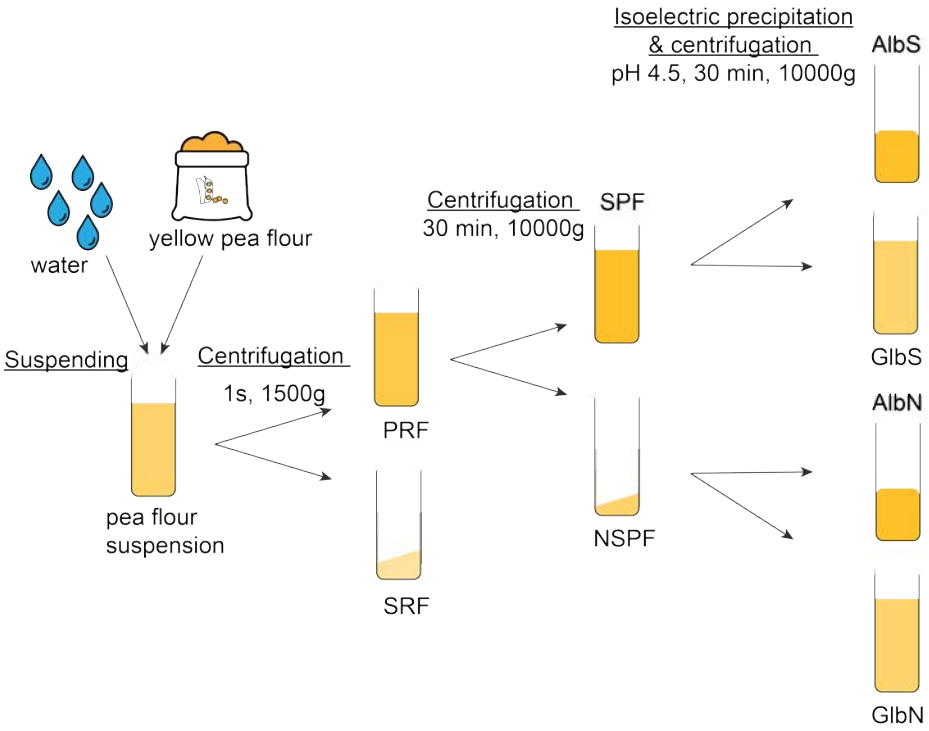


Figure 5.1 Mild wet fractionation of yellow pea flour with subsequent isoelectric precipitation to separate albumins and globulins. The fractions are starch-rich fraction (SRF), protein-rich fraction (PRF), soluble protein fraction (SPF), non-soluble protein fraction (NSPF), albumin-rich fraction from SPF (AlbS), globulin-rich fraction from SPF (GlbS), albumin-rich fraction from NSPF (AlbN), and globulin-rich fraction from NSPF (GlbN).

Scientific Inc., USA). Bovine serum albumin (BSA) with a known concentration was used to prepare a calibration curve (ThermoFisher Scientific Inc., USA). The method was performed according to the standard protocol. The absorbance of the colourimetric reaction was measured at 562 nm using a spectrophotometer (Beckman DU720 UV-Vis spectrophotometer (Beckman-Coulter Inc., USA). Protein solubility ($S$) (%) of the fractions was determined by dividing the pea protein fractions' protein content determined with BCA ($x_{p,supernatant}$) (g/g) by the initial protein content in the solution ($x_0$) (g/g) using equation 5.1:

$$S = \frac{x_{p,supernatant}}{x_0} \cdot 100\% \qquad 5.1$$

5.2.6 Rheological measurements

The linear viscoelastic response of the pea proteins in dispersion was measured during heating and cooling to determine their gelation properties (Remco Kornet, Penris, et al., 2021). Temperature and frequency sweeps were performed in a MCR301 rheometer (Anton Paar, Austria) equipped with a CC-17 concentric cylinder geometry, and a thin layer of highly liquid paraffin oil (Merck Millipore, USA) was applied on the sample surface as a solvent trap to prevent evaporation (Anton Paar, Austria). For the temperature sweeps, the samples were heated from room temperature to 95 °C with a heating rate of 3 °C/min, the temperature was held for 10 min, and subsequently, the samples were cooled to 20 °C, with a cooling rate of 3 °C/min. The temperature was kept at 20 °C for 5 min more. The storage ($G'$) and loss ($G''$) moduli were recorded as a function of temperature at a frequency of 1 Hz and a strain amplitude of 1 %. The frequency sweeps were performed at 1 % deformation (within the linear viscoelastic regime) with a frequency increase from 0.01 to 10 Hz.

### 5.2.7 SDS-PAGE

SDS-PAGE gels were prepared under non-reducing and reducing conditions. 2x Laemmli buffer (Bio-Rad Laboratories Inc., USA) was mixed 1:1 with 2 mg/ml protein solutions. For reducing conditions, the buffer was prepared with β-mercaptoethanol at a ratio of 1:20. The samples were heated to 95 °C for 10 min with a Thermomixer (Eppendorf AG, Germany) and subsequently centrifuged to remove precipitates (Sysmex B.V., The Netherlands). The samples (20 µL) and the standard marker (10 µL) (Precision Plus Protein™ Standards 10-250 kDa, Bio-Rad, USA) were loaded onto 12 % precast gels (Mini-PROTEAN® TGX™, Bio-Rad, USA). 10x TGS running buffer (Bio-Rad, Germany) was diluted to 1x TGS and poured into the buffer tank. Electrophoresis was performed at 200 V. The gels were rinsed twice with Milli-Q water and stained with Bio-Safe™ Coomassie G-250 brilliant blue (Bio-Rad, Germany) before they were scanned (GS-900™ Calibrated Densiometer, Bio-Rad, USA) for band analysis (ImageLab Software, Bio-Rad, Germany).

### 5.2.8 Size exclusion chromatography

McIlvaine buffer was prepared with 10 mM citric acid, 20 mM Na2HPO4 and 150 mM NaCl and adjusted to pH 7. The buffer was filtered with a 0.45 µm filter. Samples of all fractions were prepared in a protein concentration of 10g/L and filtered with a 0.45 µm filter. Size Exclusion Chromatography (SEC) was carried out on an Äkta Pure 25 System (Cytiva, USA) with a Superdex 200 Increase 10/300 GL column (Merck, Germany). The McIlvaine buffer was used as the eluent. Signals were measured with a UV detector at 214 nm. A calibration curve was prepared with Blue dextran (2000 kDa), Ferritin (474 kDa), Aldolase (158 kDa), Ovalbumin (43 kDa), β-Lactoglobulin (36.8 kDa) and α-lactalbumin (14.2 kDa) by correcting the retention volume for the column volume and plotted on a logarithmic scale.

## 5.3 Results & Discussion

Mild wet fractionation allows the separation of the protein-rich supernatant into soluble and non-soluble protein. Solubility is one of the main functionalities often analysed for plant proteins (Lam et al., 2018a). Thus, we analysed the fractions obtained from mild wet fractionation for their protein composition and their protein solubility over a pH range of 3-9. SPF and NSPF were further fractionated into albumin (Alb) and globulin (Glb) enriched fractions to facilitate the analysis and relate the composition with the solubility of the fractions.

### 5.3.1 Characterisation of protein-rich fractions

The protein contents based on dry mass were determined for all fractions and are listed in Table 5.1. The stream composition of each fraction is depicted in Figure 5.2. The compositions of SPF and NSPF were well in line with previously determined compositions (Möller, Li, et al., 2021). Isoelectric precipitation further separated SPF and NSPF into two fractions each. The Alb-fraction from SPF (AlbS) contained the proteins and solutes that were also soluble at pH 4.5. The Glb-fraction from SPF (GlbS) contained the proteins and polymers that precipitated at pH 4.5 or were insoluble anyhow. Also, the Alb-fraction from NSPF (AlbN) contained those components that were soluble at pH 4.5; the Glb-fraction from NSPF (GlbN) contained the components that were insoluble or precipitated at pH 4.5. The AlbN fraction was of very low quantity, probably because most of these components were fractionated into the SPF before isoelectric precipitation. Furthermore, the Alb-fractions was of lower protein purity than the Glb-fractions.

All protein fractions were separated chromatographically to elucidate their protein composition. The proteins were studied in a broad molecular mass range to include the native protein masses. In Figure 5.3, the different proteins were assigned to the respective peaks according to their molecular mass. The fractions obtained through the mild wet fractionation method are depicted in Figure 5.3 A. The PRF, from which the SPF and NSPF will be derived, is the protein frac-

Table 5.1 Protein content of all fractions obtained through mild wet fractionation with subsequent isoelectric precipitation, with standard deviation. Of those the protein yields based on the initial protein present in the pea flour are listed. A graphic representation of the streams is attached in the appendix in Appendix Figure A 5.1

| Sample | Protein content (g/100g DM) | Protein yield % |
|---|---|---|
| PRF | 53.5 ± 2.6 | 71.0 |
| SRF | 4.6 ± 0.4 | 29.0 |
| SPF | 46.2 ± 1.5 | 40.2 |
| NSPF | 65.7 ± 1.6 | 30.8 |
| AlbS | 30.6 ± 1.2 | 19.1 |
| GlbS | 80.6 ± 1.8 | 21.1 |
| AlbN | 38.6 ± 5.0 | 1.6 |
| GlbN | 66.7 ± 1.2 | 29.1 |

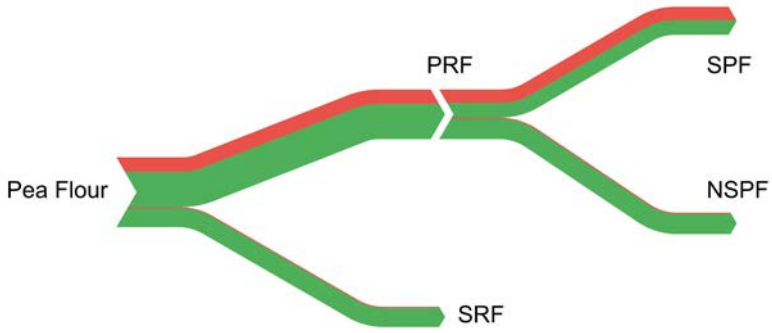


Figure 5.2 Graphical representation of the protein composition through the mild wet fractionation process, based on the protein yield of the Alb- and Glb-fractions. The red streams represent the albumin content; the green streams represent the globulin content. According to globulin contents from literature, it is assumed that SRF consists of mostly globulins (Boye, Zare, & Pletch, 2010).

tion obtained after starch extraction. Both globulins (retention volumes (RV) 10-14 ml) and albumins (RV > 14 ml) were found in this PRF fraction, as was expected. Peak determination for SPF indicated that SPF was a mixture of albumins and globulins. According to Djoullah et al. (2015), albumins and globulins are largely soluble at extraction pH 6.8, which explains the presence of both proteins in the SPF. NSPF mainly contained the globulin peaks, which corresponded to Djoullah et al. (2015) as well, as albumins are almost 100 % soluble at extraction pH 6.8. Figure 5.3 B depicts the chromatograms of the fractions obtained after isoelectric precipitation of SPF and NSPF. A clear separation into albumins and globulins was achieved through isoelectric precipitation. The globulin (Glb) fractions from SPF and NSPF consisted mainly of globulins, and the albumin (Alb) fractions from SPF and NSPF consisted mainly of albumins. The SPF chromatogram showed a peak often attributed to the albumin lipoxygenase. This enzyme catalyses the oxidation of polyunsaturated fatty acids and has been identified as a natural additive in food applications (Shi, Mandal, Singh, & Pratap Singh, 2020). The chromatograms of PRF and SPF showed an additional peak at a RV of 8.9 ml, corresponding to a molecular mass of approximately 1700 kDa, which might result from protein aggregation.

The chromatographic results were compared with SDS-PAGE analysis (Figure 5.4). Through SDS, the native proteins were separated into their subunits and are thus further referred to as protein units. In PRF and SPF, multiple protein units over the whole molecular mass range were detected. NSPF showed fewer bands, most of which were in the higher molecular mass range. The protein units detected in the albumin fractions are marked in green, and the protein units detected in the globulin fractions are marked in red. The SDS-PAGE patterns confirm the size exclusion chromatography results. In SPF, bands and peaks for both albumins (14-20 ml RV, 10-26 kDa, 94 kDa) and globulins (10-14 ml RV, >35 kDa) were pronounced. In NSPF, those were mainly pronounced for globulins. The isoelectric precipitation of the fractions resulted in a clear separation into albumins and globulins, visible in both the SEC peaks

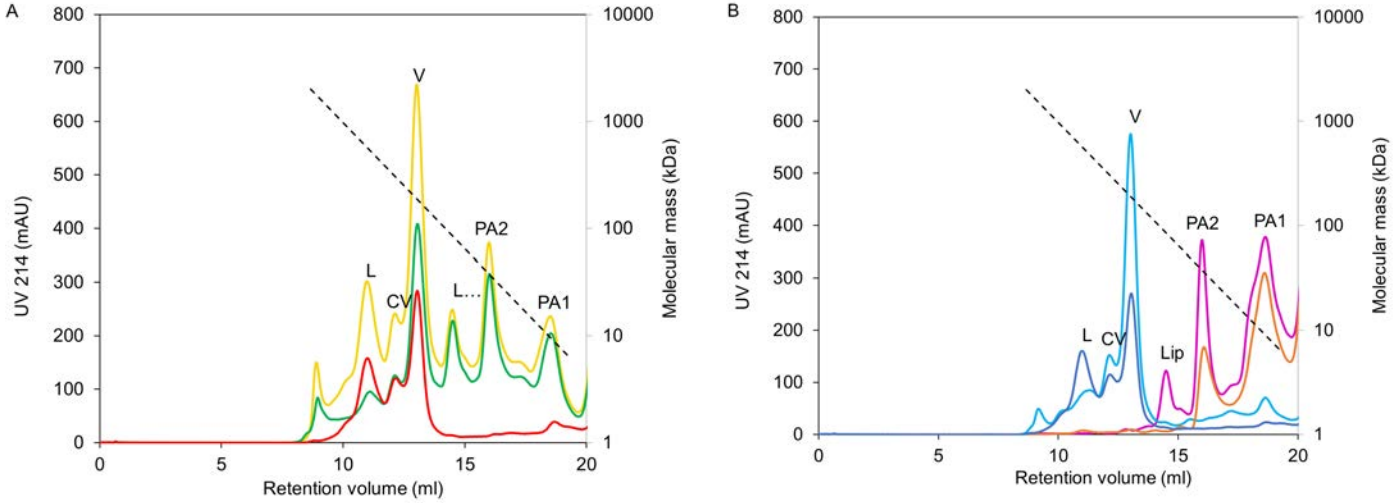


Figure 5.3 SEC chromatograms of the protein-rich fractions obtained from mild wet fractionation with subsequent isoelectric precipitation with UV detection at 214 nm as a function of the retention volume. PRF ( ), SPF ( ), NSPF ( ), Alb-SPF ( ), Glb-SPF ( ), Alb-NSPF ( ), Glb-NSPF ( ). The dashed black line indicates the molecular mass. Legumin (L), Convicilin (CV), Vicilin (V), Lipoxygenase (Lip), PA2, PA1.

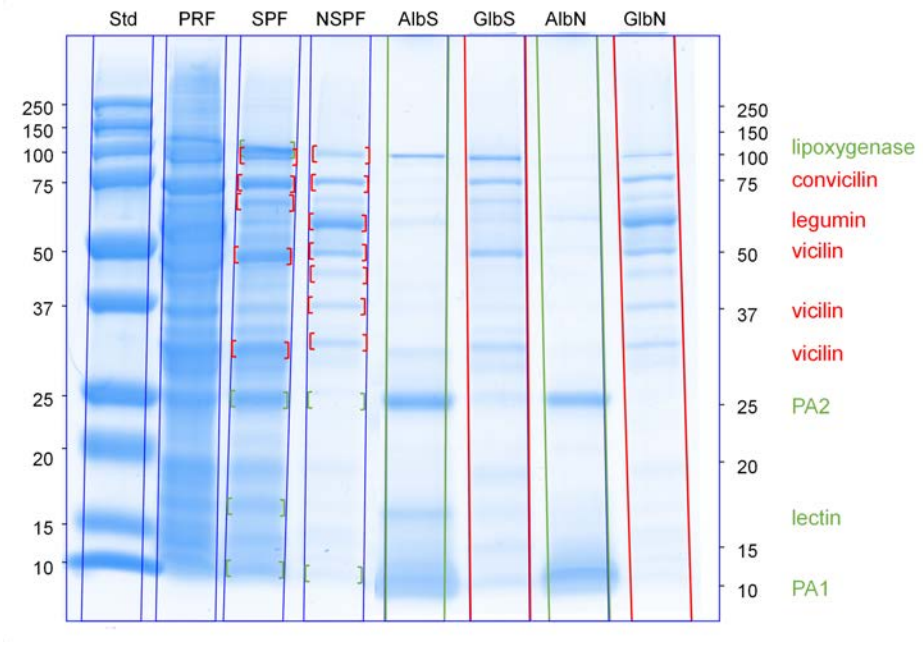


Figure 5.4 Non-reducing SDS-PAGE patterns of PRF, SPF, NSPF, ALB-SPF, GLB-SPF, ALB-NSPF and GLB-NSPF. Albumins are marked in green; globulins are marked in red. Std is the standard. Table A 5.1 lists the protein units in the respective fractions.

and the SDS-PAGE bands. The albumin fractions contained mainly low molecular mass proteins, while the globulin fractions contained high molecular mass proteins. For NSPF, only very faint bands were detected for the albumin units, indicating that NSPF hardly contained albumins. In SPF, the bands for albumins and globulins had similar intensities confirming that this fraction contained a mixture of albumins and globulins.

The protein yields of all fractions were calculated based on the initial protein present in the pea flour. The starch-rich fraction, separated after the first centrifugation step, was included in the yield calculations to account for the total protein content in the pea flour. The protein yields are depicted in Figure 5.2 in the form of the processing streams in mild wet fractionation. The first centrifugation step separates the pea flour into PRF and SRF. Around 30 g protein/100 g initial protein in the pea flour were recovered in the SRF fraction. PRF contains about 70 g protein/100 g initial pea protein and is further separated into SPF and NSPF, with around 40 g and 30 g protein/100 g initial pea protein, respectively. Protein yields and chromatograms revealed that approximately 50 % of the proteins in SPF are albumins and 50 % are globulins. NSPF, on the other hand, consists of primarily globulins, 95 % globulins and 5 % albumins, of 29 g protein/100 g initial pea protein. Therefore, the protein yield of PRF is a sum of around 20 g albumins and 50 g globulins/100 g initial pea protein. This albumin yield is in line with values obtained from literature (15-25 % albumins in pea flour, 65-80 % globulins in pea flour (Boye, Zare, & Pletch, 2010)), but the globulin value is considerably lower. Therefore, the proteins recovered in the SRF fraction are likely globulins (Figure 5.2). Previous research showed that washing the SRF fraction could decrease its protein yield to 3 g protein/100 g initial pea protein, resulting in a protein yield of 97 g protein/100 g initial pea protein in the PRF (Möller, Li, et al., 2021), thus recovering more globulins into the PRF.

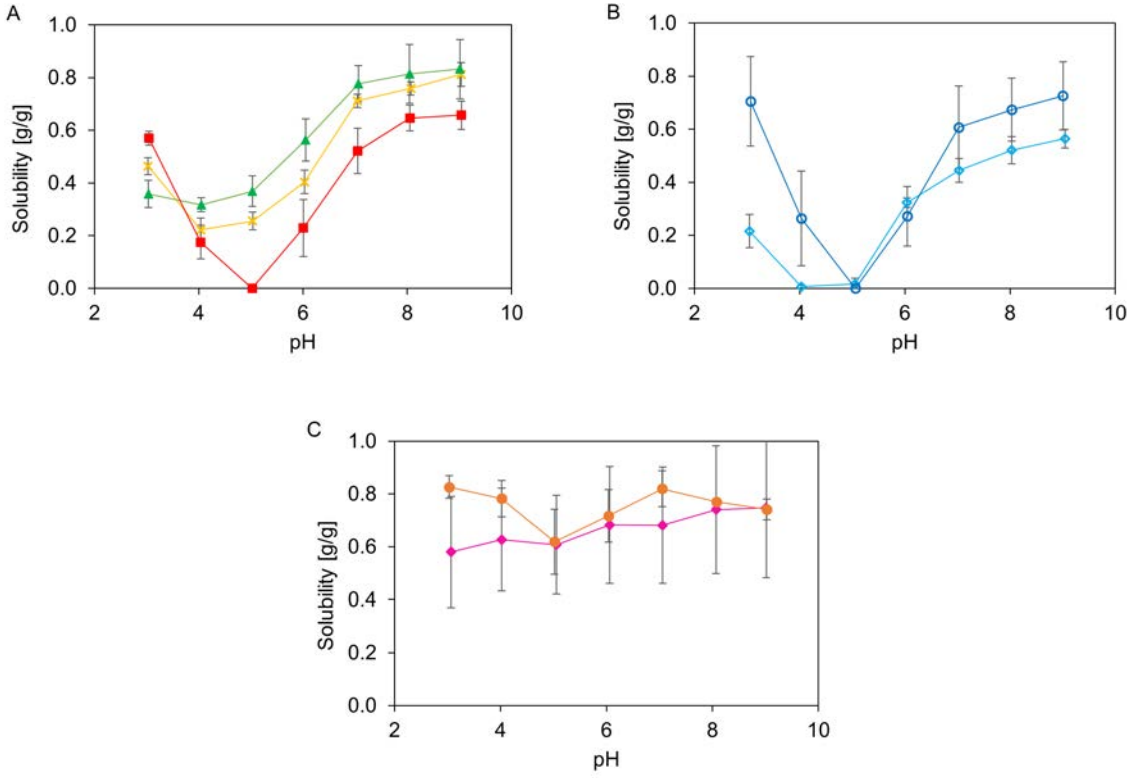


Figure 5.5 Protein solubility (%) is determined over a pH range of 3-9. PRF ( ), SPF ( ), NSPF ( ), Alb-SPF ( ), Glb-SPF ( ), Alb-NSPF ( ), Glb-NSPF ( ). All data points were determined in triplicate, and the averages with standard deviations are plotted here.

### 5.3.2 Protein Solubility

The component separation in mild wet fractionation depends on the solubility characteristics at extraction conditions. Factors that influence the protein solubility are temperature, pH, time, or solvent characteristics. Previously the solubility of the proteins in SPF and NSPF was determined at the extraction pH of 6.8 (Möller, Li, et al., 2021). Now, the protein solubility of all samples was determined in a pH range of 3-9 to find the isoelectric point of the proteins in the fractions and thus also their precipitation behaviour at pH 4.5. PRF, SPF and NSPF all contained protein that are soluble at pH 9. Their solubility decreased towards lower pH. For PRF and NSPF, the protein solubility increased again when further lowering the pH. The lowest protein solubility of PRF is around 20 %, while it decreased to around zero for NSPF. SPF has no clear negative peak but shows a decrease in protein solubility towards pH 3. At all pH values, the protein solubility of PRF is in between that of SPF and NSPF, which reflects that SPF and NSPF are separated from PRF indeed. The relationship between pH and solubility of the proteins in NSPF is most similar to that reported in the literature for pea protein isolates following a typical U-shape (Boye, Aksay, et al., 2010; Shevkani, Singh, Kaur, & Chand, 2015). The solubility profiles of the albumin and globulin fractions support the protein yield-purity results. As at the extraction pH of 6.8, most of the albumins and around half of the globulins are soluble.

The protein solubility was determined for solutions that were diluted to 0.1 % protein content. At extraction pH, PRF, SPF, and NSPF all contain at least 50 % soluble protein. Protein solubility is dependent on multiple factors, i.e., other components in the protein dispersion can influence the solubility. During mild wet fractionation the dispersions were more concentrated, thus the relevance of component interactions on solubility properties of each other might be higher. This effect has been reported for long-chain polymers, e.g. cellulose, which can occupy space and lead to a higher possibility of proteins interacting and

precipitating (Kramer, Shende, Motl, Pace, & Scholtz, 2012). Components that interacted and sedimented during MWF might resolubilize in a 0.1 % protein solution, and therefore the NSPF can contain more than 50 % soluble protein. Hence, the solution concentration can determine the separation efficiency of the fractionation.

Isoelectric precipitation into Alb and Glb-fractions resulted in different protein solubility profiles of the respective fractions. The Alb-fractions of SPF and NSPF are over the whole range soluble between 40-100 %. This is in line with the literature (Djoullah et al., 2015), where their solubility is assigned to the albumins' low surface hydrophobicity and hydrophilic nature. The albumin and globulin solubility in the literature was slightly higher. In this research, the protein fractions were freeze-dried before the solubility determination. Freeze drying generally induces protein aggregation and often results in reduced solubility of the fractions (Berghout, Venema, Boom, & Goot, 2015). The globulins follow a similar trend as NSPF, with a negative peak at pH 4-5. Glb-NSPF has the highest solubility at pH 3 and 9, while Glb-SPF is most soluble at pH 9.

### 5.3.3 Protein gelation

It was previously suggested that the protein type determines the gel firmness rather than the protein content (Kornet, Penris, et al., 2021). Therefore, the heat-induced gelation of the protein fractions in dispersions of 10 wt.% protein content was determined. The protein content was standardized as all fractions were of different protein purities. As a result, the dry matter concentrations of the Alb-rich fractions had to be taken considerably higher due to their low protein content, similarly as done by Kornet, Veenemans, et al. (2021).

The final G' of PRF and NSPF was on average around 3.2 kPa (± 1.5 kPa); the final G' of SPF was on average around 7.7 kPa (± 1.1 kPa) (Figure 5.6). That indicates that the extraction of the non-soluble proteins increased the gel firmness. The loss factor (tanδ) of all gels was around 0.2; it was highest for SPF and lowest for NSPF (Table 5.2). Thus, all three gels exhibited solid-like behaviour. The

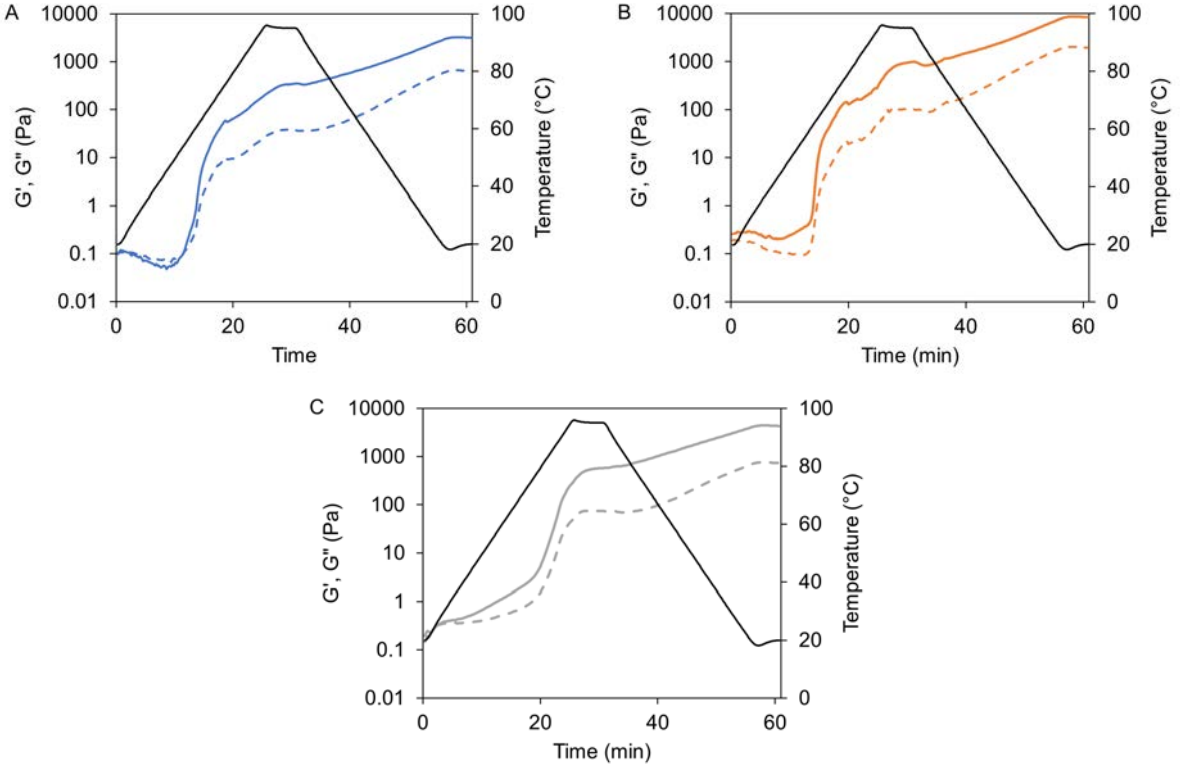


Figure 5.6 G' (solid line) and G" (dashed line) determined over a temperature sweep for PRF (A), SPF (B), and NSPF (C). All protein fractions were dispersed to a protein content of 10 wt.% and adjusted to pH 6.8. The samples were measured in duplicate and a representative curve was selected.

main proteins in PRF and NSPF are globulins; SPF consisted almost of a ratio of 1:1 globulins and albumins, as shown above. The results of the rheological experiments seem to indicate that the presence of albumins above a certain ratio enhances the firmness of a pea protein gel, which effect was also found earlier (Kornet, Veenemans, et al., 2021).

The gelation properties of the albumin- and globulin-rich fractions were also determined to better understand the contribution of the different proteins (Figure 5.7). Differences can be observed in the albumins and globulins extracted from SPF and NSPF. The G' of the albumins extracted from SPF was around 1.1 kPa (± 0.1 kPa); the G' of the albumins extracted from NSPF was only around 17 Pa (± 0.4 Pa). The opposite resulted for globulins: The globulins extracted from SPF had a G' of 187 Pa (± 52 Pa), while the globulins of NSPF had a G' of 958 Pa (± 0.1 kPa). For all gels, the loss factor was between 0.20-0.24. As the protein content of all gels was standardized the difference in G' might result from a difference in protein composition in the respective fractions. The SEC results (Figure 5.3) indicate that the albumin- and globulin-rich fractions extracted from SPF and NSPF vary in protein composition. That would mean that not only albumins and globulins form gels of different firmness, but additionally, the composition of albumins and globulins plays a role. Furthermore, the G's of PRF, SPF and NSPF were higher than those of the extracted protein fractions. That can result from the isoelectric precipitation, which can negatively affect the protein gelling capacity (Kornet, Veenemans, et al., 2021). Hence, additionally the state of the proteins influences the gelation properties. The pea protein fractions varied distinctly in protein purity. The starch content in PRF, SPF, and NSPF is considerably low (Möller, van der Padt, et al., 2021), and it was assumed that its contribution to the gelation properties of PRF, SPF and NSPF can be neglected. Hence, fractionation of pea proteins into SPF and NSPF can enhance the gelation capacity. This gelation capacity is decreased through isoelectric precipitation. Therefore, for gelation applications mild wet fractionation might be the more suitable method to obtain firmer gels.

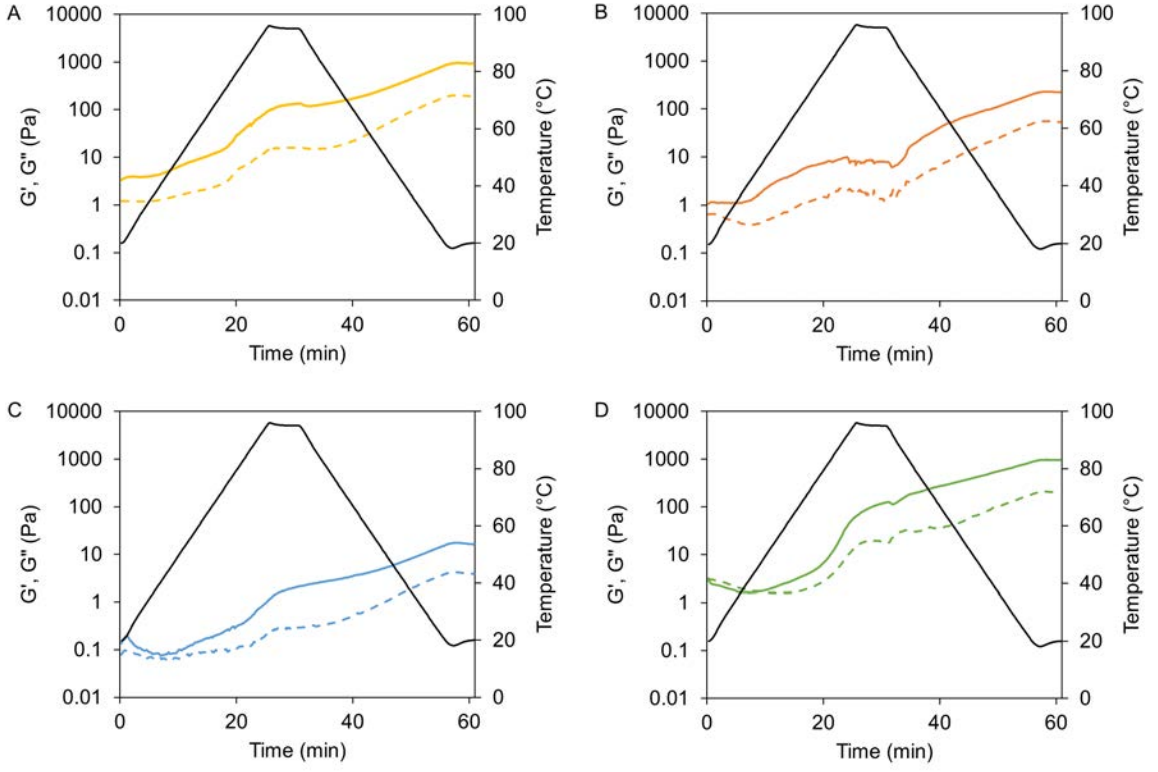


Figure 5.7 G' (solid line) and G" (dashed line) determined over a temperature sweep for AlbS (A), GlbS (B), AlbN (C), and GlbN (D). All protein fractions were dispersed to a protein content of 10 wt.% and adjusted to pH 6.8. The samples were measured in duplicate, and a representative curve was selected.

Table 5.2 Elastic modulus (G') and loss factor (tanδ) of all protein-rich gelled fractions. The averaged elastic modulus and loss factor were calculated from the last data point of the temperature sweeps determined in duplicate and are presented with standard deviations.

| | PRF | SPF | NSPF | AlbS | GlbS | AlbN | GlbN |
|---|---|---|---|---|---|---|---|
| Dry mass (wt.%) | 18.7 | 21.6 | 15.2 | 32.7 | 12.4 | 25.9 | 15.0 |
| G' (Pa) | 3496 ± 452 | 7689 ± 1099 | 3227 ± 1542 | 1015 ± 132 | 187 ± 52 | 17 ± 0.4 | 958 ± 145 |
| tanδ | 0.20 ± 0.00 | 0.23 ± 0.00 | 0.17 ± 0.00 | 0.21 ± 0.00 | 0.24 ± 0.00 | 0.24 ± 0.00 | 0.21 ± 0.02 |

### 5.3.4 The consequence for ingredient and process design

Previous research shows that the higher protein yields can be obtained through mild wet fractionation than conventional fractionation (Möller, Li, et al., 2021). In this research it becomes clear that the higher yields reported can be explained through the co-extraction of albumins. To valorise the complete protein content in the yellow pea, extraction of albumins is required. The protein purity of the SPF-albumin fraction is low, with only 31 % protein content. As reported in Section 5.3.3, the carbohydrate content in pea protein fractions obtained through a similar technique mainly consisted of small sugars and was predominantly present in the albumin-rich fraction (Kornet et al., 2020). That indicates these are present mainly in SPF. In earlier research, the membrane separation process applied to the SPF fraction (Möller, Li, et al., 2021) likely extracted most mono- and disaccharides.

The protein solubility and protein gelation analyses indicate that the protein composition and the processing history of the mild wet fractions affect their functional properties. A fractionation of PRF into SPF and NSPF can increase the protein solubility and enhance the gelation capacity in SPF. NSPF mainly contains globulins and has a higher protein purity. Other functional properties of NSPF should be investigated as it is a promising ingredient due to its high protein purity. However, the results of this research indicate that protein purity does not enhance functional properties, e.g. increased protein solubility or gelation capacity.

Mild wet fractionation consists of different steps, resulting in fractions of varying composition and functionality. The separation efficiency is dependent on the solubility characteristics of the components at extraction conditions and thus also the centrifugation settings. The first, very mild centrifugation step of mild wet fractionation separates the protein-rich fraction from the starch-rich fraction (70.4 wt.% starch (Möller, van der Padt, et al., 2021)). The second centrifugation step is applied to the protein-rich fraction, and is more intense; it separates soluble from insoluble proteins and soluble saccharides from insolu-

ble saccharides. These steps could be adjusted to vary the protein composition or protein state in the fractions, and match the functional properties to a product. That is a step towards tailored fractionation, which is based on the idea that the food ingredients should be produced according to the product requirements. For example, it might be beneficial to further fractionate the pea proteins into albumin- and globulin-rich fractions, similarly to conventional wet fractionation. Such a fractionation might be of interest for specific pure protein ingredients. This additional separation bears similarities to the fractionation into pure α-lactoglobulin for infant formula as applied in the dairy industry. The fractionation techniques presented here allow to obtain different fractions of varying functional properties. Further exploration of the effect of fractionation techniques on the composition and functional properties might result in a wide variety of ingredients to develop tailored ingredients for foods.

It was previously proposed to apply the extensive know-how from the dairy industry in plant protein fractionation and apply similar processes, such as ultrafiltration with diafiltration, to obtain plant protein isolates (Möller, Li, et al., 2021). When comparing these processes to the those studied here, it seems that that the dairy industry focusses on mild wet fractionation principles. The use of those processing steps probably explains the very good functional properties of dairy proteins (Singh, 2011). Therefore, we suggest adopting the principles of dairy protein fractionation to mild wet fractionation of pea proteins. Moreover, the dairy industry has shown how to make the best use of a raw material stream by valorising side streams, e.g. lactose, into high quality and price ingredients. Such practices could be applied to plant ingredient fractionation, to create a broad range of highly functional ingredients from one raw material.

## 5.4 Conclusions

Mild wet fractionation into SPF and NSPF results in two protein-enriched fractions with different protein compositions. This research highlights that both globulins and albumins can be soluble at neutral pH, and thus, MWF results in mixed fractions. Yield determination after isoelectric precipitation of SPF and NSPF allowed quantifying the proteins present in the fractions. SPF was an equal mixture of albumins and globulins; NSPF consisted of mostly globulins. Furthermore, it could be concluded that the protein fractions also have different functional properties, probably due to their different protein composition and the state of the proteins. The protein solubility of the albumin fractions was constant over a pH range of 3-9. In contrast, the protein solubility of the globulin fractions was low around the isoelectric point of pea globulins, which could be confirmed by the results of purified albumin and globulin fractions from the literature. The protein solubility characteristics at extraction pH supported the albumin and globulin yield detected in SPF and NSPF. SPF could form firmer gels than PRF and NSPF at the same protein concentration. Albumins and globulins extracted from SPF and NSPF had different gelling capacities; Alb-SPF formed firmer gels than Glb-SPF and Alb-NSPF, comparable to those of Glb-NSPF, and might be a result of the protein composition in these fractions. Thus, the different proteins have different functional properties and, accordingly, SPF and NSPF. Moreover, the state of the proteins also influences the functional properties of the fractions, as indicated from the lower gelation capacities of the isoelectric precipitated proteins.

Hence, mild wet fractionation offers the possibility to obtain protein-rich fractions of varying composition and functionality. By controlling the composition and processing history, the fractions' functionalities could be tailored, which could contribute to establish mild fractionation techniques in the food industry.

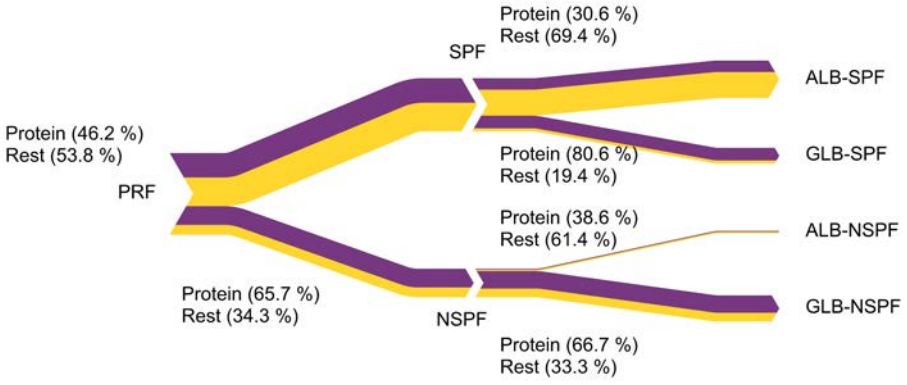


Figure A5.1 Graphical representation of the proportion of protein and rest in the protein-rich fractions obtained through mild wet fractionation with subsequent isoelectric precipitation into ALB and GLB-rich fractions based on dry mass. The purple stream represents the protein content, and the yellow stream represents the other components (Rest). The Rest was determined by difference.

Table A 5.1 proteins determined in SEC and SDS-PAGE in the respective fractions.

| Protein | PRF | SPF | NSPF | AlbS | GlbS | AlbN | GlbN |
|---|---|---|---|---|---|---|---|
| Albumin | all | Lipoxygenase<br>PA2<br>Lectin<br>PA1 | PA2<br>PA1 | Lipoxygenase<br>PA2<br>Lectin<br>PA1 | | PA2<br>PA1 | |
| Globulin | all | Convicilin<br>Vicilins | Convicilin<br>Legumin<br>Vicilins | | Convicilin<br>Vicilins | | Convicilin<br>Legumin<br>Vicilins |

# Chapter 6

## Structure analysis of multi-component pastes - The effect of water distribution on the rheological properties

Anna Cäcilie Möller, Anouk Lie-Piang, Ting Bian,
Albert van der Padt, Atze Jan van der Goot

Submitted

## Abstract

Techno-functional properties of multi-component blends and ingredients are determined by the contribution of each ingredient and the water distribution in the blends. However, ingredients can consist of multiple components, which should be considered to better understand the properties of ingredients and blends thereof. Recently, empirical models were used to describe the viscosity of mildly refined ingredient blends. While many compositions were described well by the model, blends with high fibre contents were not predicted sufficiently well. Therefore, in this research, the multi-component blends of pea protein, pea starch, and pea fibre isolates were investigated on their rheological properties as a function of the water content. The same properties were then measured for blends of two of these isolates mixed in different ratios. From the rheological experiments, predictions of the water distribution were made with the polymer blending law. The results were compared with CLSM images. A quantitative analysis of the CLSM images mostly confirmed the model predictions. The isolate ratio could describe the isolate blends sufficiently well, meaning that it was not necessary to know the exact compositions of the ingredients. It was concluded that changes in meso structure of the blends, for example a phase transition at high fibre contents, caused the lower predictability by the empirical viscosity models. This study demonstrates that the water distribution in multi-component blends plays a crucial role for their viscoelastic properties and the contribution of the individual isolates and components. Moreover, polymer blending laws that include water distribution provide extra mechanical insights into the fraction behaviour in multi-component blends.

## 6.1 Introduction

A more sustainable food industry requires reducing the use of recourses in food and food ingredient production (Govindan, 2018). This could be achieved by reducing the degree of refining. Methods that involve a lower degree of refining are dry fractionation, such as milling and air classification or simplified wet fractionation. Such milder fractionation methods focus on ingredient functionality rather than purity (Van Der Goot et al., 2016). However, the application of the ingredients obtained from mild fractionation is still limited. One reason is that mixed ingredients can affect each other's functional properties, which could result in another gel strength than expected (Saha & Bhattacharya, 2010). In our recent article, we used empirical models to describe the viscosity of these mildly refined ingredients (Lie-Piang, Möller, et al., 2021). The viscosity was described by the total amount of dry matter, the ingredient quantity, or the components present. The component models described the viscosity of the mildly refined ingredients best. Furthermore, the models indicated that interactions play a role in fully describing the multi-component ingredients' viscosity indeed. Yet, these models do not provide more insight into the mechanical phenomenon that explains these interactions. It is interesting to understand the nature of their component interactions to facilitate the application of these lower refined ingredients. The component interactions can be estimated by analysing the microstructure of component blends, e.g. by calculating the water distribution and phase behaviour between the components. As outlined below, various papers describe the microstructure of polymer blends by combining rheology measurements with a theoretical model described by Takayanagi, Harima, & Iwata (1963) called the 'polymer blending law'. The model is based on the assumption that most polymers are phase-separated inside a blend. This assumption allowed them to relate the viscoelastic moduli of the individual phases to the rheological properties of the blend

The Takayanagi model was previously used to describe the viscoelastic properties of biopolymers, in particular whey protein/cassava starch gels. Due to the

importance of water for the viscoelastic properties of biopolymers and hence the microstructure, the model was extended to include the water distribution between the biopolymers (Aguilera & Baffico, 1997).
Dekkers et al. (2016) developed a method using TD-NMR that accurately determined the water distribution in blends of soy protein isolate and wheat gluten. They compared the results to estimations of the water distribution obtained with the modified polymer blending law from rheological measurements with good agreement. Their good outcomes suggested that the modified polymer blending law is suitable to estimate the water distribution in food ingredient blends. Schreuders, Bodnar, Erni, Boom, & Goot (2020) applied the same method to blends of pea protein isolate and wheat gluten.
Thus, the consideration of water uptake per phase is a factor that can help to explain the rheological properties of biopolymer blends. Furthermore, it enables to draw conclusions on differences in rheological properties of component mixtures. For example, starch can behave differently in a starch-fibre blend than in a starch-protein blend. In Figure 6.1, the possible influence of components on each other's swelling behaviour is depicted. While each component has distinct swelling properties by itself, this swelling property might be influenced if another component is present. Accordingly, the water uptake can vary per component and can also depend on other components present. These effects are especially of importance in multi-component ingredients. Food pastes contain large amounts of water that is absorbed by the paste components. The water distribution in food pastes influences the viscoelastic properties and can be indicative for their fraction behaviour (Chou & Morr, 1979; Donmez, Pinho, Patel, Desam, & Campanella, 2021). Therefore, this study aims to investigate the contribution of protein, starch and dietary fibre to the viscoelastic properties of yellow pea pastes. By investigating how the water distribution influences the blend microstructure we expect to understand why the empirical model predicted high fibre blends less well.
Due to the multi-component character of the milder refined ingredients, it

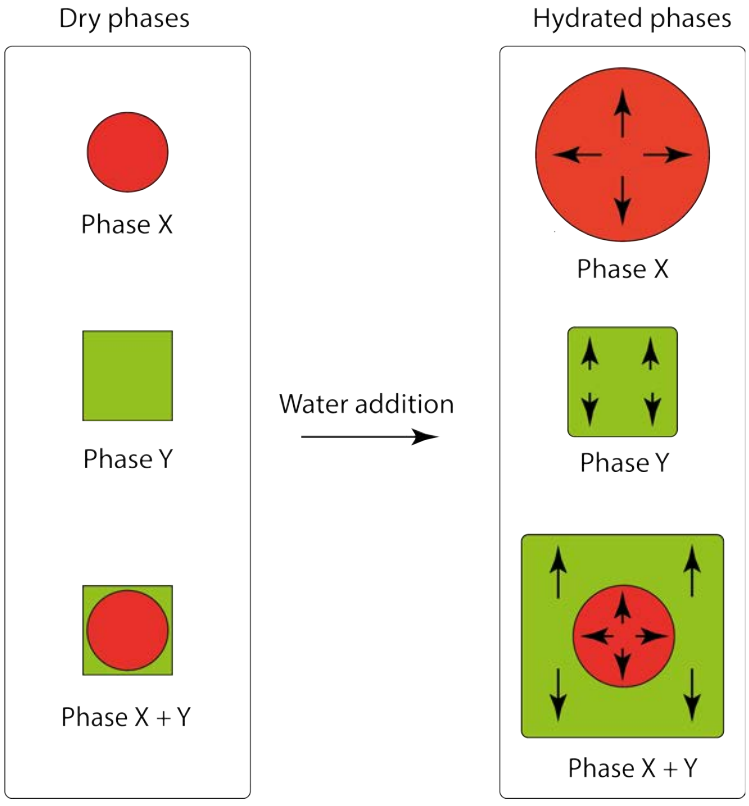


Figure 6.1: Graphical representation of three different types of swelling behaviours of single components and a blend of both components under the addition of water. The arrows depict the water induced swelling behaviour of the component phases, the arrow lengths indicates the extend of swelling.

is difficult to pinpoint the contribution of each component to the properties. Therefore, the purer commercial protein, starch and dietary fibre isolates were used in this study. Pastes were made using one ingredient or using combinations of ingredients (blends). In the latter, the water distribution per phase in the blends were determined, as a function of the starch, protein, and dietary fibre isolate concentration and component concentration. The distribution was investigated both on isolate and component basis to understand if the microstructure analysis could consider the isolate only or if an analysis on component level is required. The theory behind the polymer blending law and the approach of this research is described in the following section (Section 6.2).

## 6.2 Theory

### 6.2.1 Polymer blending law

In paste and gel formation with gelling polymers, biphasic co-gels can develop with one polymer building the continuous and the other the dispersed phase. In rarer situations, bicontinuous co-gels can be formed with biopolymer blends. In these blends, one polymer forms the first gel, which remains intact, and the other component forms a second continuous gel through the first network (Morris, 2009). For such bicontinuous blends, and blends with a dispersed phase in a continuous matrix, the modulus of the polymer blend paste $G'_b$ can be related to the moduli of the individual phases, $G'_x$ and $G'_y$. These theoretical equations were introduced by (Takayanagi et al., 1963) for polymer blends and can be described by the general form:

$$G_b'^n = \varphi_x G_x'^n + \varphi_y G_y'^n \qquad 6.1$$

The exponent n describes three phase behaviours: n = 1 is isostrain behaviour, the rigid stronger phase limits the deformation of the weaker phase, resulting in the same extent of deformation for both phases. A value of n = -1 describes

isostress behaviour, where the forces transmitted to the stronger phase are limited by the strength of the weaker phase, resulting in an approximated overall deformation from the weighted average of the individual phases. Finally, n = 0.2 describes the bicontinuous behaviour. $\varphi_x$ and $\varphi_y$ represent the volume fractions of the individual component phases.

### 6.2.2 Modified polymer blending law includes water distribution

Aguilera et al. (1997) modified the polymer blending law to include water distribution in the calculation, as water is present in high proportions in food gels. Variable *a* was introduced to describe the fraction of the original water absorbed by one phase, to include the water partition between the phases into the model. According to the hypothesis of Clark (1987), it was assumed that the total water added to form the suspensions was completely partitioned between their two phases. Consequently, the water is considered a solvent and not an extra component. Moreover, they introduced the 'effective' concentration to the model to further describe the water partition. The effective concentration is the relation between the dry matter mass fraction used in the original model and the volume fractions of the phases determined by the water partition between the phases.

The volume fractions were replaced by mass fractions to describe the behaviour of whey/starch gels. That is possible when assuming that the effect of concentration on density is limited, which seems acceptable due to the high water content of their gels (>80%) (Aguilera & Baffico, 1997). As a result, the mass fractions of the phases used in equation 6.1 can be calculated as follows in equations 6.2 and 6.3:

$$\varphi_x = \frac{m_x + m_w \cdot a}{(m_x + m_y + m_w)} \qquad 6.2$$

$$\varphi_y = \frac{m_y + m_w \cdot (1-a)}{(m_x + m_y + m_w)} \quad 6.3$$

Here, $m_x$ and $m_y$ are the dry masses of the phases, and $m_w$ is the water mass added to the blend, a is the estimated amount of water absorbed by phase *X*, and can be fitted to minimize the sum of squares (*SSE*) between the experimentally (e) measured *G'* and the predicted (p) *G'*:

$$SSE = \sum (G'_e - G'_p)^2 \quad 6.4$$

With the fitted *a*, the effective phase concentrations (wt.%) can be calculated by the difference between the mass and the phase mass:

$$c_x = \frac{100 \cdot m_x}{m_x + m_w \cdot a} \quad 6.5$$

$$c_y = \frac{100 \cdot m_y}{m_y + m_w \cdot (1-a)} \quad 6.6$$

The estimated amount of absorbed water can also be used to calculate the relative water uptake (*WU*):

$$WU_x = \frac{m_w \cdot a}{m_x} \quad 6.7$$

$$WU_y = \frac{m_w \cdot (1-a)}{m_y} \quad 6.8$$

Subsequently, Aguilera & Baffico, (1997) used the modified polymer blending law, including the absorbed water in the mass fraction to calculate the storage modulus of the two-component blends for isostrain behaviour ($n = 1$). This modified polymer blending law could also be applied for the other behaviours isostress $n = -1$ and bicontinous $n = 0.2$.

Table 6.1: The composition of pea protein isolate (PI), pea starch isolate (SI) and pea fibre isolate (FI) was determined through compositional analysis. 1 Rest was determined by difference, summarizing all non-starch, -protein, or -dietary fibre components.

| Fractions<br>Composition based on dry weight (%) | PI<br>Mean | SI<br>Mean | FI<br>Mean |
|---|---|---|---|
| Protein (N x 5.52) | 74.11 | 0.50 | 7.83 |
| Starch by starch kit | 0.39 | 91.44 | 33.76 |
| Fibre | 2.24 | 0.79 | 53.57 |
| Rest[1] | 23.26 | 7.27 | 4.84 |

## 6.3 Materials and Methods

### 6.3.1 Materials

Pea protein isolate (Nutralys F85G) (PI) and pea fibre isolate (PEA FIBRE I50M) (FI) were purchased from Roquette Frères S.A. (St. Louis, USA). Pea starch Isolate (SI) was kindly provided by Emsland Stärke GmbH (Emlichheim, Germany). For all experiments, deionized water produced with a Milli-Q purification system was used (Merck Millipore, Burlington, USA).

In this paper, those isolates will be referred to as: protein isolate (PI), starch isolate (SI) and fibre isolate (FI). In addition, the components in the isolates will be addressed as *starch*, *protein*, and *fibre*, to ensure a clear distinction between the isolates and components.

### 6.3.2 Compositional analysis

The isolates protein content was determined with the Kjeldahl method, with a nitrogen conversion factor of 5.52 for yellow pea (Holt & Sosulski, 1979). A Total

Starch Amyloglucosidase-α-Amylase Assay Kit, AOAC Method 996.11 (Megazyme International Ireland Ltd, Bray, Ireland) was used to determine the total starch content. The total dietary fibre content was determined using the AOAC method 985.29. The isolates were dried at 120 °C in an infrared moisture analyzer (MA35, Sartorius, Göttingen, Germany) to determine the dry matter. The residual component fraction was calculated by the difference between the dry matter and *protein*, *starch* and *fibre* content. The residual component fraction contains, among others, oil, ash, salt and sugars.

### 6.3.3 Sample preparation

Starch, protein and fibre isolate were dispersed in Milli-Q water (resistivity 18.2 MΩ.cm, Merck Millipore, France) in the following concentrations: SI 4-24 %w/w, PI 9-28 %w/w and FI 8-41 %w/w. The lowest concentration for the single isolate dispersions was selected based on the possibility to still determine the linear viscoelastic (LVE) region accurately. For the binary blends, starch isolate (SI), protein isolate (PI) and fibre isolate (FI) were mixed to pre-determined *component* ratios with total dry matter contents of 13 %. The SI-PI blends and the PI-FI blends were mixed to create the following *component* ratios in percentages based on the dry matter content: 20/80, 35/65, 50/50, 65/35 and 80/20 of *starch/protein* (s/p) and *protein/fibre* (p/f), respectively. For SI-FI blends, the chosen ratios were *starch/fibre* (s/f) (45/55), (50/50), (65/35) and (80/20). A lower *starch* content could not be achieved due to the high *starch* content in the fibre isolate. Therefore, the blends were prepared to achieve a predefined composition, to cover the whole range of low and high *protein*, *starch* and *fibre* contents (Appendix Figure A 6.1). The isolate mass is the ratio in which the isolates were blended based on dry matter content.

All dispersions were stirred at room temperature for 10 min before paste preparation. As the raw materials used were not pure, 'phase' is in the following replaced by 'fraction'.

### 6.3.4 Paste preparation

Of each dispersion, 17 g was placed in a starch cell C-ETD160/ST connected to an Anton Paar Rheometer MCR301 (Anton Paar, Austria) to form the pastes. The dispersions were heated, and the viscosity was determined in the process. The dispersions were stirred at 600 rpm at 50 °C for 10 s prior to the measurement. The viscosity measurements were performed at a constant rotational speed of 160 rpm, using a typical temperature-time profile for starch gelatinization for all samples (Kim, Kim, & Baik, 2012). All viscosity determinations were performed in duplicate. The obtained pastes were then left to cool and rested at room temperature for 1.5 h.

Subsequently, amplitude sweep tests were performed on the cooled pastes to determine the linear viscoelastic regime (LVE). The CP50-4 geometry was used for the *protein* samples, which allows low-viscosity measurements. All other one component and multi component pastes were determined with the PP25/P2 geometry. The gap size for all samples was set to 0.125 mm. The measurements were performed at 25 °C. A 1 % shear strain was used for all samples within the LVE and hence selected as an input parameter for frequency sweep tests. The frequency sweep tests were performed using a frequency range from 0.1-10 Hz after a 15 min recovery time (Appendix Figure A 6.2). Subsequently, the storage (*G'*) and loss moduli (*G"*) of the samples were determined as a function of the frequency.

### 6.3.5 Confocal laser scanning microscopy

For the image analysis Rhodamine B (0.008 % w/w, water) and CFW (calcofluor-white) (0.001 % w/w, water) were used to stain *protein* and *dietary fibres*, respectively. *Starch* was not stained; it was present in black granules, resulting in good contrast. The staining solutions were mixed with the dry samples and Milli-Q water at the respective blend ratios and prepared as described in Sections 6.3.3 and 6.3.4. A Zeiss LSM 520-META 18 confocal laser scanning microscope (Carl Zeiss, Oberkochen, Germany) was used to visualize the samples, with

543 and 514 nm excitation wavelengths for Rhodamine B and CFW, respectively. A magnification of 10x was used for all samples, and the ZEN 2008 software (Carl Zeiss, Oberkochen, Germany) was used to capture the images.
The image analysis to determine the area fractions of each component in the sample was performed using Matlab Software (Matlab R2016a, Mathworks, Nattick, Massachusettes, USA). Of each sample, three images of different parts in the paste were analysed, and the mean of the area fractions was determined to approximate the volume fractions of the components according to the principle of Delesse (Delesse, 1847).
The component area fractions were converted to isolate area fractions for a better comparison with the polymer blending law results:

$$isolate\,area\;fraction = \frac{component\,area\;fraction}{isolate\,component\,concentration} \cdot 100\% \qquad 6.9$$

6.3.6 Applying the modified polymer blending law in binary blends
The modified polymer blending law was applied to the isolate blends of Section 6.3.3 to determine the water uptake of the different fractions in the blends. The approach is listed below to fit the modified polymer blending law and select the best fitting model to describe the rheological properties of the isolate blends. The approach can be divided into two sections: 1) Fitting the modified polymer blending law, and 2) validation of best fitting behaviour.

1) Fitting the modified polymer blending law
The experimentally determined storage moduli of the single isolates ($G'_e$) in the specific concentration range were fitted with a power law, based on the $R^2$ to estimate the water distribution of each single isolate in the binary blends. Then, the obtained equations were used to describe the relation between the isolate contribution and the rheological properties and follow the general form in equation 6.10:

$$G'_{x,y} = b \cdot c_{x,y}{}^{a} \qquad 6.10$$

$G'_{x,y}$ is the respective fraction storage modulus, $c_{x,y}$ for the effective concentration of the respective fraction in dependence of the water absorption, and *a*, *b* and *c* are the fitting parameters.

Next, the modified polymer blending law was applied for each blend ratio at all three behaviours: isostrain $n = 1$, isostress $n = -1$ and bicontinous $n = 0.2$. Therefore, the water uptake a was obtained by fitting the storage modulus (equation 6.1) with Excel Solver Function GRG Nonlinear, minimizing the sum of squares (*SSE*< 0.01) (equation 6.4). The entire binary polymer blend calculations were based on the pea isolate concentrations. The pea isolates were not completely pure. Therefore, the isolate dry matter was used for each isolate in the calculations. This implies that the impurities of each isolate were assumed to behave the same as the primary component, i.e. *protein*, *starch*, or *dietary fibre*. For the following, it should be stressed that isolates are the ingredients used to prepare the blends, and components are the fractions of *protein*, *starch* and *dietary fibre* in these ingredients.

2) Validation of best-fitting behaviour

As described in Section 6.2.2, the water uptake a was determined by fitting a in equation 6.1 to minimize the sum of squares between the experimentally (e) measured $G'_e$ and the predicted (p) $G'_p$. For some blend ratio more than one solution was obtained for the water uptake a of isolate *X* at the same behaviour. Therefore selection criteria were defined:

1. Accuracy of the prediction: only the conditions and water uptake values that resulted in parity of the moduli were further considered. Parity was evaluated by a visual inspection of the quality of the prediction and by sum of squares *SSE*<0.01, see equation 6.4.

2. As a second criteria, the isolates' water uptake and the predicted storage modulus of the isolate blend fraction were evaluated. This criterion was required for those ratios where more than one behaviour solution resulted in parity with the experimental results. The water uptake of an isolate fraction was assumed to behave consistently to changes in ratio. This means that the water uptake does not fluctuate between high and low values with an increasing concentration of isolate *X*. The storage modulus was used to evaluate the fraction strength and together with the water uptake, an estimation of the fraction behaviour was made. The strength of the fractions ($G'_{x,y}$) and the model predictions at fraction behaviour, i.e. isostrain, isostress or bicontinuous, and the water uptake (equations 6.7, 6.8) of the phases, served to estimate which behaviour could be used best to predict the blend properties. With these two steps, one behaviour was picked for every ratio.

Validation with microscopy: the predicted fraction behaviour was compared to the phase behaviours observed from the CLSM images and to the area fractions determined by image analysis. The comparison was discussed.

## 6.4 Results & Discussion

### 6.4.1 Viscoelastic properties of protein, starch and fibre isolate pastes

The storage modulus was found to be dependent on the isolate concentration in all samples. The storage moduli of SI and FI were higher than for PI at the same concentrations. The storage modulus of PI was more concentration dependent though. The differences in the selected ranges of isolate concentrations was a result of the lowest measurable concentration of PI (9 %) and the highest measurable concentrations of SI (24 %) and FI (41 %) before slip occurred (Section 6.3.3). The storage moduli at a frequency of 1 Hz and as a function of concentration were fitted to a power law with $R^2 > 0.9$ for all isolates (Figure

6.2), which resulted in the following equations for SI, PI and FI, respectively. Here $G'_{SI,PI,FI}$ is the storage modulus and $c_{SI,PI,FI}$ is the weight fraction of the respective isolate:

$$G'_{SI} = 0.0015 \cdot c_{SI}^{6.4367} \quad 6.11$$

$$G'_{PI} = 5 \cdot 10^{-12} \cdot c_{PI}^{10.979} \quad 6.12$$

$$G'_{FI} = 0.4162 \cdot c_{FI}^{3.8642} \quad 6.13$$

The power law fits were used to determine the storage modulus of the isolate fractions in the blends at the respective concentration.

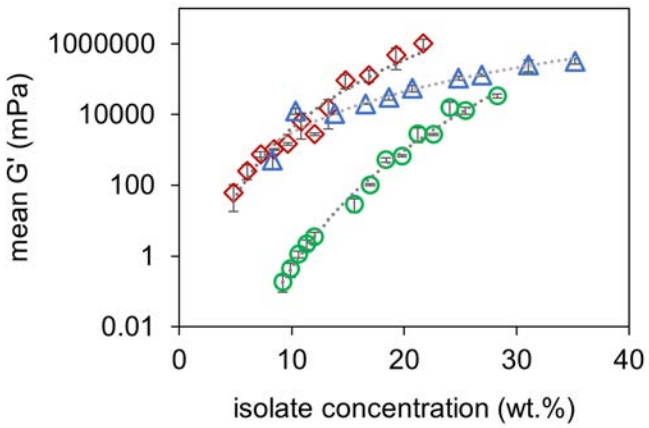


Figure 6.2: Storage modulus as a function of isolate concentration (wt.%) for PI (◯), SI (◇) and FI (△) with power law fits with R2 > 0.90 at a frequency of 1 Hz. The concentrations account for component concentrations of 4-18 % for starch, 7-20 % for protein and 4-17 % for fibre, respectively.

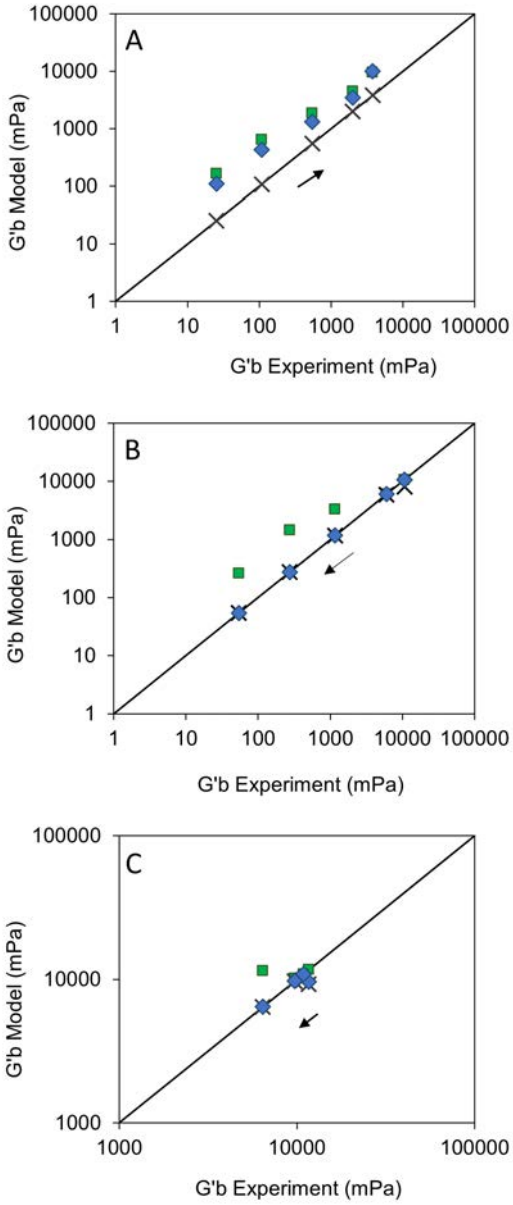


Figure 6.3: Parity plots of model predictions plotted against experimental results of G'b (blend storage modulus) of (A) starch/protein, (B) protein/fibre and (C) starch/fibre blends. For the isostress n=1 (■), isostrain n=-1 (✕) and bicontinuous n=0.2 (◆) behaviour. The arrows point in the direction of increasing concentration of the first fraction.

### 6.4.2 Prediction of mass fractions from viscoelastic properties – calculation of water uptake

To predict the water distribution in binary blends from pea isolates the polymer blending law (equation 6.1) was applied. Equations 6.11 - 6.13 were used to determine the storage moduli at the respective isolate concentrations in the blends. The water uptake of one fraction, parameter *a*, was determined by minimizing the sum of squares (equation 6.4). The mass fractions and effective concentrations (equations 6.2 - 6.6) were calculated based on this parameter. Figure 6.3 shows the parity plots of the predicted storage modulus, as results of the different models corresponding to isostrain ($n = 1$), isostress ($n = -1$) and bicontinuous ($n = 0.2$) behaviour, plotted against the storage modulus determined in the rheological experiments.

When multiple behaviours resulted in parity, the behaviour was selected based on the water uptake of the isolate fractions and the calculated storage moduli (Section 6.3.6, 2.2).

Table 6.2 summarizes the mass fractions (Section 6.2.2) calculated from the selected behaviour at the respective blend isolate ratios. Because the binary blend models were based on the isolate ratios, these ratios are also listed in the table. Although multiple behaviours resulted in parity with the experiments of several blends, the mass fractions between different behaviours varied considerably. As shown in Table 6.2, the mass fractions were not the same as the isolate ratios based on dry matter content and did not increase or decrease proportionally to the isolate ratios. This indicates that the isolate water uptake is influenced by the isolate ratio and the other isolate present. Furthermore, the mass fractions determine the effective concentration and the viscoelastic properties. Hence, the water uptake of each isolate fraction influences the viscoelastic properties of the blends. Figure 6.4 depicts the water uptake relative to the dry mass and the fraction storage modulus of the isolates for the isostrain, isostress or bicontinuous behaviour. A schematic depiction of the fraction behaviours in the blends is attached in Appendix Figure A 6.3 to aid visualization.

Table 6.2: Binary blend mass fractions of SI, PI and FI determined by rheological methods at different blend ratios of the selected behaviour, the isostrain $n = 1$, isostress $n = -1$ and bicontinuous $n = 0.2$.

| Blend | Isolate ratio | Mass fractions | | |
|---|---|---|---|---|
| | | n=1 | n=-1 | n=0.2 |
| SI/PI | 17/83 | | 22/78 | |
| | 31/69 | | 41/59 | |
| | 46/54 | | 58/42 | |
| | 61/39 | | 73/27 | |
| | 77/23 | | 84/16 | |
| PI/FI | 08/92 | 15/85 | | |
| | 23/77 | 18/82 | | |
| | 41/59 | | 29/71 | |
| | 60/40 | | 48/52 | |
| | 84/16 | | 74/26 | |
| SI/FI | 01/99 | 09/91 | | |
| | 10/90 | 18/83 | | |
| | 18/82 | | 23/77 | 24/76 |
| | 37/63 | | 49/51 | 65/35 |

#### 6.4.2.1 Starch isolate/ protein isolate

Isostress behaviour was predicted in all SI/PI blends. SI forms the stronger fraction at all ratios, which was expected based on the rheological measurements of the single ingredients (Figure 6.2).

The depiction of the isolate water uptake per isolate dry mass highlights that SI absorbed relatively more water than PI in the SI/PI blends (Figure 6.4). It was further observed that the storage moduli increased with decreasing water uptake and vice versa. The blend storage modulus was orienting along with the storage modulus of the primary fraction, shifting from PI to SI from low to high SI/PI ratios. According to the isostress behaviour, the weak PI formed a continuous network in which the strong SI was dispersed.

#### 6.4.2.2 Protein isolate/ fibre isolate

The PI/FI blends transitioned from isostrain to an isostress behaviour. The results of the selected behaviour suggested a stronger FI fraction than the PI fraction at all ratios, which is in line with the storage moduli of the single isolates (Figure 6.2). The FI absorbed more water relative to its dry mass than the PI at all ratios except for PI/FI(08/92). At this ratio, the total PI fraction absorbed almost the same amount of water as the total PI fraction at PI/FI(23/77), although the PI dry mass was by a third lower in PI/FI(08/92). The high water uptake of the PI fraction affected its storage modulus, which was a factor of a million lower than that the FI fraction in this blend. When all blends are considered, it can be concluded that the main fraction (i.e. the highest mass fraction) dominated the blend properties and determined the storage modulus in all blends.

A transition from the isostrain to the isostress behaviour was suggested for the PI/FI blends. PI built the continuous network at lower FI concentration, while FI built the continuous network at high FI concentrations. The transition of the isotrain to the isotress behaviour was between a ratio of PI/FI(23/77) and (41/59) (Figure 6.4, red line). Because the models predicted a stronger FI fraction than PI fraction at all ratios, this transition also resulted in a phase inversion. The

continuous strong FI network inverted into a strong dispersed FI at increasing PI concentration, and the weak dispersed PI inverted into a weak continuous PI network (Appendix Figure A 6.3, B).

#### 6.4.2.3 Starch isolate/ fibre isolate

In SI/FI blends, the results of the selected behaviour suggested a transition from the isostrain to the isostress or the bicontinuous behaviour between the ratios SI/FI(10/90) and (18/82). No clear selection was possible between the isostress and bicontinuous behaviour at ratios SI/FI(18/82) and (37/63) (see Table 6.2). Therefore, the water uptake was plotted with a transition from isostrain to isostress and a transition to bicontinuous behaviour for SI/FI. At all ratios, the storage moduli of the FI fraction were higher than the storage moduli of the SI fraction. The SI in the SI/FI(01/99) blend absorbed a high amount of water relative to its dry mass. At all other ratios, the water uptake was similar to those of SI/PI and PI/FI. SI absorbed more water than FI at all ratios; however for all ratios FI formed the stronger fraction. Again the blend storage modulus was similar to the storage modulus of the primary fraction. Compared to the SI/PI and PI/FI blends the relation between fraction strength and water uptake was inversed in SI/FI; the fraction that absorbed less water was the stronger fraction. CLSM images and image analysis might provide more insight into the fraction behaviour of the blends, and specifically for SI/FI into which model predicts the blend behaviour best. The predictability of the blends will be assessed in the next Section.

### 6.4.3 Identifying the fraction behaviour in binary blends

The estimations from the polymer blending law on the water distribution over the isolates were compared to the CLSM images (Figure 6.5). Only *protein* and *fibre* were stained for better contrast; the *starch* component then appears black in the images, just as the residual components. Notably, the analysis does not distinguish between the complete isolates, but rather the stained components

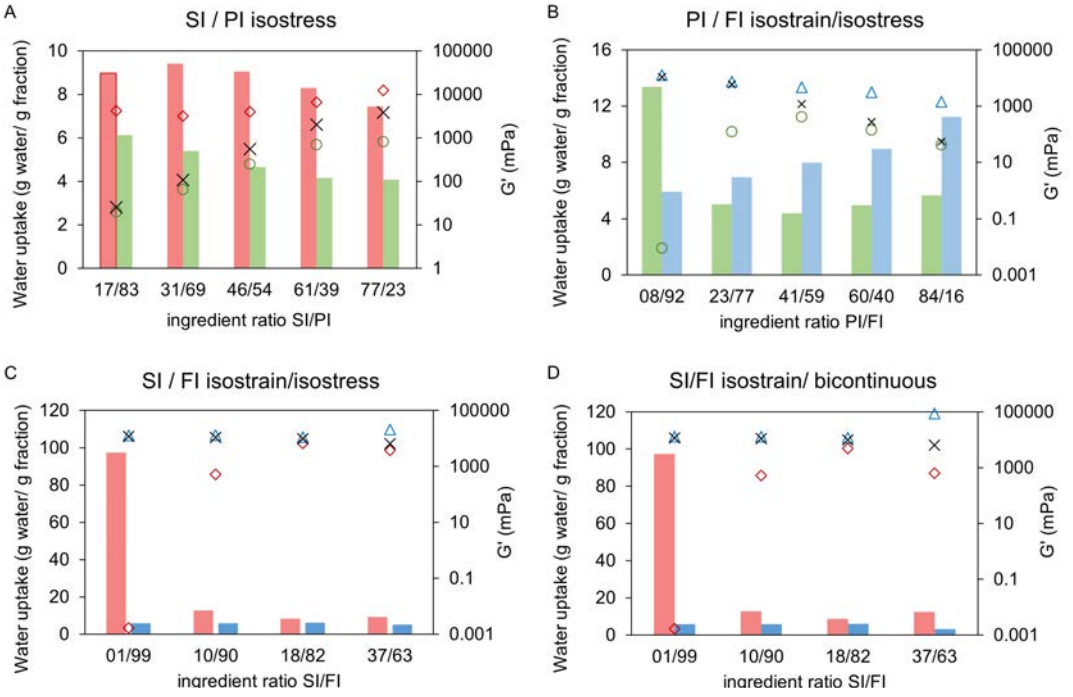


Figure 6.4: Depiction of the relative water uptake (equations 6.7, 6.8) per isolate dry mass at isostrain, isostress or bicontinuous fraction behaviour, as bar chart, PI (■), SI(■) and FI(■) and the predicted storage modulus for the single isolates and the isolate blends over the blend ratios. The symbols represent the storage moduli (G') of PI (○), SI (◇), FI (△) and (×) the blend of the respective isolates. The red lines indicate the transition from isostrain to isostress or bicontinuous behaviour, respectively. In (A) starch isolate/protein isolate blends, in (B) protein isolate/fibre isolate blends and in (C) and (D) starch isolate/fibre isolate blends with a transition to isostress and bicontinuous, respectively.

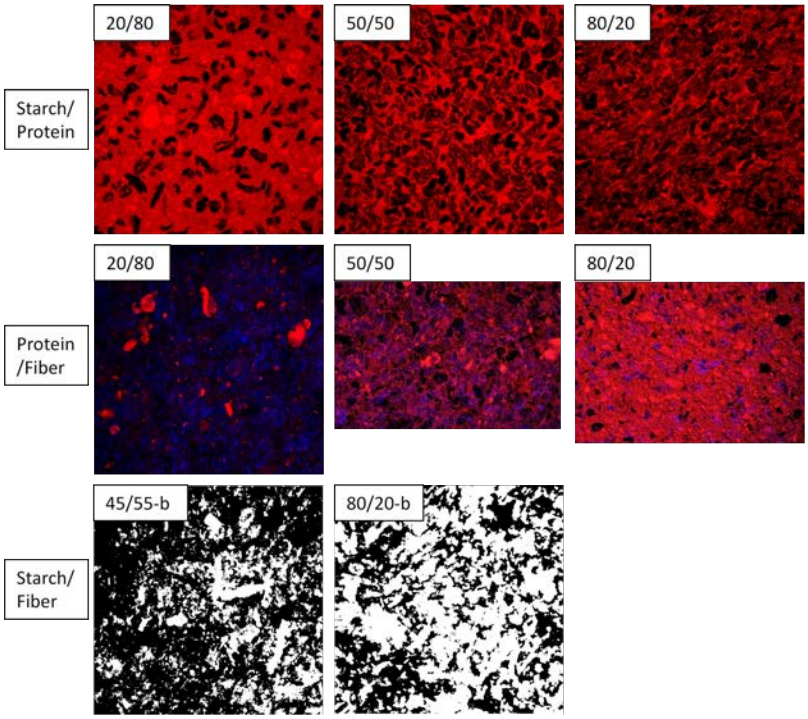


Figure 6.5: CLSM images of SI/PI, PI/FI and SI/FI binary blends. For the SI/FI blend the binarized images are depicted for better visibility. Protein is stained red and fibre is stained blue, starch appears as black. In the binarized images of SI/FI blends, fibre is white and starch is black. For complete overview see Appendix Figure A 6.4.

in those blends. Therefore, the relative area fractions were quantified by image analysis of the stained components *protein* and *fibre* in the CLSM images, listed in Table 6.3 (binarized images Appendix Figure A 6.4). The area fractions were used to estimate the volume fractions of the components in the paste. The unstained areas were added to *starch*. Isolate area fractions were calculated from the component area fractions (equation 6.9) and the isolate composition for a better comparison.

The mass fractions (polymer blending law) and the component area fractions were comparable, indicating that the polymer blending law predicted the fraction behaviour well. In the SI/PI blend, PI formed the continuous and SI the dispersed phase for all component ratios according to the result analysis from the polymer blending law. The mass fractions (polymer blending law) and the component area fractions (CLSM) of SI/PI(17/83) and (46/54) are comparable, indicating that the polymer blending law predicted the fraction behaviour well. A continuous red *protein* network was still visible at SI/PI ratio of (77/23), with distinct *starch* granules dispersed (Figure 6.5, Appendix Figure A 6.4). The *starch* fraction in this blend appeared more entangled, possibly interrupting the continuous *protein* network. The isolate area fraction of SI is much lower, and that of PI is much higher than predicted by the polymer blending law. That could be a result of such a network interruption, which is not reflected in the isostress, isostrain, or bicontinuous fraction behaviour. Therefore, the CLSM images possibly suggest that the influence of SI and PI on each other at high SI concentrations follows another behaviour than predicted by the model. In the PI/FI blend, according to the polymer blending law analysis, a transition from an isostrain to an isostress fraction behaviour occurred between PI/FI(08/92) and (41/59) and therewith, an inversion from a continuous FI to a continuous PI fraction. In CLSM images at PI/FI(08/92) the FI's black and blue *starch* and *fibre* formed a continuous matrix in which the red stained *protein* was dispersed. The inaccurate prediction of PI/FI(41/59) might result from the phase inversion, hence a discontinuity in viscosity that could lead to a lower predictability by the

Table 6.3: Area fractions determined with image analysis of CLSM images of the binary blends. Component area fractions were converted to isolate area fractions to take the impurity of the isolates into account.

| Blend | Isolate ratio | mass fractions (Table 6.2) | component area fraction | | | Mass fractions | | |
|---|---|---|---|---|---|---|---|---|
| | | | *starch* | *protein* | *fibre* | SI | PI | FI |
| *SI/PI* | 17/83 | 22/78 | 22 | 78 | | 19 | 81 | |
| | 46/54 | 58/42 | 52 | 48 | | 47 | 53 | |
| | 77/23 | 84/16 | 60 | 40 | | 55 | 45 | |
| *PI/FI* | 08/92 | 15/85 | 63 | 9 | 28 | | 20 | 80 |
| | 41/59 | 29/71 | 19 | 57 | 24 | | 64 | 36 |
| | 84/16 | 74/26 | 22 | 66 | 12 | | 79 | 21 |
| *SI/FI* | 01/99 | 09/91 | 47 | | 53 | 13 | | 87 |
| | 37/63 | 65/35 | 77 | | 23 | 60 | | 40 |

polymer blending law in that range.
The predictability around phase inversions could be improved by following the approach of Schreuders et al. (2020). They used $n$ as a fitting parameter to predict the fraction behaviour of *protein* blends between different behaviours, such as isostrain and bicontinuous. That way the morphology of blends undergoing a phase transition might be more accurately described.
Two behaviours resulted in a good prediction for the SI/FI blend; a transition from isostrain to isostress or a transition from isostrain to bicontinuous. The predicted isostress fraction behaviour described a continuous FI fraction with SI dispersed, which did not correspond with the image observation. The image might instead depict a bicontinuous fraction behaviour; at SI/FI(37/63), the *fibre* (blue) and *starch* (black) agglomerates rather resemble bicontinuous behaviour.

To validate the polymer blending law, the calculated isolate area fractions were used as input for the mass fractions $\varphi$ (equation 6.1), at all ratios. The water uptake a was newly obtained by fitting the storage modulus, minimizing the sum of squares (Section 6.3.6). The validation confirmed the selected behaviours at all ratios. However, for some ratios also bicontinuous behaviour was validated, e.g. at high *starch* concentration in SI/PI, or around the phase transition in PI/FI and SI/FI. That supports the hypothesis that at changing fraction behaviours the parameter $n$ should consider such changes ( $-1 < n < 0.2$/ $0.2 < n < 1$), e.g. by extending the range of possible fraction behaviours.
In general, it is remarkable that the isolate models could mostly predict the blends well, even though the isolates varied in component purity. The similarity of the storage moduli of SI and FI in the blend's concentration range could be an explanation for the good description of the blends that contained FI. In this context, it cannot be expected that an equally good prediction would be the result, with an impure fibre isolate containing *protein* instead of *starch*. We conclude from these findings that, within this concentration range, a prediction based on the isolate concentration can describe the blends' microstructure.

That might be useful, when quick approximations of a blend microstructure are required. For more thorough insight into the morphology, e.g. phase transitions in multi-component blends, models based on composition might be more informing.
The insights gained in this research can be linked to our previous work (Lie-Piang, Möller, et al., 2021), where we used empirical models to describe the viscosity of mildly refined ingredient blends. Similarly there, the blend viscosity could also be described well by the ingredient concentration. We conclude that to predict high *fibre* contents in mildly refined ingredients, the empirical models need to be trained more in that range, due to the change in phase behaviour we observed here.

## 6.5 Conclusions

The fraction behaviour in binary blends of protein, starch and fibre isolate could be determined by the modified polymer blending law for biopolymers. The selection from different fraction behaviours was possible by evaluating the parity between the model predictions and the experiments, the storage modulus of the blends, and the water uptake of the single fractions in the blends. The relative water uptake correlated with the strength of the isolate fraction in the blend. The predicted mass fractions and the isolate ratios (wt.%) were not the same, nor did they increase proportionally. This indicated that the water distribution did influence the blend properties. CLSM images confirmed the microstructure suggested by the modified polymer blending law. We found that the prediction based on the isolate concentration described the microstructure of the binary blends well for most SI/PI, PI/FI and SI/FI blends. In addition, we showed that the phases transition at increased fibre contents, and hence the microstructure altered when changing fibre contents. The model predictions were less good around these phase inversions, as at these concentrations, the component behaviours and thus the water distribution between the fractions

varied. Therefore, when phase inversions or network interruptions occur, the polymer blending law should also consider other behaviours than isostress, isostrain and bicontinuous.

The modified polymer blending law provides a tool with which mechanical explanations and quantifications of the water distribution and the structure in multi-component blends can be obtained. These tools can facilitate the application of lower refined ingredients in foods by providing more insight into the mechanical phenomenon that explain the fraction behaviour.

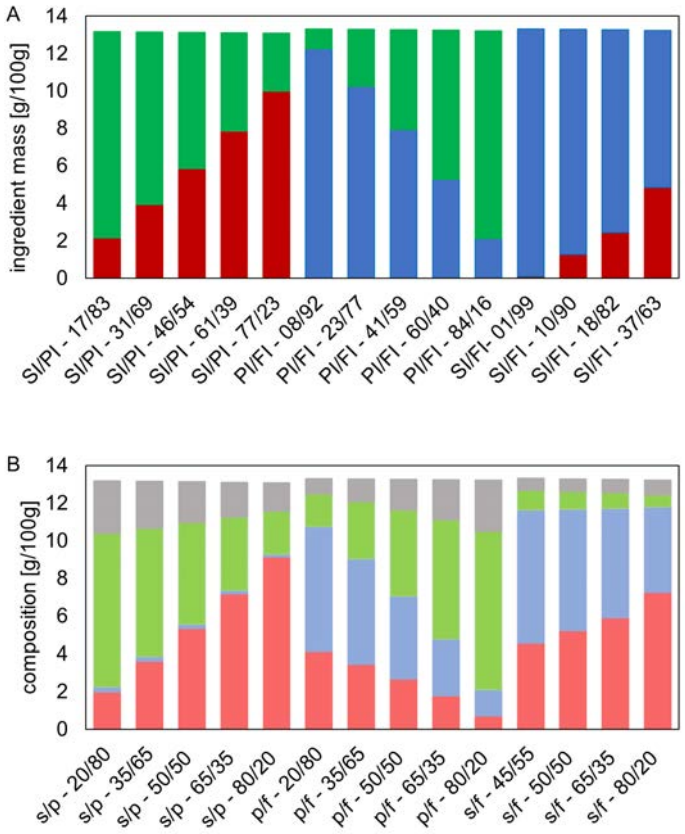


Figure A 6.1: Compositions of binary blends depicted in isolate mass (A), SI (■), PI (■) and FI (■) and in component mass (B), *starch* (■), *protein* (■) and *fibre* (■), both based on dry matter content. *Starch*, *protein* and *fibre* where here abbreviated by s, p and f and followed by the component ratio to describe the binary blend. The rest (■) was calculated by difference from the isolate masses.

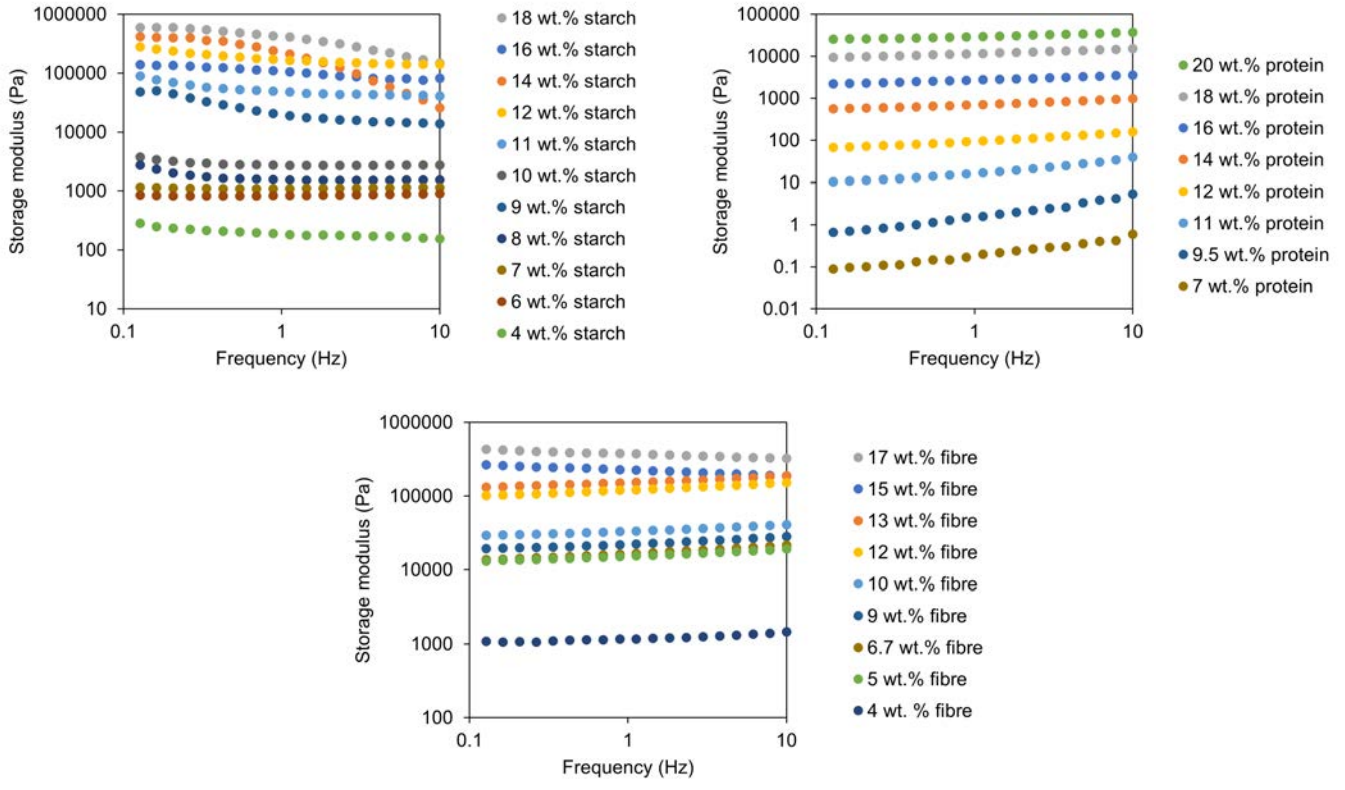


Figure A 6.2 Storage modulus plotted over Frequency of (A) Starch (4-18 wt.%), (B) Protein (7-20 wt.%), and (C) Fibre (4-17 wt.%).

Table A 6.1 Binary blend mass fractions of SI, PI and FI determined by rheological methods at different blend ratios of the isostrain n=1, isostress n=-1 and bicontinuous n=0.2. **Bold** ratios are the selected behaviours based on Section 6.4.7. *Italic* ratios were not in parity with the experimental blend modulus.

| Blend | Isolate ratio | Mass fractions | | |
|---|---|---|---|---|
| | | n=1 | n=-1 | n=0.2 |
| SI/PI | 17/83 | *34/66* | **22/78** | *18/82* |
| | 31/69 | *51/49* | **41/59** | *32/68* |
| | 46/54 | *64/36* | **58/42** | *46/54* |
| | 61/39 | *76/24* | **73/27** | *62/38* |
| | 77/23 | *87/13* | **84/16** | *88/12* |
| PI/FI | 08/92 | **15/85** | *04/96* | 02/98 |
| | 23/77 | **18/82** | *12/88* | 12/88 |
| | 41/59 | *26/74* | **29/71** | 48/52 |
| | 60/40 | *42/58* | **48/52** | 71/29 |
| | 84/16 | *66/34* | **74/26** | 87/13 |
| SI/FI | 01/99 | **09/91** | *01/99* | *0/100* |
| | 10/90 | **18/83** | *10/90* | 07/93 |
| | 18/82 | *23/77* | **23/77** | **24/76** |
| | 37/63 | *44/56* | **49/51** | **65/35** |

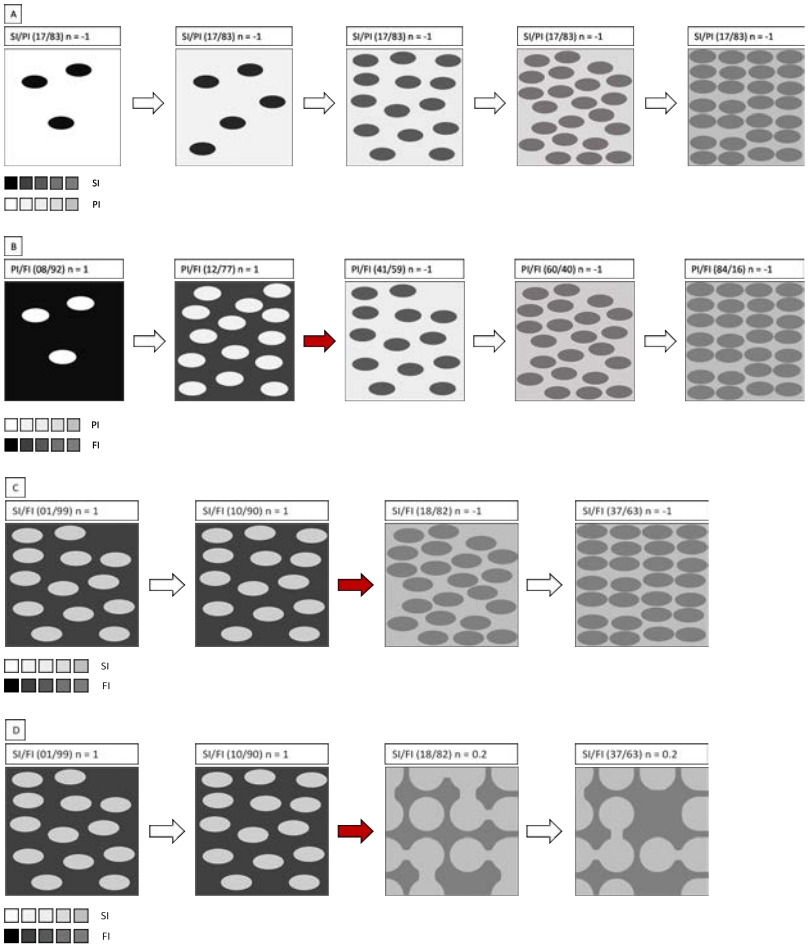


Figure A 6.3: Estimated behaviour of (A) SI/PI, (B) PI/FI and (C) SI/FI at SI/PI concentrations of (17/83), (31/69), (46/54), (61/39) and (77/23) for (A); at PI/FI concentrations of (08/92), (23/77), (41/59), (60/40) and (84/16) for (B) and at SI/FI concentrations of (01/99), (10/90), (18/82), (37/63) for an isostrain to isostress transition (C) and for an isostrain to bicontinuous transition (D). Colour from light to dark refers to increasing concentrations of the respective isolate. Red arrows indicate a phase inversion.

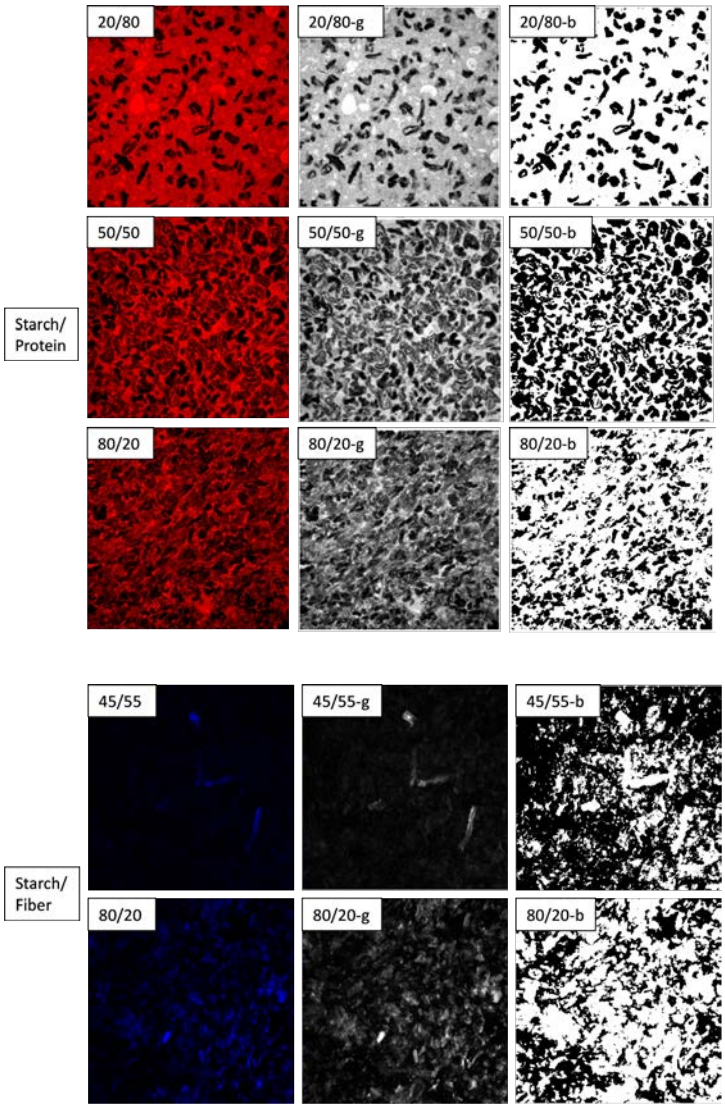


Figure A 6.4-1: CLSM images of binary blends, with image analysis conversion to graythresh images (g) and binarized images (b) for phase quantification. For Protein/Fibre the images were converted to graythresh and binarized images for the blue and the red stain (graythresh-red (g/b), binarized-red (b/r), graythresh-blue (g/b), binarized-blue (b/b))

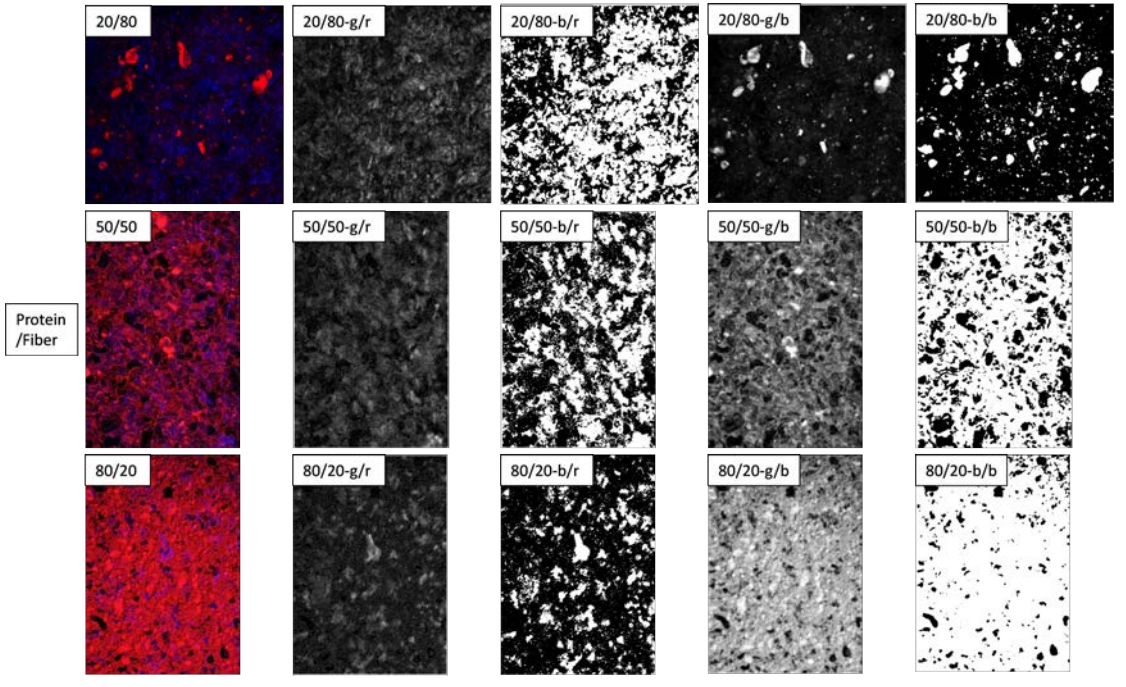


Figure A 6.4-2: CLSM images of binary blends, with image analysis conversion to graythresh images (g) and binarized images (b) for phase quantification. For Protein/Fibre the images were converted to graythresh and binarized images for the blue and the red stain (graythresh-red (g/b), binarized-red (b/r), graythresh-blue (g/b), binarized-blue (b/b))

# Chapter 7

## A novel process to produce stratified structures in food

Anna Cäcilie Möller, Atze Jan van der Goot, Albert van der Padt

Submitted

## Abstract

A method to create stratified structures with static mixing elements initially developed for the plastic polymer industry is investigated here as a new route for structuring food dispersions. Food dispersions of different viscosities were structured with static mixing elements to investigate the potential of the method for foods. Differently coloured chocolates were used as the model products. The viscosity of the chocolate was controlled through the addition of pea fibre. The first step was the formation of 2 to 8 layers, with the two differently coloured chocolates. Then, the chocolate dispersions were layered into 256 layers with an approximate layer thickness of 60 μm. Layer formation was facilitated when using similar paste viscosity and when slip was induced through wall coating with vegetable oil. Uniaxial cutting tests of the layered chocolate indicated that layering resulted in different mechanical properties, parallel and perpendicular to the layers. Fibre orientation in the direction of flow was observed, resulting in the potential to induce anisotropy, additional to the layers. The higher viscous dispersions, wheat dough and melt cheese, could also be structured into layers, although the force constraints of the experimental set-up were reached. Mid-stream additions were added to produce strand structures instead of layers, resulting in higher hierarchy structures but less uniformity.

## 7.1 Introduction

Recently, renewed interest was shed on laminar mixing methods by which two or more fluids are extruded into layers that are stretched and folded on top of each other, respectively. The key element of this compounding process is a static mixer into which two or three fluid streams are fed in parallel, forming layers, due to the laminar flow conditions (at low Reynold numbers). This is in contrast to mixing processes in mixers that are based on turbulent fragmentation and reorientation of the volumes to be mixed. Similarly as in microfluidic processes, streams of fluid are directly controlled by the geometry of the device. Such repetitive stretching and folding has been demonstrated for polymer melts but also for oil/water emulsions (Hofmann, Bayles, & Vermant, 2021; Schaller, Neerincx, & Meijer, 2017). The application of laminar fractal mixing for food structuring has so far not been discussed. Natural food structures are heterogeneous, complex and mostly anisotropic. Structural and textural properties in food influence our perception and taste experience (Lillford, 2016). Therefore, methods to produce structures in foods are widely applied. Especially recently, efforts have been undertaken to copy existing product structures from novel raw materials to mimic 'traditional' foods, such as meat. These methods include extrusion and 3D printing (Nachal, Moses, Karthik, & Anandharamakrishnan, 2019; Sandoval Murillo, Osen, Hiermaier, & Ganzenmüller, 2019). Extrusion is widely applied in food production to obtain specific shapes and textures. Extrusion is still considered a complex process, due to the fact that multiple sections are highly linked through an interdependency of the process conditions and ingredient properties (Pietsch, Karbstein, & Emin, 2018). Consequently, extrusion is still difficult to control. 3D food printing, usually extrusion based, offers the production of custom made foods (Liu, Zhang, Bhandari, & Wang, 2017), and flexible and rapid prototyping (Ma, Schutyser, Boom, & Zhang, 2021). So far the application of 3D printing for food is still limited by its scalability.

In this chapter, the potential of laminar fractal mixing is discussed and demonstrated for the structural design of food. In particular of multi-compo-

nent food formulations. Laminar fractal mixing exploits the combination of different channel elements. These elements can be arranged differently, to design pre-defined structures according to controlled assembly and product requirements. As an example, layers can be continuously formed from macro to microscale. In bakery industry, laminar structuring could lead to process improvements, by avoiding dough weakening during common kneading processes (Cappelli, Bettaccini, & Cini, 2020; Muscalu, Voicu, Istudor, & Tudor, 2020). In other applications the method can lead to new flavour experiences, potentially by combining materials of different texture and composition, i.e. a protein network and a fat phase. Furthermore, variation in taste, such as sweetness of the phases can be exploited for taste sensation. Stretching of fluid material in a channel can induce orientation of the components in the fluid. Orientation in fluid flow has been shown for fibre-like structures in polymer melts (Kugler et al., 2020), as well as for food polymers, i.e. caseins micelles during Mozzarella cheese production (McMahon, Fife, & Oberg, 1999), and could thus introduce additional anisotropy into the structures.

As the method is dependent on laminar flow conditions the material properties are important to ensure structure formation solely based on laminar flow in the channel geometry. Viscosity differences, normal stress differences or interfacial tension between the materials can induce distortions, making it less trivial to reach the intended structure (Neerincx et al., 2021). Furthermore, the smallest achievable domain size that can be obtained by this relatively easy compounding method is limited by the balance between the interfacial, inertial and viscous forces (Hofmann et al., 2021). This research aims to investigate the applicability of laminar fractal mixing to produce pre-defined structures with food materials. At first, the theory of the structuring method is reviewed, followed by an elaboration on its potential to produce anisotropic substructures. Then, first experiments are presented that describe the possibilities to form uniform layers and strands with food materials of different viscosities. Finally, the potential of laminar fractal mixing in food processing is discussed.

## 7.2 Theory

### 7.2.1 Principle of layer multiplication

Laminar fractal mixing is based on the baker's transformation. This operation received its name from dough kneading in the baking trade. It includes a stretching step of the material, whereafter the stream is either folded, or cut and stacked onto each other (Figure 7.1).

Fractal mixers are static mixers, hence no parts of the mixer itself are moving. Within the mixers, the stream of stacked fluids is split, stretched and once again stacked onto each other, resulting in an exponential layer multiplication, upon repetition (Neerincx & Meijer, 2013). Figure 7.1 demonstrates the fundamental steps of fractal mixing. Fluid volumes, here marked in black and white for the explanation, are stretched and then folded, or cut and stacked, to fill the size of the original volume element. Different channel designs were designed to enable this operation. Examples are shown in Figure 7.2. The scheme in (A) is a Chen mixer with elements for stretching and folding, (B) shows a stretching and stacking element. These mixers were improved with the objective to optimise the regularity of the layering even after multiple repetitions of the operation. Mixers that contained initially rotating operations of the fluid stream (Figure 7.2) (Neerincx, Denteneer, & Meijer, 2011; Neerincx, Hellenbrand, & Meijer, 2011; Neerincx & Meijer, 2013; Schaller et al., 2017), were in more recent developments avoided to minimize distortions of the structures (Neerincx et al., 2021). The optimized mixing scheme is depicted in Figure 7.3. The design was focused on a constant cross section of the flow. The first stretching in the direction of the flow is induced by a vertical compression step. The compression is subsequently reversed by a lateral extension, to return to the original channel cross section. Thereby layering the volumes and avoiding interface rotation.

Further developments included the addition of layers oriented perpendicular to the initial layer surface (Figure 7.5, B, C). With subsequent layer multiplication

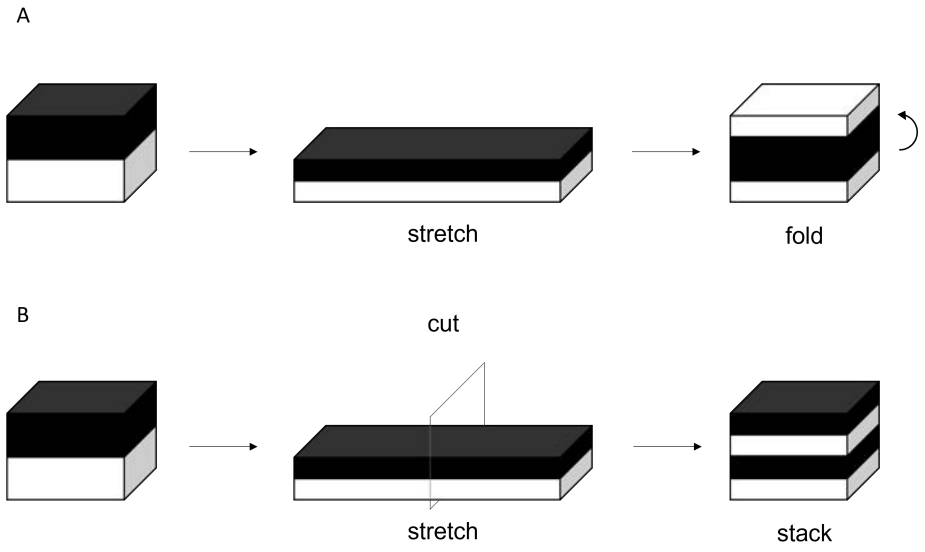


Figure 7.1 Principle of the baker's transformation either by (A) stretching followed by folding, or (B) by stretching followed by cutting and stacking. Graphic adopted from (Schaller et al., 2017).

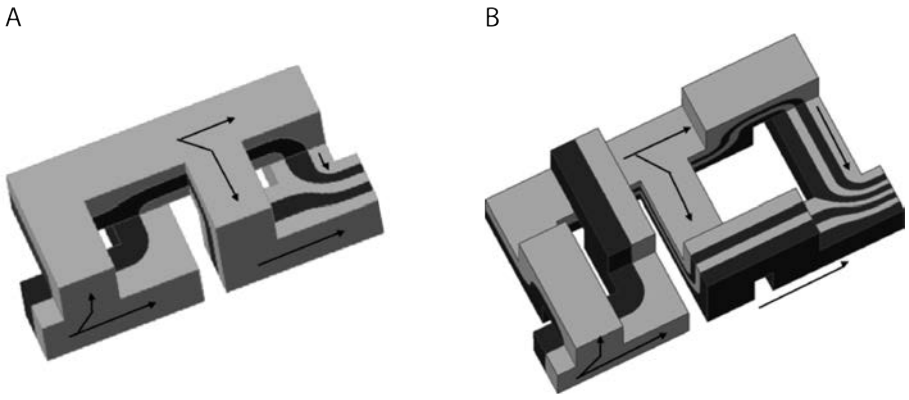


Figure 7.2 The Chen mixer (A) makes use of the stretching-folding operation, the Dentincx mixer (B) makes use of the stretching-stacking operation. Both mixers include interface rotation to reorient layers parallel to each other for layer multiplication. Images reprinted with permission (Schaller et al., 2017).

the perpendicular layer addition increases the hierarchy of the structures. By repeating the layer additions and multiplication steps, higher hierarchy structures could be formed (Neerincx et al., 2021; Schaller et al., 2017).
Layer formation through laminar fractal mixing has been demonstrated to yield uniform structures of polymer melts, as well as of Nivea cream samples (Neerincx et al., 2021; Schaller et al., 2017). However, the formation of microstructures, in particular those with a more complex pattern resulted in less uniform structures. Even though the replacement of the rotation operation improved the uniformity of the hierarchical structures a lot (Neerincx et al., 2021), vertical stretching of horizontal layers still distorted the layers, comparable to previous results (Neerincx & Meijer, 2013).
So far, the method development and application of laminar fractal mixing was mainly focused on structural uniformity. The stacking has been shown to result in layer multiplication, stretching of the liquid stream caused layer thinning and served to maintain the continuity of the process (Hofmann et al., 2021; Schaller et al., 2017). We noted that the stretching step in this structuring process can have additional promising effects on the substructure of the different fluids in the stream, such as the orientation of the material in the flow direction. These effects have so far not been further described for laminar fractal mixing, and their potential benefits are therefore elaborated on in the following Section.

### 7.2.2 Stretching to induce fibre orientation in fluid flow

In a fluid, containing fibre-like components, a convergence of the channel induces extensional flow, which may result in orientation of these components in the direction of flow (Hsiao, Sasmal, Ravi Prakash, & Schroeder, 2017; Rivlin, 1948). Such fibre orientation could introduce an additional level of anisotropy in the substructure of the layers.
The latest laminar static mixer geometries include a short stretching step (Figure 7.3), according to the baker's transformation. The stretch is induced by

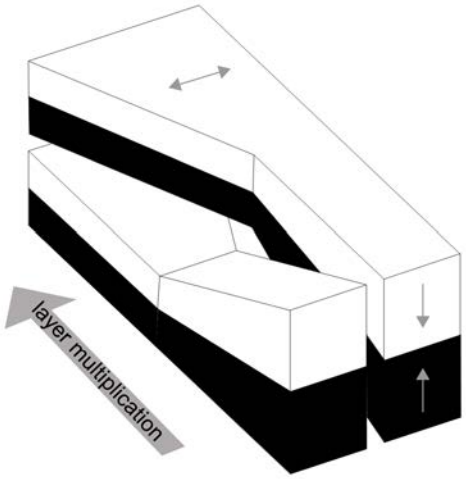


Figure 7.3 Layer multiplication with converging and diverging channel adopted from (Neerincx et al., 2021), grey arrows indicate the vertical compression of the stream through the converging channel, and the lateral extension of the stream through the divergence of the channel.

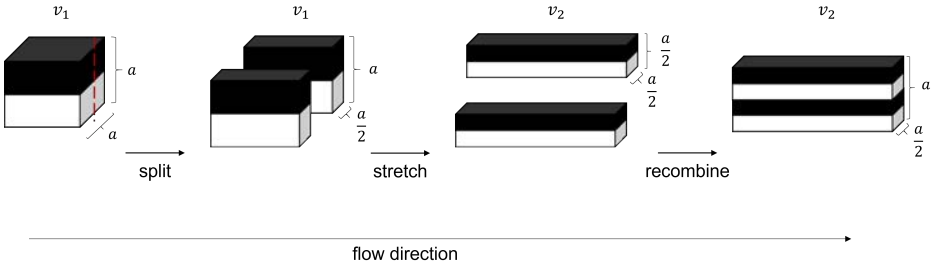


Figure 7.4 Layer multiplication with stretch induced by vertical convergence to half of the channel cross section, with subsequent stream recombination to retain extensional stress on fluid. $v_1$ is the flow velocity before channel convergence, $v_2$ is the flow velocity after channel convergence.

converging the channel geometry in the vertical direction. Accordingly, the convergence can induce extensional flow, which induces extensional stress on the fluid. In order for a fibre-like component or molecule to orient in a fluid flow, it needs to be exposed to the extensional flow for sufficient time or distance (Vincent & Agassant, 1985). Subsequent to stretching the material, the channel diverges into the horizontal direction (Figure 7.3), which can result in decrease of the extensional stress. Materials can be constrained in te stretched conditions for a longer time and distance, by avoiding the channel divergence. Recombination of the stretched layers at the reduced channel cross section area allows to keep the flow velocity constant after stretching (v2), and maintain the extension on the fluid (Figure 7.4). The iterative decrease of the channel dimensions could be overcome by the addition of layers perpendicular to the original layers, and concurrently also increase the hierarchical structure of the material.

## 7.3 Experimental

### 7.3.1 Materials

Multiflux elements were drawn in SolidWorks Software (Dassault Système SolidWorks Corp., France) according to the cutting-stretching-stacking design of (Neerincx et al., 2021) and processed in PreForm 3.22.1 (Formlabs Inc., USA) for 3D printing. The elements were 3D printed from Grey Resin V4 (Formlabs Inc., USA) on a Form 2 SLA 3D Printer (Formlabs Inc., USA) with a layer thickness of 0.16 mm.

Milk chocolate, dark chocolate and white chocolate (Delicata, Albert Heijn, The Netherlands), cheddar melt cheese (Cheddar Kaas, Jumbo, The Netherlands), wheat flour (Albert Heijn the Netherlands), and dill (Dille Vers, Jumbo, The Netherlands) were purchased from local supermarkets (Albert Heijn, the Netherlands; Jumbo, The Netherlands). Stained cocoa butter (white and black) was purchased online (BrandNewCake, The Netherlands). Yellow pea fibre isolate

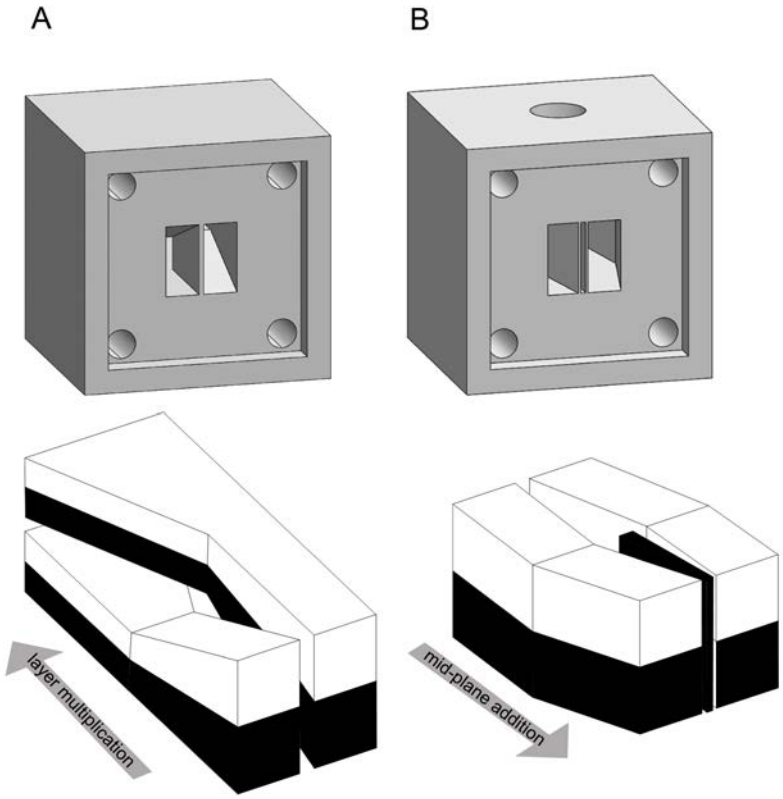


Figure 7.5 Flow profile in Multiflux elements (A) splitting serpentine element for layer multiplication and (B) mid-plane addition element. Geometry adopted from (Neerincx et al., 2021).

was purchased from Roquette Frères S.A. (St. Louis, USA), sodium caseinate powder was kindly provided by FrieslandCampina (The Netherlands).

### 7.3.2 Chocolate preparation

The chocolates were melted in a water bath at 40 °C. Black and white stained chocolate samples were made by mixing 200 g chocolate (white or milk) with 15 g white or black stained cocoa butter, respectively. To adjust the viscosity of white and milk chocolate, 5 g yellow pea fibre isolate was added to the milk chocolate mix, and 15 g pea fibre isolate was added to the white chocolate mix to increase the viscosity of the dispersion.

### 7.3.3 Melt cheese and wheat dough preparation

The cheddar melt cheese was tempered at 60 °C before the structuring experiments. 120 g wheat flour was mixed with 60 ml water and kneaded until a smooth dough was obtained. The dough was rested at 4 °C, overnight.

### 7.3.4 Structuring in static mixer

#### 7.3.4.1 Chocolate structuring

The Multiflux elements were assembled into a structuring channel. For layer formation the channel was assembled with up to 7 splitting serpentine elements (Figure 7.5A), an inlet and outlet part, and homogenizer elements (*'H'* and *'I'*), placed before and after the splitting serpentine elements, to improve layer thickness uniformity (van der Hoeven, Wimbergen-Friedl, & Meijer, 2001), (Figure 7.6).

The tempered materials were filled into pre-heated stainless steel syringes connected to the Multiflux elements. The syringes were mounted in a Texture Analyser Instron 5564 (Instron, USA), which allowed to set a constant force and record the displacement over time. A constant force was set to 150 N to obtain volumetric flow rates, which resulted in a shear rate of 0.3 $s^{-1}$ in the structuring channel. The channel was placed above a water bath of 40 °C to pre-heat the

elements prior to structuring, and to avoid early solidification of the chocolate at the walls.
By adding two differently coloured dispersions to the Multiflux channel, 4, 8, 16, 32, 64, 128 and 256 layers were formed. The layer formation of the stained chocolate mixes was calculated with the following equation (Neerincx et al., 2021):

$$b = 2^{n+1} \qquad 7.1$$

With *b* the number of resulting layers and n the number of layering operations. One layering operation results in 4 layers, two in 8 layers, three in 16 layers, up to seven, which gives 256 layers. With a channel width of 15 mm, the layer thickness after 7 folding operations corresponds to a theoretical layer thickness of approximately 60 µm. That is the maximum number of layers with which a layer thickness > 30 µm can be obtained. 30 µm is the limit for particle size above which the human palate can feel particles (Tiefenbacher, 2017), which we connect here to the layer thickness.

7.3.4.2 Wheat dough and melt cheese structuring
One stainless streel syringe was pre-heated for the melt-cheese sample, the other one was kept at room temperature. The pumps were connected to the Multiflux elements and a constant force of 1800 N was set, resulting in a shear rate of 0.02 s-1. Due to the higher viscosities of the wheat dough and melt cheese, higher forces were necessary to push the materials through the channel. The set force was limited by the constraints from the texture analyser, and this force did give lower low shear rate in case of this combination of materials compared to the shear rate obtained with chocolates. .
The Multiflux elements were placed into the freezer after structure formation to shorten the solidification time of the chocolate and to fixate the structure of the wheat dough-melt cheese samples. Subsequently, structures were collected and cross sections were prepared through cutting. The structures were photo-

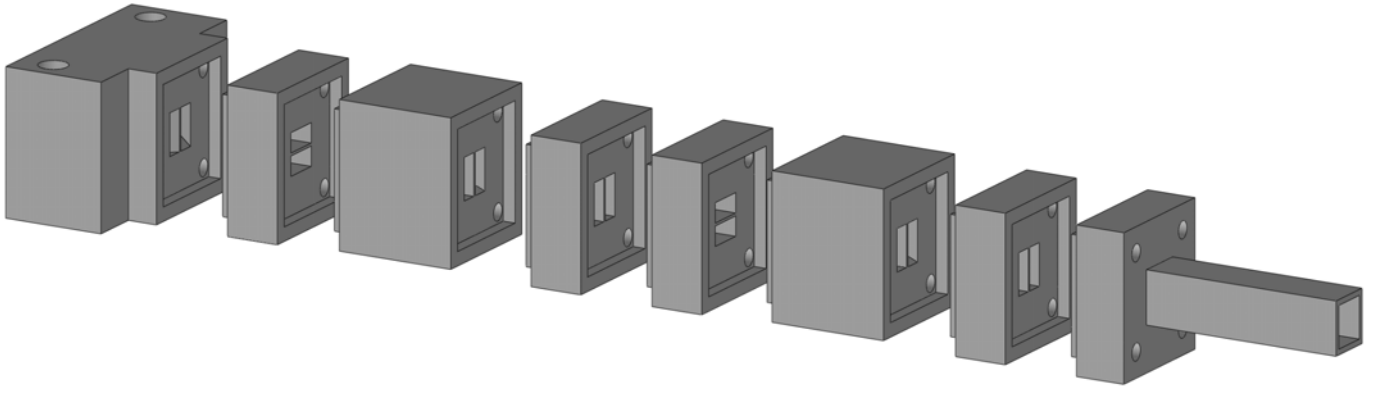

Figure 7.6: From left to right the layer formation set-up contains the following elements: Feed (F), Pressure Homogenizer (H), Splitting Serpentine Mixer (S), Pressure Homogenizer (I), H, S, I, Outlet (O). The set-up was extended for up to seven Splitting Serpentine Mixers to obtain 256 layers, with a layer thickness of ~ 60µm.

graphed with a Sony α6000 camera (Sony, Japan) equipped with a macrolens (Tokina, Japan).

7.3.4.3 Formation of hierarchical structures with mid-plane additions
Hierarchical structures were formed by adding a mid-plane to the layered structures (Neerincx et al., 2021). Four splitting serpentine elements were combined with the pressure homogenizer elements to a channel to produce 16 layers, followed by the mid-plane addition element (Figure 7.5) to form simple strand structures.

7.3.5. Rheological measurements
Rheological properties of the coloured chocolate, melt cheese and wheat dough were determined using the MCR-502 rheometer (Anton Paar GmbH, Graz, Austria). A cone-plate geometry (Ø 50 mm, CP50-4) was used and the shear rate was set to increase from 0.1 $s^{-1}$ - 100 $s^{-1}$ (chocolate), or 0.001 $s^{-1}$ – 10 $s^{-1}$ (cheese and dough). This was done to compare the flow responses of the materials with each other to allow conclusions of their influence on the layer formation.
The apparent viscosity was calculated at the respective shear rate in the channel, as:

$$\eta = \frac{\tau}{\gamma} \qquad 7.2$$

With $\eta$ representing the apparent viscosity, $\tau$ the shear stress, and $\gamma$ the shear rate.

7.3.6 Cutting tests
Uniaxial cutting of the structured chocolate samples was done with a Warner Bratzler blade in a TA.XT plusC Texture analyzer (Stable Micro Systems, UK) to determine the cutting force. The chocolate products were trimmed to a sample width and length of 15 mm and equal sample heights. The peak force was

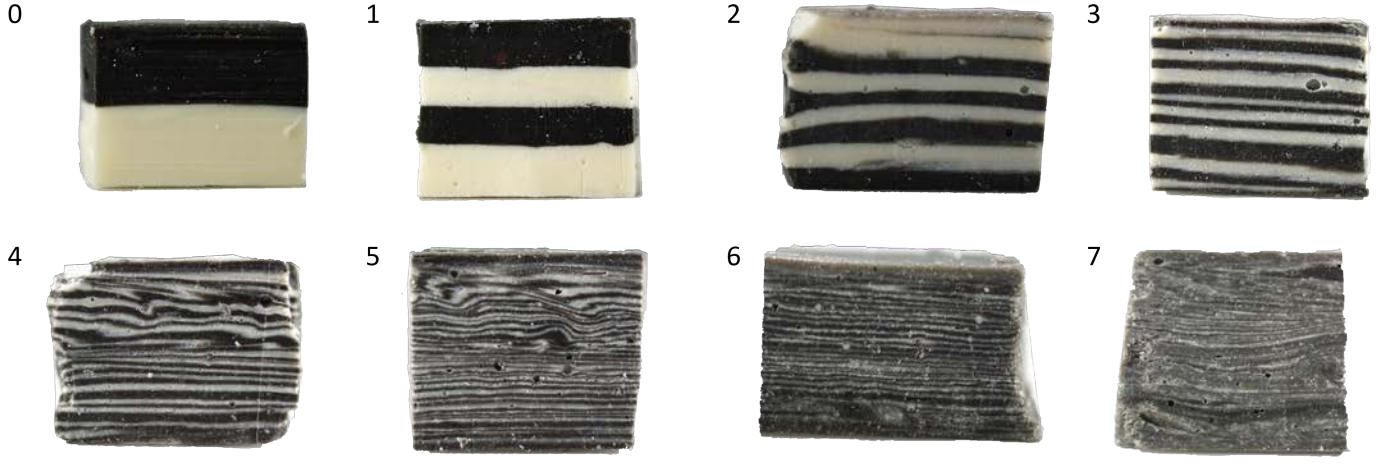


Figure 7.7: Images of layer formation with stained milk chocolate and stained white chocolate. (0) are the combined chocolates before the layering operations, (1) 1st layering operation, (2) 2nd layering operation, (3) 3rd layering operation, (4) 4th layering operation, (5) 5th layering operation, (6) 6th layering operation and (7) 7th layering operation.

used from the tests and compared for parallel and perpendicular cut chocolate samples.

## 7.4 Results

7.4.1 Formation of 256 layers with white and black stained chocolate mixes

Milk and white chocolate were stained with black and white cocoa butter, respectively for better distinction of the layers. The viscosities were adjusted with yellow pea fibre isolate. The viscosities of the black and white stained chocolate mixes were similar over a temperature decrease from 40 to 20 °C (Figure A 7.1). Hence, during cool down in the channel, they remained in the same range. The volumetric flow of the chocolate through the channel was approximately 14 ml/min, which corresponded to a shear rate of around 0.5 $s^{-1}$. The viscosity of the chocolates and the shear stress on the chocolates was approximately the same in this range (apparent viscosity $\eta_{white}$=32 Pa·s ± 6 Pa·s, $\eta_{black}$=33 Pa·s ± 5 Pa·s) (Figure A 7.1), and might thus not induce distortions during layer formation (Neerincx et al., 2021).

The layer formation of stained chocolate mixes in the Multiflux channel is depicted in Figure 7.7. Mostly uniform straight layers were produced. The layers were still countable after five layering operations, thus 64 layers.

7.4.2 Structural anisotropy

The mechanical properties of the product were determined parallel and perpendicular to the layers. It was assumed that the layered structure would affect the material stiffness. The required force to cut the 8 layer and 16 layer structures was higher when cut perpendicular to the layers than that of parallel cut samples. Moreover, cutting the samples along the layers resulted in even breakage, which was not the case when cut perpendicular to the layers (Figure 7.8). The peak cutting force was not determined for 4 layers, as the structures were too instable and broke too quickly along the layer surfaces during cutting

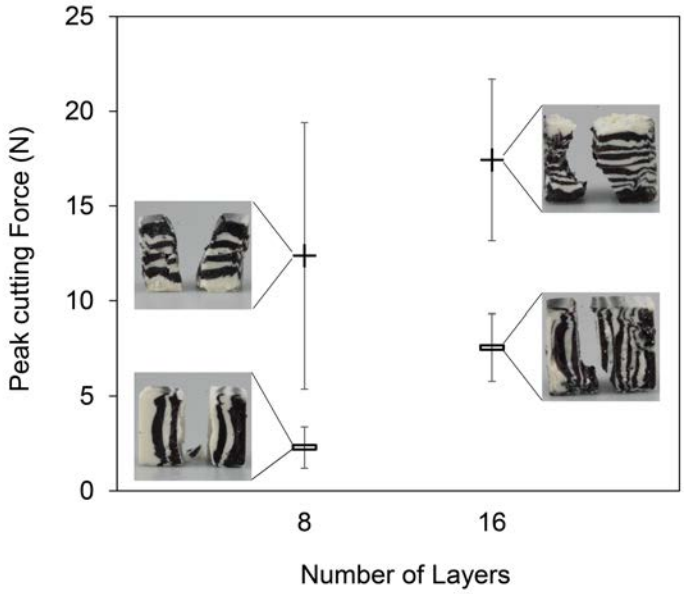


Figure 7.8: The cutting force was measured as the peak force required to cut samples. The cutting force was determined for a structure of 8 layers, and 16 layers, with cuts parallel (▭) and perpendicular (+) to the layers. Cutting profiles are depicted in images next to the corresponding modulus, for a better comparison of the structures.


Figure 7.9: Structured wheat dough and melt cheese into 0) 2 layers, 1) 4 layers, and 2) 8 layers.

for sample preparation.

### 7.4.3 Layer formation with high viscosity dispersions

The structure formation in the Multiflux mixer was additionally tested with wheat dough and melt cheese to investigate if two different materials of higher viscosities could also be structured. While the melt cheese was heated for the experiments, the wheat dough was kept at room temperature. The apparent viscosity of the wheat dough and melt cheese was about a factor 10 higher than those of the chocolate (Figure A 7.2). Accordingly higher force was required to push the material through the channel (Section 7.3.4). The volumetric flow that could be achieved with the set-up was 0.7 ml/min. That also leads to a longer residence time of the material in the channel. The corresponding shear rate was calculated to be around 0.02 $s^{-1}$. Although, the viscosities profiles differed, and were of different magnitude at the respective shear rate (apparent viscosity $\eta_{cheese}$= 39 MPa·s ± 15 MPa·s, $\eta_{dough}$= 23 MPa·s± 4 MPa·s), layers could be produced

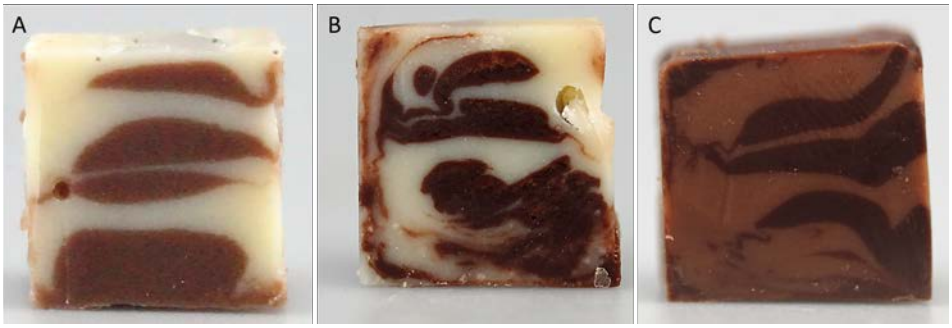


Figure 7.10: Layer formation (8 layers) of (A) milk and white chocolate, (B) dark and white chocolate, and (C) dark and milk chocolate.

(Figure 7.9). The cheese layer thickness was bigger than the dough layer thickness, possibly induced through differences in viscoelastic properties of the materials under stress (Figure A 7.2).

### 7.4.4 Factors influencing layer formation

For the structure formation with the splitting serpentine geometry, it has been previously described that matching viscosities are a prerequisite to produce uniform structures (Neerincx et al., 2021). To determine the range of viscosity dark, milk and white chocolate was used as a model material. All three varied in viscosity and shear stress over a shear rate of 0.01 to 100 $s^{-1}$, but followed similar viscosities curves (Figure A 7.3, A). At the corresponding shear rate in the structuring channel, layer formation of milk (apparent viscosity $\eta_{milk}$ = 18 Pa·s ± 0 Pa·s) and white chocolate ($\eta_{white}$ = 12 Pa·s ± 2 Pa·s) (Figure 7.10 A), white ($\eta_{white}$ = 12 Pa·s ± 2 Pa·s) and dark chocolate ($\eta_{dark}$ = 75 Pa·s ± 3 Pa·s) (Figure 7.10 B), and milk ($\eta_{milk}$ = 85 Pa·s ± 1 Pa·s) and dark chocolate ($\eta_{dark}$ = 190 Pa·s ± 56 Pa·s) (Figure 7.10 C) resulted in non-uniform layers, or distorted structures. The distinctly different viscosity properties of the three chocolate samples (Figure A 7.3), compared to those of the white and black stained chocolate samples, underline the importance of similar viscosity properties to avoid distortions. Hence, the similarity of the material viscosities is very relevant, while the magnitude of the material viscosity is less relevant, as uniform layers could be formed with the white and black stained chocolate samples, at relatively low apparent viscosities.

### 7.4.5 Structure formation of higher hierarchical level

A mid-plane addition element was added to the Multiflux channel to produce strands instead of layers (Figure 7.5 A) (Neerincx et al. 2021). For the production of strands by a mid-plane addition, white and black stained chocolate, as well as melt cheese and wheat dough were used to see if both materials could produce similar structures. After the mid-plane addition in the chocolate samples, the


Figure 7.11: The structure design (A) to produce a tree structure from 16 layers through a mid-plane addition, adapted from (Neerincx et al., 2021) and the experimental results with (B) white and black stained chocolate, and (C) melt cheese and wheat dough. (A and B) depict the structure after one mid-plane addition, (C and D) depict the structure after a subsequent layering operation.

tree structure described by Neerincx et al. (2021) were clearly observable, and all 16 branches could be observed (Figure 7.11 B). However, the branches were slightly bended towards the middle from both sides. Mid-plane addition in the cheese dough sample resulted in a more distorted structure. The mid-addition is clearly present, while the branches are even more bended. Due to the distortions not all 16 expected branches were visible. Neerincx et al. (2021) pointed out that these distortions are a result of normal stress differences in viscoelastic fluids, or differences in viscosities. The distortions of the 'branches' in the cheese-dough sample could be additionally induced through the elastic properties of the dough phase that formed wavy structures upon relaxation. The results in Section 7.4.4 already highlighted the importance of similar viscosities for layer formation. Here, it becomes obvious that in order to create hierarchical structures similar viscosities are even more important, as evidenced by the fact that the cheese dough structures are more distorted. Furthermore, the bended branches of the chocolate sample indicate that formation of hierar-

chical structure is even more difficult, as these distortions will likely enhance with subsequent hierarchy increases. The structures obtained by Neerincx et al. (2021) with black and white stained Nivea cream samples, were more uniform at slightly higher viscosities of 50 Pa and similar viscosity profiles. The lesser uniformity of the chocolate structure might be a result of the crystallization properties of the chocolate samples that could occur at the geometry wall, due to cool down of the geometry and material during structuring.

## 7.5 Discussion

The layer and structure formation via this laminar fractal structuring process seems a promising process for various food applications to produce layers or strand-like structures. We could show with our experiments that food dispersions of varying but matching viscosities can be layered in the Multiflux channel. The structure formation with the wheat dough and melt cheese was restricted by the maximum force of the experimental set-up. Schaller et al. (2017) connected the Multiflux channel to two single-screw extruders to process polystyrene and amorphous polyamide at high temperatures (200°C and 270 °C, respectively). A similar set-up here would allow to push higher viscosity dispersion through the channel and extend the possibilities to apply the method for foods.

The method offers additionally the potential to structure food dispersions on a substructure level. The convergence of the structuring channel to induce stretching of the fluid has the additional effect of component orientation in the stream. When polymer chains, such as proteins are exposed to an extensional flow for a sufficient amount of time or distance, those polymer chains can stretch and orient in the fluid (Hsiao et al., 2017; Rivlin, 1948). Such an alignment could induce an additional fibre formation in the food dispersion on a microscale. Protein alignment in food dispersions occurs for example in Mozzarella cheese kneading, i.e. oriented casein micelle chains. Fibre formation on

Figure 7.12: Cross section of four layer melt cheese sample, showing alignment of dill leaf in flow direction.

different length scales, strands on macroscale, and oriented and stretched molecules on microscale could result in enhanced anisotropy. Such structural levels could add to the elasticity and texture of the strands and hence to the textural properties of food.

In order to understand if an orientation in the direction of flow could be achieved in the Multiflux channel, even at the conditions tested in this research, dill leaves were added to melt cheese. The dill leaves were only added to one syringe filled with melted cheese and up to four layers were formed. Indeed, orientation in the direction of flow could be visualized by orienting a dill leaf in a four layer melt cheese sample (Figure 7.12). This indicates that anisotropy can be induced also within the layers, through orientation in the direction of flow. The continuity of the process, as well as its scalability makes it attractive for the production of a variety of food products. These include layered pastry, or novel chocolate structures, such as presented above. Layers can provide texture expe-

riences, and allow the combination of materials with different flavour profiles, e.g. differences in sweetness or saltiness (Kistler, Pridal, Bourcet, & Denkel, 2021). Furthermore, the strand formation in combination with the potential orientation of food proteins has potential to produce novel food structures with anisotropy at different length scales.

## 7.5 Conclusions

The static Multiflux mixer allowed the formation of stratified structures with food materials. The materials, which resulted in the most homogeneous layers after only two layer duplications were used to produce up to 256 layers of an estimated layer thickness of 60 μm. Chocolate served as a model material, due to its melting and solidification properties at intermediate temperatures. Layer formation with higher viscosity materials, such as wheat dough and melt cheese, could also be achieved. The presence of layer in chocolate-based product resulted in anisotropy in the mechanical properties. The required cutting force was lower when the product was cut in parallel direction, than when it was cut perpendicular to the layers. Probably, additional anisotropy can be induced in the structures in each layer as indicated by the oriented dill leaf in the direction of flow. The application of higher forces could open even new opportunities for structure formation, i.e. easing the fixation of the structures, and investigating the potential to induce orientation at smaller length scale in protein-rich dispersions.

# Appendix

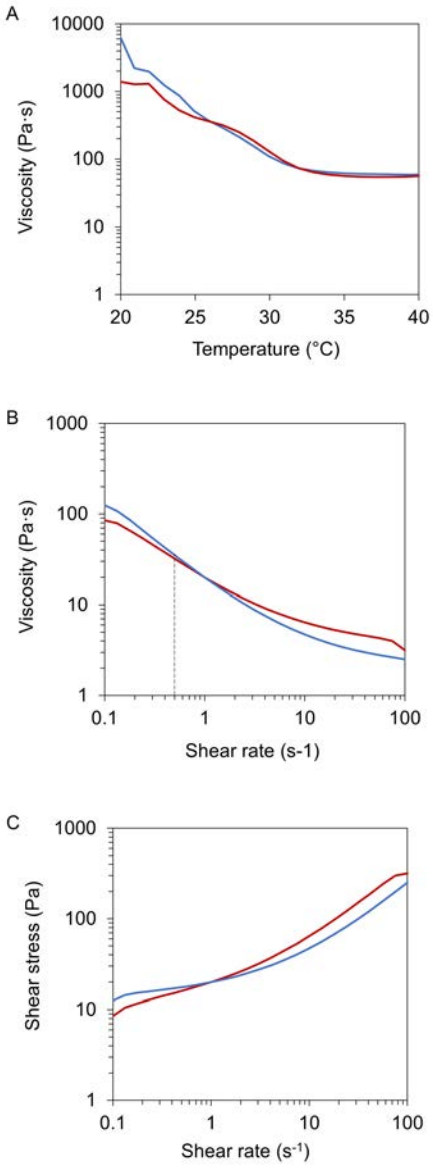


Figure A 7.1 Viscosity of black (▬) and white (▬) stained chocolate mixes (A) over a temperature ramp from 40 °C to 20 °C, (B) over shear rate at 35 °C and (C) shear stress against shear rate. Viscoelastic properties were determined in duplicate and a representative curve was selected.

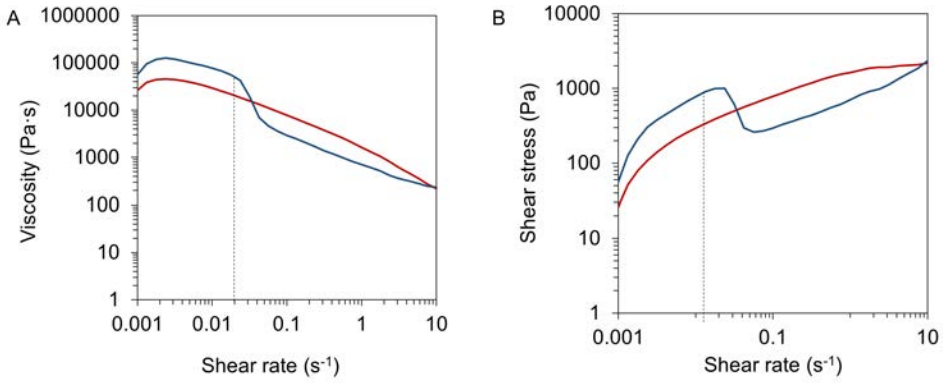


Figure A 7.2 Viscosity of wheat dough (▬) at 25 °C and melt cheese (▬) at 40 °C at increasing shear rates. Shear stress plotted against shear rate for the same samples (B). Viscoelastic properties were determined in duplicate and a representative curve was selected.

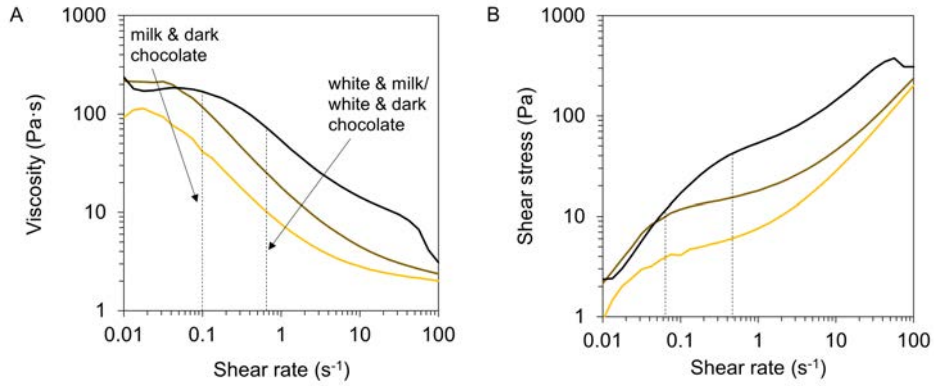


Figure A 7.3 Viscosities at the respective shear rates (dotted lines) in the structuring channel are depicted in (A), the shear stress against the shear rate is depicted in (C) for dark (▬), milk (▬) and white (▬) chocolate. Viscoelastic properties were determined in duplicate and a representative curve was selected.

# Chapter 8

## General Discussion

Plant protein fractionation is a process that begins with the structural break-up of the seed. For yellow peas, this can entail dehulling of the seed or can start with milling the whole seed. The structural break-up of the pea cotyledon determines the potential of the fractionation process (Pelgrom et al., 2015), and should therefore be considered part of the fractionation process. Recently, Geerts, et al. (2018) proposed to focus on functionality and thus on making more subtle changes to the raw material structure instead of aiming at complete break-up. This research continued on that path, and aimed to investigate pea protein fractionation from the structured crop. Furthermore, the properties of the resulting ingredients, and their potential to be used in product application was analysed. This chapter summarises the main findings of the previous chapters and discusses the challenges and opportunities resulting from the presented research.

## 8.1 Main findings

The research described in this thesis, started with developing routes that allow better use of the whole seeds from the dried yellow pea seed. Abrasive milling was evaluated as a pre-fractionation method for peas on its potential to enrich components before milling by removing the outer bran layer. *Chapter 2* highlights that abrasive milling did not serve as a method to pre-fractionate the pea cotyledon into protein and starch enriched fractions. Nevertheless, it is suitable for effectively removing and collecting the testa and embryonic axis that are rich in fibre and protein, respectively. Next, *Chapter 3* focuses on the structure of the pea cotyledon, specifically to describe the form in which protein and starch are present in it. In addition, the structural changes of these constituents during milling, air classification, and solubilisation in water were determined. It was concluded that the insufficient break-up and particle adhesion after milling the pea cotyledon limited the complete separation of the constituents through air classification. However, solubilisation of pea flour in water induced

further disentanglement of the particles and thus led to better separation. A relationship between structure and purity of fractions could be established and thus be used to elaborate on the potential of a fractionation method.
In *Chapter 4*, an additional driving force created by the use of water was investigated in the mild wet fractionation process. It was found that it is possible to use the mild wet fractionation process to extract high purity and yield protein and starch fractions. Compared to conventional wet fractionation, it was evaluated that similar fractions can be produced through this method. However, the presented mild wet fractionation method offered the advantage to omit chemicals, recirculate water and limit changes to the native state of the constituents. Additionally, the applied process steps during mild wet fractionation were similar to fractionation steps frequently applied in dairy industry. Thus, it was suggested to use dairy processing as a reference to evaluate the upscaling potential of the process. The protein fractions obtained through mild wet fractionation were further examined in *Chapter 5*. The protein composition of the different fractions varied, which was assumed to affect the functional properties. Therefore, the protein solubility and the gelation properties of the protein fractions were determined. Albumin containing fractions were in general more soluble than globulin containing fractions. Furthermore, the composition affected the gelation properties of the protein-rich fractions. The soluble protein gels were stronger than the non-soluble protein gels. This effect could be linked to the protein composition of the fractions. Moreover, the state of the proteins influenced the gelation properties as well; isoelectric precipitation decreased the gelation capacity of the fractions. Due to the influence of the composition and protein state on the functional properties, the separation into albumins and globulins might be desirable depending on the application and required functional properties. The pea protein fractionation applied in this process was compared to whey protein fractionation, pointing out the potential of using known techniques from the dairy industry.
For using the mildly fractionated ingredients, insight into their functional prop-

erties, particularly their structuring properties, is required.
Therefore, *Chapter 6* describes the use of the modified polymer blending law as a tool to provide mechanical explanations and quantifications of the water distribution and the structure in pea ingredient pastes. It was concluded that the viscoelastic properties and the contribution of the isolates and components are highly dependent on the water distribution. The insights obtained in this chapter can facilitate the application of mild fractionated ingredients and provide more mechanistic insight into the microstructure of multi-component blends. *Chapter 7* presents a novel method with which food materials can be structured. The application of this method for food ingredients is evaluated by producing products with ingredients of specific viscosities, within a distinct range. Furthermore, the opportunities to structure plant ingredients with this method into novel food products are discussed.

In this thesis we aimed to investigate the role of structure in fractionation and in the fractions' functional properties. We investigated the component interactions before, during, and after fractionation. The results show the dependency between the fractionation route and the structuring potential of the ingredients into a food matrix. Mild wet fractionation was demonstrated to be a promising route to separate pea into its constituents. The presence of water promotes particle disentanglement and results in enhanced separation. Furthermore, the process allows to obtain highly purified fractions with high yields. The obtained mild fractions varied in functional properties; harsher processing steps like isoelectric precipitation negatively impact the protein gelation. Moreover, the application of such ingredients requires to consider the effect of other components on the final functional properties of these newly formed ingredients. For most applications specific properties are required, and therefore a good understanding of ingredients functional properties in different conditions is essential. Altogether, the role of structure in crops, ingredients, and food should be connected by looking at the food production chain from raw materials, via

ingredients to final food products.

## 8.2 Comparison of different fractionation methods

This thesis investigates the complete and efficient valorisation of the pea seed to further develop the use of plant-based ingredients in foods. Mild fractionation methods usually aim to reduce the energy and water requirements, reduce the degree of refinement in the process or reduce the losses. Dry fractionation (DF) requires less energy and water compared to conventional wet fractionation (CWF) (Schutyser & van der Goot, 2011). However, the protein purity achievable by dry fractionation will remain limited. A hybrid fractionation method was proposed to increase the protein purity of these fractions, which is a combination of DF followed by an aqueous fractionation. This process increased the protein purity of the protein-rich fraction and required less water than CWF (Pelgrom et al., 2015). However, protein yield has not been considered for these processes. Lie-Piang, Braconi, Boom, & van der Padt (2021) investigated the impact of the fractionation method on the environment taking the protein yield into account. They determined that the global warming potential (GWP) of DF yellow pea protein was much lower than CWF pea protein. Still, the global warming potential of the hybrid fractionation method was only slightly lower than that of CWF pea protein. This outcome can be explained by considering that the protein yield of the protein fractions was highest for CWF (82 %) and lowest for the hybrid method (~28 %). The hybrid method includes the yield loss occurring in DF and requires an energy-intensive drying step. The mild wet fractionation (MWF) process developed by Geerts, Nikiforidis, van der Goot, & van der Padt (2017) was also included in the analysis; it yielded more than double the protein (87 %) than hybrid fractionation but only had a slightly lower GWP. The high GWP of all wet processes mostly results from the final drying steps. The mild wet fractionation method was further developed in this thesis and can now provide protein fractions with increased yield and purity through

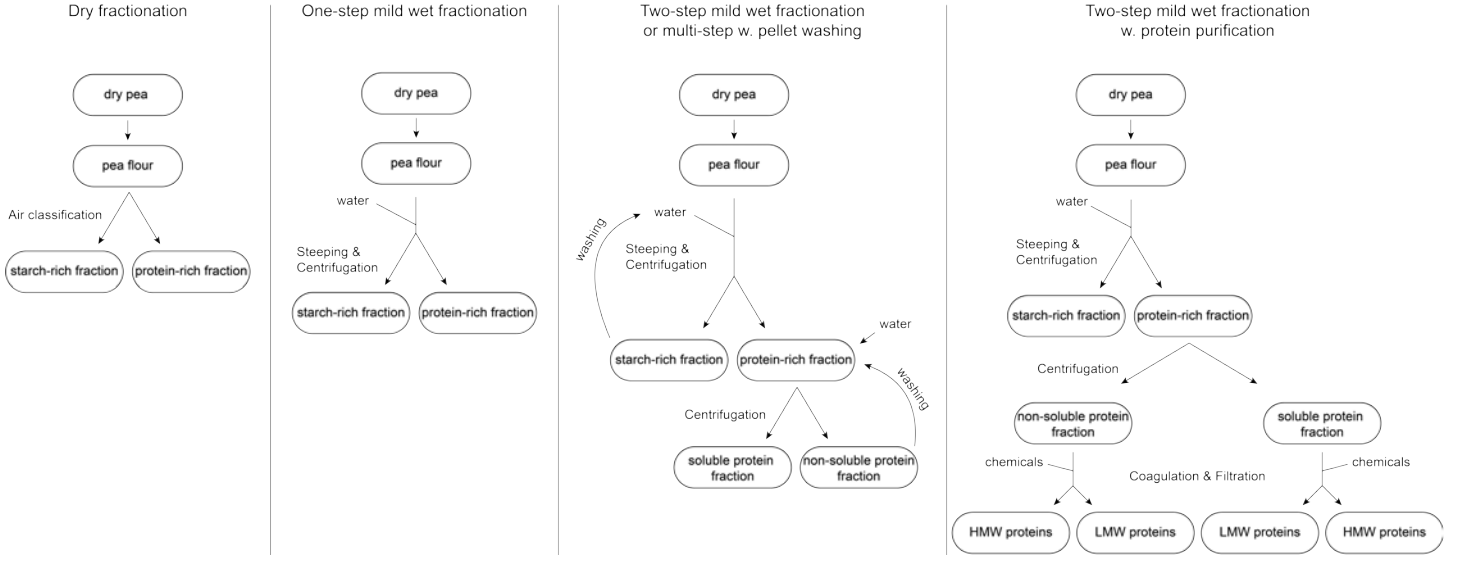


Figure 8.1 Portfolio of mild fractionation methods for tailored fractionation into varying ingredients.

washing and membrane filtration processes (*Chapter 4*).The comparison of fractionation methods through the protein yield helps to estimate the efficiency of a process. However, investigating the mild wet fractionation processes (*Chapters 4* and *5*) also considers the protein purity and functional properties. Especially the functional properties are not related to the protein yield and purity of a fraction and should therefore be considered in a comparison of fractionation methods. In this way, the most optimal fractionation method per application should be evaluated based on the ingredient functionality, similar to the approach introduced by Lie-Piang et al. (2021).

## 8.3 Mild fractionated ingredients: enriched or pure?

Focusing on ingredient functionality instead of purity in plant ingredients production has already been proposed (Van Der Goot et al., 2016). The newly proposed aim is to tailor the fractionation process to the required product application. The developed MWF process as described in *Chapter 4* can offer highly purified fractions with native protein functionality. Moreover, the process allows further fractionation into component classes, such as starch, protein, dietary fibres, and even different proteins and saccharides (*Chapter 5*). To be able to tailor the fractionation method to the product application, it is necessary to have options to choose from, like varying composition, purity, and functionality. Consequently, the motto should be "fractionate as much as necessary" instead of "as much as possible" to optimally benefit from the concept of tailored fractionation. Such approach will result in a portfolio of fractionation to obtain enriched fractions.

In case of MWF we now see the following possibilities: One step MWF followed by ultrafiltration to obtain isolates, two-step MWF followed by ultrafiltration for a further separation based on component solubility, and MWF with subsequent protein fractionation for specific pure ingredients, such as albumins, globulins or specific saccharides (Figure 8.1). In *Chapter 5* it becomes clear that

the amount of processing steps not only influences the yield and purity of the fractions but additionally the composition and functional properties. Therefore, the intended application of the fractions also needs to be considered to evaluate which fractionation steps should be applied. Moreover, the analysis of the GWP (Lie-Piang, Braconi, et al., 2021) highlights the impact of the final drying step on the energy requirements of a process. It could therefore be considered to omit drying steps for specific applications. For example, the soluble protein fraction obtained through MWF could be processed into a product without drying, similar to processes applied to cow's milk.

## 8.4 The relevance of a thorough understanding of the structure and structure formation

The protein composition influences the functional properties of an ingredient (Kornet, Veenemans, et al., 2021). However, both the protein composition and the other components present in an ingredient determine these properties (*Chapter 6*). That highlights that the application of ingredients in foods to obtain specific properties is not straight forward, and cannot be determined by summing up the contribution of every single component. Therefore, to develop tailored fractionation, the functional properties of an ingredient need to be thoroughly studied, as well as their behaviour in ingredient blends or even products. Empirical models can facilitate the application of different ingredients in foods to obtain specific structural properties (Lie-Piang, Möller, et al., 2021). They are also suitable for better insight into component interactions and their effect on the properties (*Chapter 6*). Such approach accounts for the whole final product, which is needed to establish a link between ingredient functionalities and product properties. In *Chapter 7* a novel route to produce stratified structures in food is introduced. It was found that to obtain uniform structures the viscosity of the food materials needed to be controlled and adjusted. In addition, the experiments also revealed that the flow properties induced by a

convergence of the die geometry can influence the structure formation. Such a convergence can contribute to extensional flow in the channel geometry and induce orientation of fibre-like components in the dispersion (Hsiao et al., 2017). The alignment of dill fibres in a cheese melt could be seen as a proof (*Chapter 7*) that such an orientation was achieved in the structuring channel. With yellow pea ingredients, alignment of proteinaceous phases might contribute to attractive products. These multi-layer or hierarchical structures ultimately need to be solidified to fixate the structure. Based on the experiments so far, we think that laminar fractal mixing is promising to structure food materials. Anisotropy can be created on different length scales, which might make the method also suitable to produce novel structures from protein-rich plant ingredients, such as from yellow pea.

## 8.5 The dairy industry is an example to establish a link between the ingredient and food industry

The concept of a close collaboration between the ingredient producing industry and the product production industry is not new. For example, in the dairy industry, the standard procedure is that the dairy factory purchases the farmer's raw material (milk). Then, the milk is processed into various products, such as cheeses, butter, and cream, and ingredients like whey protein and purified lactose. These different products and ingredients might be produced in different factories, but these factories are commonly part of the same head organisation. In comparison, in plant ingredient and product production, primarily large companies produce the ingredients, i.e., protein isolate, starch isolate, in single extensive facilities, while various other companies carry out product production in which those ingredients are used.

For a more detailed comparison of milk and pea, a list of products and ingredients produced from milk and yellow pea are depicted in Figure 8.2. The graphic shows potential products that can be produced from wet fractionated pea. Most

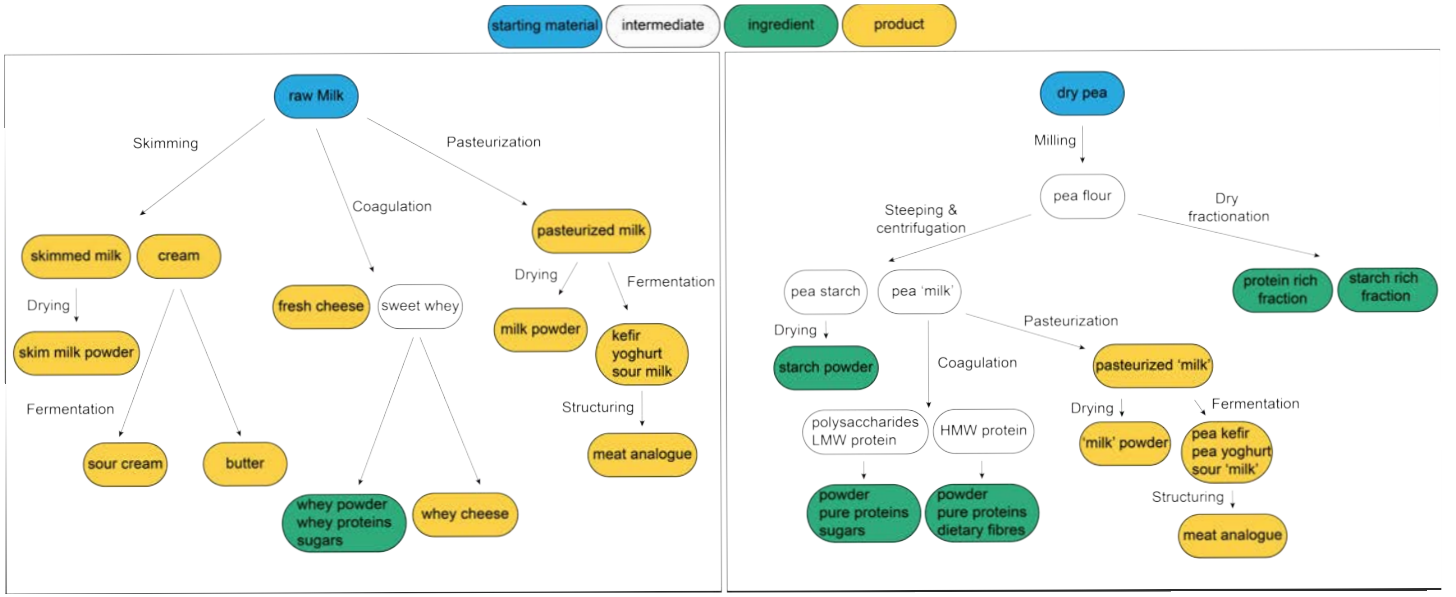


Figure 8.2 Graphical representation of milk ingredients and products, and pea ingredients and potential products, and their production pathways, respectively.

of those are adopted from dairy products, such as pasteurized 'pea milk', pea yoghurt or pea 'milk powder'. The manufacture of such products would strongly benefit if drying processes could be omitted, hence the products would be produced straight from the protein-rich 'pea milk'. This concept requires a more integrative plant product production. The harvested crops could be purchased from the farmers and processed into respective ingredients and products under the head of one company. In addition to starch-rich crops, oil-rich crops could be processed to expand the portfolio to oil-rich products (Romero-Guzmán, Jung, Kyriakopoulou, Boom, & Nikiforidis, 2020).
Moreover, the yellow pea crop contains around 2 % of oil (Tulbek, Lam, Wang, Asavajaru, & Lam, 2016), mostly neglected in pea protein fractionation (Lam, Can Karaca, Tyler, & Nickerson (2018), *Chapters 3, 4,* and *5*). Nevertheless, the oil might accumulate in one fraction through mild wet fractionation, thus accounting for a more significant part. An analysis of the oil content in the fractions could indicate if oil-containing products could also be produced from yellow pea.

## 8.6 Future research

Future research could be focussed on upscaling the mild wet fractionation process. In *Chapter 4,* it was proposed to use decanters and ultrafiltration coupled with diafiltration to obtain protein isolates from the soluble protein fraction. Upscaling experiments of mild wet fractionation could aim to purify the fractions with ultrafiltration further and evaluate the possibilities of decreasing the fractions' water content. Through ultrafiltration small peptides can be extracted from the protein fraction, which might contribute to an improved flavour profile of the fraction, as protein hydrolysates can develop bitter taste (Aluko, 2017). Furthermore, the extraction of small sugars from the protein fractions could be tested with ultrafiltration with different membranes, as proposed in *Chapter 5*. Such research could be conducted in close collaboration with the

dairy industry to use their vast knowledge of these processes.
Functional properties include ingredients' structuring ability and sensory and aesthetic attributes. These attributes open another large field of research that needs to be explored for these mildly fractionated ingredients. The complete valorisation of the pea components leads to the co-extraction of antinutritional components, which are naturally present in plants. 2S albumin, a specific pea albumin protein, was described to be resistant to proteolytic degradation and heat denaturation and is considered to have allergenic potential (Dziuba et al., 2014; Sirvent, Palomares, Cuesta-Herranz, Villalba, & Rodríguez, 2012). As pointed out in *Chapter 5*, commercial pea protein isolates, usually obtained through isoelectric precipitation lack albumins. However, the mildly fractionated protein fractions contain these albumins. Therefore, their allergenicity should be further investigated, to apply mildly fractionated protein in products for human consumption. Alternatively, methods might need to be developed to reduce the allergenic potential of these proteins.
During this research, it was observed that the aqueous protein fractions are very prone to spoilage. Therefore, a pasteurisation or UHT step could be beneficial to prolong the shelf life and suppress enzymatic degradation. Furthermore, the sensory attributes of the mildly fractionated ingredients require special focus. Pea proteins are often ascribed grassy, green and bean-like off-flavours, which lowers consumer acceptance. Therefore, different studies describe research on the aroma profile of different pea proteins from pea protein isolates, to quantify the contributing factors and develop flavour optimization of pea protein ingredients.
Functional ingredients of the mildly refined fractions could be better analysed with a product application in mind. Product applications could be inspired by dairy products or soy products, using coagulation or fermentation to specifically alter the structure, e.g., milk fermentation to produce yoghurt or soy protein coagulation to produce tofu. The application of old processes might result in novel products from plant sources.

## 8.7 Concluding remarks

This research once more confirms the heterogeneous, complex nature of raw materials, food ingredients and food products. In case of ingredients and products, it became apparent that both the composition and the structure determine the final ingredient or product properties.

Currently, ingredient producing industries build an intermediate step between the food assembly industry and the agro-industry, each as rather individual facilities. The food assembly industry purchases existing plant-based ingredients and develops novel food products, i.e. meat analogues, by intense processing and the addition of other ingredients. For a more efficient food production chain, a closer collaboration between, or even integration of the ingredient producers and the food assembly industry could be beneficial to develop ingredients that fulfil the product requirements. The process of de-structuring the raw material and re-structuring the ingredient into a food product should be closely linked and investigated using this new perspective. That could also help make these industries more efficient, avoid the production of low-value side streams and improve the ingredient properties.

## References


Aguilera, J. M., & Baffico, P. (1997). Structure-Mechanical Properties of Heat-Induced Whey Protein / Cassava Starch Gels. Journal of Food Science, 62(5), 1048–1054.

Aluko, R. E. (2017). Structural Characteristics of Food Protein-Derived Bitter Peptides. Bitterness, (2017), 105–129. https://doi.org/10.1002/9781118590263.ch6

Assatory, A., Vitelli, M., Rajabzadeh, A. R., & Legge, R. L. (2019). Dry fractionation methods for plant protein, starch and fiber enrichment: A review. Trends in Food Science and Technology. https://doi.org/10.1016/j.tifs.2019.02.006

Augustin, M. A., Riley, M., Stockmann, R., Bennett, L., Kahl, A., Lockett, T., … Cobiac, L. (2016). Role of food processing in food and nutrition security. Trends in Food Science and Technology. https://doi.org/10.1016/j.tifs.2016.08.005

Bain, J. M., & Mercert, F. V. (1966). Subcellular organization of the developing cotyledons of Pisum Sativum L. Australian Journal of Biological Sciences, 19, 49–67.

Berghout, J. A. M., Venema, P., Boom, R. M., & Goot, A. J. Van Der. (2015). Comparing functional properties of concentrated protein isolates with freeze-dried protein isolates from lupin seeds. Food Hydrocolloidsydrocolloids, 51, 346–354. https://doi.org/10.1016/j.foodhyd.2015.05.017

Berk, Z. (2013). Membrane Processes. In Food Process Engineering and Technology (pp. 259–285). https://doi.org/10.1016/B978-0-12-415923-5.00010-1

Bertoft, E., Qin, Z., & Manelius, R. (1993). Studies on the Structure of Pea Starches Part 4: Intermediate Material of Wrinkled Pea Starch. Starch - Stärke, 45(12), 420–425. https://doi.org/10.1002/star.19930451203

Boukid, F., Rosell, C. M., & Castellari, M. (2021). Pea protein ingredients: A mainstream ingredient to (re)formulate innovative foods and beverages. Trends in Food Science and Technology, 110, 729–742. https://doi.org/10.1016/j.tifs.2021.02.040

Boursier, B; Delevarre, M; Lis, J; Marquilly, P. (2008). Textured pea proteins. United States Patent Application Publication. https://doi.org/10.1037/t24245-000

Boye, J. I., Aksay, S., Roufik, S., Ribéreau, S., Mondor, M., Farnworth, E., & Rajamohamed, S. H. (2010). Comparison of the functional properties of pea, chickpea and lentil protein concentrates processed using ultrafiltration and isoelectric precipitation techniques. Food Research International, 43(2), 537–546. https://doi.org/10.1016/j.foodres.2009.07.021

Boye, J., Zare, F., & Pletch, A. (2010). Pulse proteins : Processing, characterization, functional properties and applications in food and feed. Food Research International, 43(2), 414–431. https://doi.org/10.1016/j.foodres.2009.09.003

Cappelli, A., Bettaccini, L., & Cini, E. (2020). The kneading process: A systematic review of the effects on dough rheology and resulting bread characteristics, including improvement strategies. Trends in Food Science and Technology, 104(August), 91–101. https://doi.org/10.1016/j.tifs.2020.08.008

Chao, D., Jung, S., & Aluko, R. E. (2018). Physicochemical and functional properties of high pressure-treated isolated pea protein. Innovative Food Science and Emerging Technologies, 45(February 2017), 179–185. https://doi.org/10.1016/j.ifset.2017.10.014

Chou, D. H., & Morr, C. V. (1979). Protein-water interactions and functional properties. Journal of the American Oil Chemists' Society, 56, A53–A62. https://doi.org/10.1007/BF02671785

Clark, A. H. (1987). Application of network theory to food systems. (J. M. V. Blanshard & P. Lillford, Eds.), Food structure and behaviour.

Colonna, P., Gallant, D., & Mercier, C. (1980). Pisum sativum and vicia faba carbohydrates : Studies of fractions obtained after dry and wet protein extraction processes. Journal of Food Science, 45, 1629–1636.

Craig, S., Goodchild, D. J., & Millerd, A. (1979). Immunofluorescent localization of pea storage proteins in glycol methacrylate embedded tissue. Journal of Histochemistry and Cytochemistry, 27(10), 1312–1316. https://doi.org/10.1177/27.10.390032

Croy, R. R. D., Gatehouse, J. A., Evans, I. M., & Boulter, D. (1980a). Characterisation of the Storage Protein Subunits Synthesised In Vitro by Polyribosomes and RNA from Developing Pea (Pisum sativum L.) I. Legumin. Planta, 148(1), 49–56.

Croy, R. R. D., Gatehouse, J. A., Evans, I. M., & Boulter, D. (1980b). Characterization of the Storage Protein Subunits Synthesised In Vitro by Polyribosomes and RNA from Developing Pea (Pisum sativum L.) II. Vicilin. Planta, 148(1), 57–63.

Croy, R. R., Hoque, M. S., Gatehouse, J. A., & Boulter, D. (1984). The major albumin proteins from pea (Pisum sativum L). Purification and some properties. The Biochemical Journal, 218(3), 795–803. https://doi.org/10.1042/bj2180795

de Almeida Costa, G. E., da Silva Queiroz-Monici, K., Pissini Machado Reis, S. M., & de Oliveira, A. C. (2006). Chemical composition, dietary fibre and resistant starch contents of raw and cooked pea, common bean, chickpea and lentil legumes.

Food Chemistry, 94(3), 327–330. https://doi.org/10.1016/j.foodchem.2004.11.020

Dekkers, B. L., Kort, D. W. de, Grabowska, K. J., Tian, B., As, H. Van, & van der Goot, A. J. (2016). A combined Rheology and Time Domain NMR approach for determining water distribution in Protein Blends. Food Hydrocolloids, 60, 525–532. https://doi.org/10.1017/CBO9781107415324.004

Delesse, A. (1847). Precede mechanique pour determine la composition de roches (extrait). CR Acad Sci (Paris), 25, 544–560.

Djoullah, A., Djemaoune, Y., Husson, F., & Saurel, R. (2015). Native-state pea albumin and globulin behavior upon transglutaminase treatment. Process Biochemistry, 50(8), 1284–1292. https://doi.org/10.1016/j.procbio.2015.04.021

Donmez, D., Pinho, L., Patel, B., Desam, P., & Campanella, O. H. (2021). Characterization of starch–water interactions and their effects on two key functional properties: starch gelatinization and retrogradation. Current Opinion in Food Science, 39, 103–109. https://doi.org/10.1016/j.cofs.2020.12.018

Dziuba, J., Szerszunowicz, I., Nałecz, D., & Dziuba, M. (2014). Proteomic analysis of albumin and globulin fractions of pea (Pisum sativum L.) seeds. Acta Scientiarum Polonorum, Technologia Alimentaria, 13(2), 181–190. https://doi.org/10.17306/J.AFS.2014.2.7

Funke, A., & Ziegler, F. (2010). Hydrothermal carbonization of biomass: A summary and discussion of chemical mechanisms for process engineering. Biofuels, Bioproducts and Biorefining, 4, 160–177. https://doi.org/10.1002/bbb.198

Gajewski, A. (1989). Measuring the charging tendency of polystyrene particles in pneumatic conveyance. Journal of Electrostatics, 23, 55–66.

Gavazzi-April, C., Benoit, S., Doyen, A., Britten, M., & Pouliot, Y. (2018). Preparation of milk protein concentrates by ultrafiltration and continuous diafiltration: Effect of process design on overall efficiency. Journal of Dairy Science, 101(11), 9670–9679. https://doi.org/https://doi.org/10.3168/jds.2018-14430

Geerts, M. E. J., Mienis, E., Nikiforidis, C. V., van der Padt, A., & van der Goot, A. J. (2017). Mildly refined fractions of yellow peas show rich behaviour in thickened oil-in-water emulsions. Innovative Food Science and Emerging Technologies, 41, 251–258. https://doi.org/10.1016/j.ifset.2017.03.009

Geerts, M. E. J., Nikiforidis, C. V., van der Goot, A. J., & van der Padt, A. (2017). Protein nativity explains emulsifying properties of aqueous extracted protein components from yellow pea. Food Structure, 14(September), 104–111. https://doi.

org/10.1016/j.foostr.2017.09.001

Geerts, M. E. J., Strijbos, M., van der Padt, A., & van der Goot, A. J. (2017). Understanding functional properties of mildly refined starch fractions of yellow pea. Journal of Cereal Science, 75, 116–123. https://doi.org/10.1016/j.jcs.2017.03.025

Geerts, M. E. J., van Veghel, A., Zisopoulos, F. K., van der Padt, A., & van der Goot, A. J. (2018). Exergetic comparison of three different processing routes for yellow pea (Pisum sativum): Functionality as a driver in sustainable process design. Journal of Cleaner Production. https://doi.org/10.1016/j.jclepro.2018.02.158

Goldstein, J. I., Newbury, D. E., Michael, J. R., Ritchie, N. W. M., Scott, J. H. J., & Joy, D. C. (2018). Microscopy and X-Ray Microanalysis. https://doi.org/10.1007/978-1-4939-6676-9

Gonzalez-Perez, S., & Arellano, J. B. (2009). Vegetable Protein Isolates. In G. O. Phillips & P. A. Williams (Eds.), Handbook of Hydrocolloids (2nd editio, pp. 1–27). Woodhead Publishing Limited.

Govindan, K. (2018). Sustainable consumption and production in the food supply chain: A conceptual framework. International Journal of Production Economics, 195(November 2015), 419–431. https://doi.org/10.1016/j.ijpe.2017.03.003

Henning, D. R., Baer, R. J., Hassan, A. N., & Dave, R. (2006). Major advances in concentrated and dry milk products, cheese, and milk fat-based spreads. Journal of Dairy Science, 89(4), 1179–1188. https://doi.org/10.3168/jds.S0022-0302(06)72187-7

Higgins, T. J. V., Chandler, P. M., Randall, P. J., Spencer, D., Beach, L. R., Blagrove, R. J., … Inglis, A. S. (1986). Gene structure, protein structure, and regulation of the synthesis of a sulfur-rich protein in pea seeds. Journal of Biological Chemistry, 261(24), 11124–11130. https://doi.org/10.1016/S0021-9258(18)67357-0

Hofmann, M., Bayles, A. V., & Vermant, J. (2021). Stretch, fold, and break: Intensification of emulsification of high viscosity ratio systems by fractal mixers. AIChE Journal, 67(5). https://doi.org/10.1002/aic.17192

Holt, N. W., & Sosulski, F. W. (1979). Amino Acid Composition and Protein Quality of Field Peas. Canadian Journal of Plant Science, 59(3), 653–660. https://doi.org/10.4141/cjps79-103

Horn, R. G., & Smith, D. T. (1992). Contact Electrification and Adhesion Between Dissimilar Materials. American Association for the Advancement of Science, 256(5055), 362–364.

Hsiao, K.-W., Sasmal, C., Ravi Prakash, J., & Schroeder, C. M. (2017). Direct observation

of DNA dynamics in semidilute solutions in extensional flow. Journal of Rheology, 61(1), 151–167. https://doi.org/10.1122/1.4972236

Huang, A. H. C. (1985). Protein Bodies. In H.-F. Linskens (Ed.), Cell Components. Springer-Verlag Berlin Heidelberg.

Karami, Z., & Akbari-adergani, B. (2019). Bioactive food derived peptides: a review on correlation between structure of bioactive peptides and their functional properties. Journal of Food Science and Technology, 56(2), 535–547. https://doi.org/10.1007/s13197-018-3549-4

Kim, H. S., Kim, B. Y., & Baik, M. Y. (2012). Application of ultra high pressure (UHP) in starch chemistry. Critical Reviews in Food Science and Nutrition, 52(2), 123–141. https://doi.org/10.1080/10408398.2010.498065

Kistler, T., Pridal, A., Bourcet, C., & Denkel, C. (2021). Modulation of sweetness perception in confectionary applications. Food Quality and Preference, 88, 104087. https://doi.org/10.1016/j.foodqual.2020.104087

Kornet, R., Venema, P., Nijsse, J., van der Linden, E., van der Goot, A. J., & Meinders, M. B. J. (2020). Yellow pea aqueous fractionation increases the specific volume fraction and viscosity of its dispersions. Food Hydrocolloids, 99(2020), 105332. https://doi.org/10.1016/j.foodhyd.2019.105332

Kornet, R., Penris, S., Venema, P., van der Goot, A. J., Meinders, M. B. J., & van der Linden, E. (2021). How pea fractions with different protein composition and purity can substitute WPI in heat-set gels. Food Hydrocolloids, 120, 106891. https://doi.org/10.1016/j.foodhyd.2021.106891

Kornet, R., Veenemans, J., Venema, P., van der Goot, A. J., Meinders, M., Sagis, L., & van der Linden, E. (2021). Less is more: Limited fractionation yields stronger gels for pea proteins. Food Hydrocolloids, 112, 106285. https://doi.org/10.1016/j.foodhyd.2020.106285

Kornet, R., Yang, J., Venema, P., van der Linden, E., & Sagis, L. M. C. (2022). Optimizing pea protein fractionation to yield protein fractions with a high foaming and emulsifying capacity. Food Hydrocolloids, 126(December 2021), 107456. https://doi.org/10.1016/j.foodhyd.2021.107456

Kosson, R., Czuchajowska, Z., & Pomeranz, Y. (1994). Smooth and wrinkled peas. 2. Distribution of protein, lipid, and fatty acids in seed and milling fractions. Journal of Agricultural and Food Chemistry, 42(1), 96–99. https://doi.org/10.1021/jf00037a015

Kramer, R. M., Shende, V. R., Motl, N., Pace, C. N., & Scholtz, J. M. (2012). Toward a

molecular understanding of protein solubility: Increased negative surface charge correlates with increased solubility. Biophysical Journal, 102(8), 1907–1915. https://doi.org/10.1016/j.bpj.2012.01.060

Kugler, S. K., Dey, A. P., Saad, S., Cruz, C., Kech, A., & Osswald, T. (2020). A flow-dependent fiber orientation model. Journal of Composites Science, 4(3), 1–22. https://doi.org/10.3390/jcs4030096

Kwetkus, B. A. (1998). Particle triboelectrification and its use in the electrostatic separation process. Particulate Science and Technology, 16:1, 55–68. https://doi.org/10.1080/02726359808906784

Ladha-Sabur, A., Bakalis, S., Fryer, P. J., & Lopez-Quiroga, E. (2019). Mapping energy consumption in food manufacturing. Trends in Food Science and Technology. https://doi.org/10.1016/j.tifs.2019.02.034

Lam, A. C. Y., Can Karaca, A., Tyler, R. T., & Nickerson, M. T. (2018a). Pea protein isolates: Structure, extraction, and functionality. Food Reviews International, 34(2), 126–147. https://doi.org/10.1080/87559129.2016.1242135

Lam, A. C. Y., Can Karaca, A., Tyler, R. T., & Nickerson, M. T. (2018b). Pea protein isolates: Structure, extraction, and functionality. Food Reviews International, 34(2), 126–147. https://doi.org/10.1080/87559129.2016.1242135

Lambert, G. M., & Baird, D. G. (2017). Evaluating Rigid and Semiflexible Fiber Orientation Evolution Models in Simple Flows. Journal of Manufacturing Science and Engineering, Transactions of the ASME, 139(3), 1–7. https://doi.org/10.1115/1.4034664

Lie-Piang, A., Braconi, N., Boom, R. M., & van der Padt, A. (2021). Less refined ingredients have lower environmental imparct - A life cycle assessment of protein-rich ingredients from oil- and starch bearing crops. Journal of Cleaner Production, 292. https://doi.org/10.1016/j.jclepro.2021.126046

Lie-Piang, A., Möller, A. C., Köllmann, N., Garre, A., Boom, R., & van der Padt, A. (2021). Functionality-driven food product formulation – An illustration on selecting sustainable ingredients building viscosity. Food Research International, 152(December 2021), 110889. https://doi.org/10.1016/j.foodres.2021.110889

Lillford, P. J. (2016). The impact of food structure on taste and digestibility. Food and Function, 7(10), 4131–4136. https://doi.org/10.1039/c5fo01375e

Lipnizki, F., Boelsmand, J., & Madsen, R. F. (2002). Concepts of industrial-scale diafiltration systems. Desalination, 144(1–3), 179–184. https://doi.org/10.1016/S0011-

9164(02)00309-0

Liu, Z., Zhang, M., Bhandari, B., & Wang, Y. (2017). 3D printing: Printing precision and application in food sector. Trends in Food Science and Technology, 69, 83–94. https://doi.org/10.1016/j.tifs.2017.08.018

Ma, Y., Schutyser, M. A. I., Boom, R. M., & Zhang, L. (2021). Predicting the extrudability of complex food materials during 3D printing based on image analysis and gray-box data-driven modelling. Innovative Food Science and Emerging Technologies, 73(April), 102764. https://doi.org/10.1016/j.ifset.2021.102764

MacGregor, A. W. (2003). Barley - Origin Adaptation, and Production. Food Technology, 379–382.

McMahon, D. J., Fife, R. L., & Oberg, C. J. (1999). Water Partitioning in Mozzarella Cheese and Its Relationship to Cheese Meltability. Journal of Dairy Science, 82(7), 1361–1369. https://doi.org/10.3168/jds.S0022-0302(99)75361-0

Möller, A. C., Li, J., van der Goot, A. J., & van der Padt, A. (2021). A water-only process to fractionate yellow peas into its constituents. Innovative Food Science & Emerging Technologies, 75(December 2021), 102894. https://doi.org/10.1016/j.ifset.2021.102894

Möller, A. C., van der Padt, A., & van der Goot, A. J. (2021). From raw material to mildly refined ingredient – Linking structure to composition to understand fractionation processes. Journal of Food Engineering, 291. https://doi.org/10.1016/j.jfoodeng.2020.110321

Mondor, M., Tuyishime, O., & Drolet, H. (2012). Production of pea protein concentrates by ultrafiltration: Influence of hollow-fibre module. Innovative Food Science and Emerging Technologies, 14, 135–138. https://doi.org/10.1016/j.ifset.2012.02.003

Morris, E. R. (2009). Functional Interactions in Gelling Biopolymer Mixtures. In Modern Biopolymer Science (First Edit, Vol. 53, pp. 167–198). Elsevier Inc. https://doi.org/10.1016/B978-0-12-374195-0.00005-7

Morris, V. J., & Groves, K. (2013). Introduction. Food Microstructures: Microscopy, Measurement and Modelling. https://doi.org/10.1016/B978-0-85709-525-1.50022-1

Muneer, F., Johansson, E., Hedenqvist, M. S., Plivelic, T. S., Markedal, K. E., Petersen, I. L., … Kuktaite, R. (2018). The impact of newly produced protein and dietary fiber rich fractions of yellow pea (Pisum sativum L.) on the structure and mechanical properties of pasta-like sheets. Food Research International. https://doi.org/10.1016/j.foodres.2018.01.020

Muscalu, G., Voicu, G., Istudor, A., & Tudor, P. (2020). Bread dough rheological behavior under the influence of the geometry of the kneading arms. Revista de Chimie, 70(9), 295–307. https://doi.org/10.37358/RC.20.9.8340

Nachal, N., Moses, J. A., Karthik, P., & Anandharamakrishnan, C. (2019). Applications of 3D Printing in Food Processing. Food Engineering Reviews, 11(3), 123–141. https://doi.org/10.1007/s12393-019-09199-8

Neerincx, P. E., Denteneer, R. P. J., & Meijer, H. E. H. (2011). A fully polymeric mouldable microfluidic device. Part 1: The process of design. Macromolecular Materials and Engineering, 296(12), 1081–1090. https://doi.org/10.1002/mame.201100047

Neerincx, P. E., Hellenbrand, S. J. M., & Meijer, H. E. H. (2011). A fully polymeric mouldable microfluidic device. Part 2: Designing the process. Macromolecular Materials and Engineering, 296(12), 1091–1100. https://doi.org/10.1002/mame.201100048

Neerincx, P. E., Hofmann, M., Gorodetskyi, O., Feldman, K., Vermant, J., & Meijer, H. E. H. (2021). One-step creation of hierarchical fractal structures. Polymer Engineering and Science, 61(4), 1257–1269. https://doi.org/10.1002/pen.25677

Neerincx, P. E., & Meijer, H. E. H. (2013). Fractal Structuring in Polymer Processing. Macromolecular Chemistry and Physics, 214(2), 188–202. https://doi.org/10.1002/macp.201200394

Nikbakht Nasrabadi, M., Sedaghat Doost, A., & Mezzenga, R. (2021). Modification approaches of plant-based proteins to improve their techno-functionality and use in food products. Food Hydrocolloids, 118(April), 106789. https://doi.org/10.1016/j.foodhyd.2021.106789

Osborne, T. B. (1909). The vegetable proteins. In Monographs on biochemistry. (p. xiii 125p.). London, New York [etc.] Longmans, Green and Company. https://doi.org/ Retrieved from catalog.hathitrust.org/Record/001034229

Otto, T., Baik, B., & Czuchajowska, Z. (1997). Microstructure of Seeds, Flours, and Starches of Legumes. Cereal Chemistry Journal, 74(4), 445–451. https://doi.org/10.1094/CCHEM.1997.74.4.445

Parada, J., & Aguilera, J. M. (2007). Food microstructure affects the bioavailability of several nutrients. Journal of Food Science, 72(2), 21–33. https://doi.org/10.1111/j.1750-3841.2007.00274.x

Passe, D; Fouache C; Verrin, J-M; Bureau, S. (2008). Pea protein composition. United States Patent Application Publication. https://doi.org/10.1037/t24245-000

Pelgrom, P. J. M., Berghout, J. A. M., van der Goot, A. J., Boom, R. M., & Schutyser, M.

A. I. (2014). Preparation of functional lupine protein fractions by dry separation. LWT - Food Science and Technology, 59(2P1), 680–688. https://doi.org/10.1016/j.lwt.2014.06.007

Pelgrom, P. J. M., Boom, R. M., & Schutyser, M. A. I. (2014). Functional analysis of mildly refined fractions from yellow pea. Food Hydrocolloids, 44, 12–22. https://doi.org/10.1016/j.foodhyd.2014.09.001

Pelgrom, P. J. M., Boom, R. M., & Schutyser, M. A. I. (2015). Method Development to Increase Protein Enrichment During Dry Fractionation of Starch-Rich Legumes. Food and Bioprocess Technology, 8(7), 1495–1502. https://doi.org/10.1007/s11947-015-1513-0

Pelgrom, P. J. M., Schutyser, M. A. I., & Boom, R. M. (2013). Thermomechanical Morphology of Peas and Its Relation to Fracture Behaviour. Food and Bioprocess Technology, 6(12), 3317–3325. https://doi.org/10.1007/s11947-012-1031-2

Pelgrom, P. J. M., Vissers, A. M., Boom, R. M., & Schutyser, M. A. I. (2013). Dry fractionation for production of functional pea protein concentrates. Food Research International, 53(1), 232–239. https://doi.org/10.1016/j.foodres.2013.05.004

Peng, Y., Kersten, N., Kyriakopoulou, K., & van der Goot, A. J. (2020). Functional properties of mildly fractionated soy protein as influenced by the processing pH. Journal of Food Engineering. https://doi.org/10.1016/j.jfoodeng.2019.109875

Pernollet, J. C. (1978). Protein bodies of seeds: Ultrastructure, biochemistry, biosynthesis and degradation. Phytochemistry, 17(9), 1473–1480. https://doi.org/10.1016/S0031-9422(00)94623-5

Pietsch, V. L., Karbstein, H. P., & Emin, M. A. (2018). Kinetics of wheat gluten polymerization at extrusion-like conditions relevant for the production of meat analog products. Food Hydrocolloids, 85(July), 102–109. https://doi.org/10.1016/j.foodhyd.2018.07.008

Ratnayake, W. S. (2021). Utilizing side streams of pulse protein processing : A review, (August), 1–15. https://doi.org/10.1002/leg3.120

Ratnayake, W. S., Hoover, R., & Warkentin, T. (2002). Pea starch: Composition, structure and properties - A review. Starch/Staerke, 54(6), 217–234. https://doi.org/10.1002/1521-379X(200206)54:6<217::AID-STAR217>3.0.CO;2-R

Reichert, R. D., & Youngs, C. G. (1978). Nature of the residual protein associated with starch fractions from air classified field peas. Cereal Chemistry. Retrieved from https://www.aaccnet.org/publications/cc/backissues/1978/Documents/

chem55_469.pdf

Rivlin, R. S. (1948). Normal Stress Coefficient in Solutions of Macromolecules. Nature, 161(4093), 567–568.

Romero-Guzmán, M. J., Jung, L., Kyriakopoulou, K., Boom, R. M., & Nikiforidis, C. V. (2020). Efficient single-step rapeseed oleosome extraction using twin-screw press. Journal of Food Engineering, 276. https://doi.org/10.1016/j.jfoodeng.2019.109890

Roquette-Frères. (n.d.). No Title. Retrieved from https://www.roquette.com/food-and-nutrition/dairy/alternative-proteins

Roy, F., Boye, J. I., & Simpson, B. K. (n.d.). Bioactive proteins and peptides in pulse crops: Pea, chickpea and lentil. Food Research International, 43(2), 432–442. https://doi.org/10.1016/j.foodres.2009.09.002

Saha, D., & Bhattacharya, S. (2010). Hydrocolloids as thickening and gelling agents in food: A critical review. Journal of Food Science and Technology, 47(6), 587–597. https://doi.org/10.1007/s13197-010-0162-6

Saldanha do Carmo, C., Varela, P., Poudroux, C., Dessev, T., Myhrer, K., Rieder, A., … Knutsen, S. H. (2019). The impact of extrusion parameters on physicochemical, nutritional and sensorial properties of expanded snacks from pea and oat fractions. Lwt, 112(January), 108252. https://doi.org/10.1016/j.lwt.2019.108252

Sandoval Murillo, J. L., Osen, R., Hiermaier, S., & Ganzenmüller, G. (2019). Towards understanding the mechanism of fibrous texture formation during high-moisture extrusion of meat substitutes. Journal of Food Engineering, 242(August 2018), 8–20. https://doi.org/10.1016/j.jfoodeng.2018.08.009

Schaller, R., Neerincx, P. E., & Meijer, H. E. H. (2017). Hierarchical and Fractal Structuring in Polymer Processing. Macromolecular Materials and Engineering, 302(6), 1–14. https://doi.org/10.1002/mame.201600524

Schieber, A. (2017). Side Streams of Plant Food Processing As a Source of Valuable Compounds: Selected Examples. Annual Review of Food Science and Technology, 8(1), 97–112. https://doi.org/10.1146/annurev-food-030216-030135

Schreuders, F. K. G., Bodnar, I., Erni, P., Boom, R. M., & Goot, A. J. Van Der. (2020). Water redistribution determined by time domain NMR explains rheological properties of dense fibrous protein blends at high temperature. Food Hydrocolloids, 101, 105562. https://doi.org/10.1016/j.foodhyd.2019.105562

Schutyser, M. A. I., Pelgrom, P. J. M., van der Goot, A. J., & Boom, R. M. (2015). Dry fractionation for sustainable production of functional legume protein concentrates.

Trends in Food Science and Technology, 45(2), 327–335. https://doi.org/10.1016/j.tifs.2015.04.013

Schutyser, M. A. I., & van der Goot, A. J. (2011). The potential of dry fractionation processes for sustainable plant protein production. Trends in Food Science and Technology, 22(4), 154–164. https://doi.org/10.1016/j.tifs.2010.11.006

Shevkani, K., Singh, N., Kaur, A., & Chand, J. (2015). Structural and functional characterization of kidney bean and field pea protein isolates : A comparative study. Food Hydrocolloids, 43, 679–689. https://doi.org/10.1016/j.foodhyd.2014.07.024

Shi, Y., Mandal, R., Singh, A., & Pratap Singh, A. (2020). Legume lipoxygenase: Strategies for application in food industry. Legume Science, 2(3), 1–15. https://doi.org/10.1002/leg3.44

Silventoinen, P., Sipponen, M. H., Holopainen-Mantila, U., Poutanen, K., & Sozer, N. (2018). Use of air classification technology to produce protein-enriched barley ingredients. Journal of Food Engineering. https://doi.org/10.1016/j.jfoodeng.2017.11.016

Singh, H. (2011). Milk Protein Products: Functional Properties of Milk Proteins. Encyclopedia of Dairy Sciences: Second Edition, 887–893. https://doi.org/10.1016/B978-0-12-374407-4.00352-6

Sirvent, S., Palomares, O., Cuesta-Herranz, J., Villalba, M., & Rodríguez, R. (2012). Analysis of the structural and immunological stability of 2S albumin, nonspecific lipid transfer protein, and profilin allergens from mustard seeds. Journal of Agricultural and Food Chemistry, 60(23), 6011–6018. https://doi.org/10.1021/jf300555h

Takayanagi, M., Harima, H., & Iwata, Y. (1963). Viscoelastic Behavior of Polymer Blends and Its Comparison with Model Experiments. Memoirs of the Faculty of Engineering, Kyushu University (Vol. 23). Retrieved from https://www.jstage.jst.go.jp/article/jsms1963/12/116/12_116_389/_article/-char/ja/

Tanger, C., Engel, J., & Kulozik, U. (2020). Influence of extraction conditions on the conformational alteration of pea protein extracted from pea flour. Food Hydrocolloids, 107(March), 105949. https://doi.org/10.1016/j.foodhyd.2020.105949

Tiefenbacher, K. F. (2017). Adjuncts—Filling Creams, Inclusions, Cacao and Chocolate. Wafer and Waffle. https://doi.org/10.1016/b978-0-12-809438-9.00005-3

Tiwari, B. K., Gowen, A., & McKenna, B. (2011). Pulse Foods Processing, Quality and Nutraceutical Applications. (B. K. Tiwari, A. Gowen, & B. McKenna, Eds.).

Tulbek, M. C., Lam, R. S. H., Wang, Y. C., Asavajaru, P., & Lam, A. (2016). Pea: A Sustain-

able Vegetable Protein Crop. Sustainable Protein Sources. Elsevier Inc. https://doi.org/10.1016/B978-0-12-802778-3.00009-3

UniProt Consortium. (2019). UniProt: a worldwide hub of protein knowledge. https://doi.org/https://doi.org/10.1093/nar/gky1049

Van Der Goot, A. J., Pelgrom, P. J. M., Berghout, J. A. M., Geerts, M. E. J., Jankowiak, L., Hardt, N. A., … Boom, R. M. (2016). Concepts for further sustainable production of foods. Journal of Food Engineering, 168, 42–51. https://doi.org/10.1016/j.jfoodeng.2015.07.010

van der Hoeven, J. C., Wimbergen-Friedl, R., & Meijer, H. E. H. (2001). Homogeneity of Multilayers Produced With a Static Mixer. Polymer Engineering and Science, 41(1).

Van Donkelaar, L. H. G., Noordman, T. R., Boom, R. M., & Van Der Goot, A. J. (2015). Pearling barley to alter the composition of the raw material before brewing. Journal of Food Engineering, 150, 44–49. https://doi.org/10.1016/j.jfoodeng.2014.10.024

Vincent, M., & Agassant, J. F. (1985). Experimental and theoretical study of short fiber orientation in diverging flows. Rheologica Acta, 24(6), 603–610. https://doi.org/10.1007/BF01332594

Vojdani, F. (1996). Solubility. In G. M. Hall (Ed.), Methods of testing protein functionality (1st ed., pp. 11–60).

Vose, J. R., Basterrechea, M. J., Gorin, P. A. J., Finlayson, A. J., & G, Y. C. (1976). Air Classification of field peas and horsebean flours: Chemical studies of starch and protein fractions. Cereal Chemistry, 53(6), 928–936.

Wang, J., Smits, E., Boom, R. M., & Schutyser, M. A. I. (2015). Arabinoxylans concentrates from wheat bran by electrostatic separation. JOURNAL OF FOOD ENGINEERING, 155, 29–36. https://doi.org/10.1016/j.jfoodeng.2015.01.008

Wu, Y. V., & Nichols, N. N. (2005). Fine grinding and air classification of field pea. Cereal Chemistry, 82(3), 341–344. https://doi.org/10.1094/CC-82-0341

Yang, J., Kornet, R., Diedericks, C. F., Yang, Q., Berton-Carabin, C. C., Nikiforidis, C. V., … Sagis, L. M. C. (2022). Rethinking plant protein extraction: albumin — from side stream to an excellent foaming ingredient. Food Structure, 31(January), 100254. https://doi.org/10.1016/j.foostr.2022.100254

Zayas, J. F. (1997). Solubility of Proteins. In Functionality of Proteins in Food (pp. 6–75).

Zhao, H., Shen, C., Wu, Z., Zhang, Z., & Xu, C. (2020). Comparison of wheat, soybean,

rice, and pea protein properties for effective applications in food products. Journal of Food Biochemistry, 44(4), 1–12. https://doi.org/10.1111/jfbc.13157

## Summary

In this thesis the process of yellow pea from structured seed to structured product is investigated. New milder fractionation methods are of interest to produce novel functional food ingredients with lower impact on the raw material and the environment. The narrative in this thesis is driven by the structure of the raw material before mild fractionation, the structure remaining in the mild fractions, and the structure when reassembling the fractions into food matrices. The aim is to understand how interactions between the different components, in dry and in wet state, influence the efficiency of the process as well as the functional properties of the fractions.

As a starting point a pre-fractionation method of the pea seed was studied to combine the structural break-up of the seed with the fractionation of the constituents (*Chapter 2*). While pearling resulted in size reduction and separation of the testa and embryonic axis from the cotyledon fractions, the enrichment in protein or starch content in the cotyledon fractions was limited. However, the dietary fibre rich testa and the protein rich embryonic axis could be separated and collected with this method, which might make promising ingredients in food application, when harvested prior to fractionation.

Dry and mild wet fractionation are both methods that can be used to separate yellow pea flour into protein and starch-enriched fractions, although both processes return different purities and yields. In *Chapter 3*, the structure and composition of the flour particles before and after fractionation are investigated with scanning electron microscopy and energy-dispersive X-ray spectroscopy to understand the opportunities and limitations of the fractionation methods. It was found that adhesion between smaller and bigger particles, after milling, hinders full separation of yellow peas into their pure components with dry fractionation. Mild wet fractionation introduces an additional driving force with water; water solubilized reduced particle adhesion, which resulted in enhanced separation. Hence, in this chapter a relationship between the structure and the

fraction purity could be established, which allowed better judgement on the performance of the different fractionation processes.

In *Chapter 4* mild wet fractionation was further developed to achieve maximum separation with efficient water use. Chemicals were omitted and only water was used to separate protein and starch. Multiple washing steps of the starch and non-soluble protein fraction were applied to extract more protein from the starch fraction and to enhance the separation of soluble and non-soluble protein. Ultrafiltration of the soluble protein fraction concentrated the fraction and concurrently increased the protein purity, due to the extraction of small solutes into the permeate. The potential to upscale the method was assessed by comparing the fractionation of pea protein to whey protein fractionation. It was concluded that the method has potential for upscale use in industry, as it can produce protein isolates with composition and properties comparable to currently available protein isolates, yet by omitting chemicals in the process.

Yellow pea contains a variety of different proteins, amongst which albumins and globulins account for the major part. The protein composition of the soluble and non-soluble protein fraction, obtained through mild wet fractionation was investigated by further fractionating the fractions with isoelectric precipitation (*Chapter 5*). Furthermore, the functional properties, protein solubility and gelation, of the soluble and non-soluble protein fraction were determined. The compositional analysis showed that with mild wet fractionation both albumins and globulins can be extracted from yellow pea. The functional properties varied with protein type, composition and protein state, and isoelectric precipitation had a decreasing effect on the gelation capacity of the protein fractions.

The influence of composition on the functional properties was also treated in *Chapter 6*. The functional properties of multi-component blends and ingredients depend on the contribution of each ingredient and the water distribution in the blend. Therefore, the rheological properties as a function of the water content, were investigated for multi-component blends of pea protein, pea starch, and pea fibre isolates. The rheological experiments were used to make

predictions of the water distribution with the polymer blending law. CLSM images of the blends were used to compare the results; a quantitative analysis of the images could confirm the model predictions. Water distribution in multi-component blends was demonstrated to play a crucial role for the viscoelastic properties of such blends. Furthermore, further mechanical insight can be gained regarding the behaviour of fractions in multi-component blends, using the polymer blending law, in which the water distribution between the ingredients was included.

In *Chapter 7* a novel processing route to create stratified structures for food products is introduced. The core of the process is a channel consisting of static mixing elements that have previously been used to multiply layers and produce hierarchical fractal structures from non-food polymers. Here, it was investigated if the technique is also suitable to structure food materials. Chocolate dispersions were used as model food dispersions and layered into 256 layers uniform layers. Layering of the chocolate samples resulted in different mechanical properties, parallel and perpendicular to the layers. Experiments were repeated with wheat dough and melt cheese, thus higher viscous dispersions of different viscoelastic properties, and eight uniform layers could be produced. Structuring strands instead of layers was possible with the chocolate dispersions. However, distortions were visible and these became more pronounced after structure multiplication. The method allowed to structure food dispersions and when operated with higher forces could be promising to also structure higher viscous food materials.

Finally, *Chapter 8* discusses the thesis' main findings and conclusions. Different fractionation methods are compared in light of the findings in this thesis. The opportunities of mild fractionation are discussed, especially by comparing the pea fractionation process to common processes in dairy industry. An approach to only fractionate as much as necessary is introduced. Key element of that approach is a better link between fractionation method and ingredient requirements for best use in food products. The chapter presents an outlook to bring

the application of mild fractionated ingredients further, by proposing a closer collaboration between the ingredient production industry and the food assembly industry. It also include a future outlook on the use of fractal structuring for food purposes.

## Acknowledgements

Thanks to everyone who contributed to this work during the past 4 years, which I am happy to now see summarized in this thesis. These years truely were a journey of ups and downs and I am grateful for the wonderful people who accompanied me throughout.

Starting, I would like to thank my promotors Albert and Atze Jan for their support, encouragement and knowledge. Thanks for giving me room and motivating me to develop, and guiding me whenever necessary. Especially the beginning wasn't easy and I am grateful for your support and advice during that time.

Of course I also received a lot more help during my PhD time. Thanks to our technicians at FPE, Jos, Maurice, Wouter, Jarno, Martin and Lyneth, for your assistance, patience and enthusiasm when working with me. Jos and Maurice, thank you for almost always smiling at me when I came into your offices with yet another question. Thank you to our secretaries, Ilona, Marjan, Evelyn and Chantal for quick replies, kind reminders and all the other administrative support.

Thanks to my co-authors Anouk, Andrea, Jan and Miek, I enjoyed our collaborations a lot. It was inspiring and very instructive.

I would also like to thank my students, Katrien, Junni, Nienke, Arno, Leonie, Ting, Judith, Senna and Pragya, I appreciated your thrive, enthusiasm and feedback.

I also want to express my gratitude to my colleagues at FPE. For inbetween talks, refreshing coffee breaks, smiles in the hallway, and the good times we had during lab outjes, borrels, or the PhD trip. The atmosphere all of you create is very welcoming and the support offered by each colleague was very valuable for me. Thanks a lot to my office mates Ivanna, Murat, Loes, Aadi, Zulhaj, Zhaojun and Birgit for laughs, chats, dinners and sharing software hacks.

A special thanks also to my Nederlandse lunch vrienden, for helping me improve my Dutch; to the Red Brows, for having fun becoming the best of the

worst teams; and the Cool party kids for drinking and dancing with me from my first week onwards.
I am especially greatful to my roomies, Pina, Andrea and Anouk, for creating a home with me, for becoming my close friends and for sharing my affinity for good food and drinks.
Schlussendlich möchte ich mich noch bei meiner Familie bedanken. Danke für Eure Unterstützung, für Euren Rat, für Eure Appreciation und Liebe.

## About the author

Anna Cäcilie Möller was born in Enschede (NL) in 1991. In 2012 she started her BSc in Technology and Biotechnology of Foods at Technical University Munich (TUM). Thereafter, Anna continued with her Master studies at TUM in Technology and Biotechnology of Foods. She completed her studies with her master thesis where she characterized the surface and foaming properties of pea proteins. In 2018 Anna started her PhD in the Food Process Engineering Group of Wageningen University. Her research focused on the process to transform yellow peas from structured seeds into structured products and how component interactions influence the processes. The results of Anna's PhD research are presented in this thesis.

## Publications

**Möller, A. C.**, van der Padt, A., & van der Goot, A. J. (2021), Abrasive milling: A method to pre-fractionate testa and embryonic axis from yellow pea. Lwt, 151, 112087.

**Möller, A. C.**, van der Padt, A., & van der Goot, A. J. (2021), From raw material to mildly refined ingredient – Linking structure to composition to understand fractionation processes. Journal of Food Engineering, 291, 110321.

**Möller, A. C.**, Li, J., van der Padt, A., & van der Goot, A. J. (2022), A water-only process to separate yellow pea into its constituents. Innovative Food Science and Emerging Technologies, 75, 102894.

**Möller, A. C.**, van der Padt, A., & van der Goot, A. J. (2022), Influence of the fractionation method on the protein composition and functional properties. Innovative Food Science and Emerging Technologies, 81, 103144.

**Möller, A. C.**, Lie-Piang, A., Bian, T., van der Padt, A. & van der Goot, A. J., Structure analysis of multi-component biopolymer blends - The effect of water distribution on the viscoelastic properties. Submitted.

**Möller, A. C.**, van der Goot, A. J & van der Padt, A., A novel continuous process to produce stratified structures in food. Submitted.

Lie-Piang, A., **Möller, A. C.**, Köllmann, N., Garre, A., Boom, R., & van der Padt, A. (2022), Functionality driven food product formulation - An illustration to select sustainable ingredients building viscosity. Food Research International, 152, 110889.

Bühler, J. M., Schlangen, M., **Möller, A. C.**, Bruins, M. E., van der Goot, A. J. (2022), Starch in Plant-Based Meat Replacers: A New Approach to Using Endogenous Starch from Cereals and Legumes. Starch - Stärke, 74, 2100157.

Rivera del Rio, A., **Möller, A. C.**, Boom, R. M., Janssen, A. E. M. (2022), Gastro-duodenal in vitro digestion of conventional and mildly processed pea protein ingredients. Food Chemistry, 387, 132894.

## Overview of the completed training activities

### Courses

| | |
|---|---|
| Food Proteins: functionality, modifications and analysis (VLAG, NL) | 2018 |
| Han-Sur Lesse Winterschool (WUR & TUDelft, BE) | 2019 |
| EIT Food Entrepreneurial Summerschool (EIT Food, Madrid, ES) | 2019 |
| 17th European School on Rheology (KU Leuven, BE) | 2019 |
| Engineering Project Management: Mastering Complexity (TUDelftX, online) | 2021 |
| Project Engineering Management: Preparing for success (TUDelftX, online) | 2021 |

### Conferences

| | |
|---|---|
| Science and Technology for meat analogues (Wageningen, NL) | 2018 |
| 33rd EFFoST conference (Rotterdam, NL)[2] | 2019 |
| LCA Food (online)[2] | 2020 |
| 34th EFFoST conference (online)[1] | 2020 |
| Plant Protein Science and Technology Forum (AOCS, online)[1,2] | 2021 |
| 35th EFFoST conference (Lausanne, CH)[1] | 2021 |

### General Courses

| | |
|---|---|
| VLAG PhD Week (VLAG, NL) | 2019 |
| Introduction to R for statistical analysis (PE&RC, NL) | 2020 |
| Project and Time Management (WGS, NL) | 2020 |
| Applied statistics (VLAG, NL) | 2020 |
| Career Perspectives (WGS, NL) | 2021 |
| Introduction to LateX (PE&RC, NL) | 2019 |
| PhD workshop Carousel (WGS, NL) | 2019 |

Other activities

| | |
|---|---|
| Preparation of research proposal | 2018 |
| FPE weekly group meetings | 2018-2022 |
| Journal club Food structuring biweekly meetings | 2018-2021 |
| Project Cluster meetings (MFFF) quarterly | 2018-2022 |
| PhD study tour to Singapore[1,2] | 2022 |
| Lecturer Online Summer/Winterschool Biotechnology, agriculture & food | 2021-2022 |

[1] Oral presentation
[2] Poster presentation

This thesis was part of the 'Novel Process Routes' project, financially supported by the Institute for Sustainable Process Technology (ISPT) and by TKI-E&I with the supplementary grant 'TKI-Toeslag' for Topconsortia for Knowledge and Innovation (TKI's) of the Dutch Ministry of Economic Affairs and Climate Policy. The author would like to thank all members of the ISPT Consortium for their contribution: Cosun, DSM, FrieslandCampina, Pentair, NIZO, RHDHV, TU Delft and Wageningen University.
More information can be found at *https://ispt.eu/projects/novel-process-routes*

Cover design by Vincent Möller
Printed by Proefschriftmaken.nl